Proceeding

8th International Conference on Creative Technlogy

2020 CreTech

Multidisciplinary

to Drive Economy and Social

5-7 August 2020

Grand Pacific Sovereign Resort and Spa
Cha-am, Petchaburi, Thailand

UTK RAJAMANGALA KRUNGTHEP
For Further Information
Rajamangala University of Technology Krungthep
Tel : +(66) 2 287 9600 EXT 1177 Fax : +(66) 2 287 9684
utkcretech@mail.rmutk.ac.th
http://utkcretech.rmutk.ac.th

8th CreTech 2020

8th CreTech International conference 2020

Research proceeding for 8th International conference at Grand Pacific Sovereign Resort & Spa, Petchaburi, Thailand.

By Rajamangala University of Technology Krungthep, 2 Nanglingi Road, Thungmahamek, Sathorn, Bangkok, 10120, Thailand

Published on August, 2020

8th International Conference on Creative Technology
Welcoming Message

Dear Excellecies, distinguished guests, ladies and gentlemen,

On behalf of the CreTech 2020 organizing committee, it is my great pleasure and honor to welcome all of you at the opening ceremony of the 8th International Conference on Creative Technology here in Grand Pacific Sovereign Resort & Spa, Petchaburi, Thailand. We are very delighted to see all researchers from many educational institutes to share and exchange your precious experiences as well as valuable studies diverse fields through not only oral presentation but academic posters in creative technologies, and education research in the concept of "Driving Economy and Society with Agriculture 4.0". This conference provides a forum for accessing to the most up-to-date and reliable knowledge from both commercial and academic worlds, sharing best practice in the fields as well as learning about case studies of successfully integrated technologies. The meeting provides an opportunity to highlight the recent developments apart from identifying emerging future areas of growth. We also expect to provide technical demonstrations, and numerous opportunities for informal networking.

The success of the conference is ultimately depended on all the people who have worked with us in planning and organizing both the technical program and supporting social arrangements. In particular, we would like to thank to the Program Chairs for their smart advice and brilliant suggestions on organizing the technical program; the Program Committee for their thorough and timely reviewing of the papers, and our sponsors who have helped us to diminish the costs of CreTech 2020 for all participants.

We would like to say thank you again to precipitate CreTech 2020 conference. I hope that you will enjoy all forums and activities we offer.

Yours sincerely,

Alongkorn Ponlaboot
Advisor to the minister of Agriculture and cooperatives
Honorary Chair, CreTech 2020

Call for Papers

Registration http://utkcretech.rmutk.ac.th

All accepted papers will be published in the proceeding of CreTech conference.
Selected papers will be published in UTK Research Journal (TCI)

2020 CreTech

8th International Conference on Creative Technlogy
4th National Conference on Creative Technlogy

Grand Pacific Sovereign Resort and Spa

Cha-am, Petchaburi, Thailand

5-7 Aug 2020

Multidisciplinary

to Drive Economy and Social

Call for Papers Oral & Poster

Topics of interests include but are not limited to

Track 1 **Engineering and Technology**
Engineering, Energy, Information Technology
Logistics, Aviation, and Related Area

Track 2 **Sciences and Technology**
General and Applied Science, Food Science
Food Safety, Product Development, Biotechnology
Agricultural Science, and Related Area

Track 3 **Creative technology**
Architecture, Product Design, Fashion Design,
Textile Design, Packaging Design, and Related Area

Track 4 **Business, Tourism, and Economics**
Management, Marketing, Financial and Banking
Tourism and Hospitality, Economics and Related Area

Track 5 **Social Sciences and Humanities**
Teaching and Education, Languages and Ontologie
and Related Area

Registration International Conference

Registration due date	Registration Type	Fee (Thai Baht)
Early-bird Registration (Before 21 July, 2020)	Regular Paper	6,500
	Student Paper	3,000
	Additional Paper	3,500
	Partioipant	3,500
Onsite Registration (From 5-6 Aug, 2020)	Regular Paper	8,000
	Student Paper	5,500
	Additional Paper	4,000
	Participant	4,000

Registration National Conference

Registration due date	Registration Type	Fee (Thai Baht)
Early-bird Registration (Before 21 July, 2020)	Regular Paper	4,000
	Student Paper	2,500
	Additional Paper	2,000
	Partioipant	2,000
Onsite Registration (From 5-6 Aug, 2020)	Regular Paper	5,000
	Student Paper	3,000
	Additional Paper	2,500
	Participant	2,500

Important Dates

26 Jun 2020 Paper submission (Full paper)

10 July 2020 Notification of full paper acceptance

17 July 2020 Final full paper submission deadline

21 July 2020 Early-bird registration deadline

22 July – 6 Aug 2020 Standard registration deadline

5-6 Aug 2020 On site registration

5-7 Aug 2020 Conference day

UTK RAJAMANGALA KRUNGTHEP
For Further Information
Rajamangala University of Technology Krungthep
Tel : +(66) 2 287 9600 EXT 1177 Fax : +(66) 2 287 9684
utkcretech@mail.rmutk.ac.th
http://utkcretech.rmutk.ac.th

Content

CreTech 2020
8th International Conference on Creative Technology
Multidisciplinary to Drive Economy and Social
http://utkcretech.rmutk.ac.th

The comparison of parameter estimation for mathematical model of the reheating furnace pusher type.

Narongrid Rorsena[1], Warisa Yomsatieankul[1], Tareerat Tanutpanit[1*]

[1]Department of Mathematics, Faculty of Science King Mongkuts University of Technology Thonburi Bangkok, Thailand.

*Corresponding author. E-mail: tareerat@yahoo.com.

ABSTRACT

The significance of iron rolling production is temperature control in the reheating furnace. The problem is that if the temperature in the furnace is overheat during production plan of iron, it cause excessive energy consumption. Moreover, the experience – based adjustment of the worker may affect to the change physical of characteristics of the furnace which directly effect to the quality of the product. In this study, we apply mathematical model to express the behavior of the change of temperature in furnace, estimate and compare the parameters of the mathematical model by using Levenberg Marquardt algorithm and Nelder - Mead algorithm. The results show that although the error from both algorithms are not different but the performance of the Levenberg Marquardt algorithm is better than Nelder - Mead algorithm due to the cost of computational.

Keywords: Reheating furnace Pusher type, Levenberg Marquardt algorithm, Nelder - Mead algorithm

1. INTRODUCTION

The iron rolling industry is important in the manufacture of iron especially in construction business. The factory A have a 24 hours production plan which will proceed as follows : the production started from 08.00 a.m. and ceased production during 06.30 p.m. - 09.30 p.m. due to the high cost of electricity and reducing the fuel, which is one cost of production, but there is still working to prepare for production at 09:30 p.m. For heating process the factory uses the reheating furnace pusher type to make the steel soft and easy to iron. The structure of reheating furnace pusher type consists of three zones as shown in figure 1. The first is the preheating zone which is responsible for removing moisture from the iron. The next zone is the heating zone. In this zone, there are 6 burners which serve directly heat the iron around 1120 - 1200 degrees Celsius. And the last zone is soaking zone. There are also 6 burners like heating zone. The temperature in this zone is around1150-1250 degrees celsius.

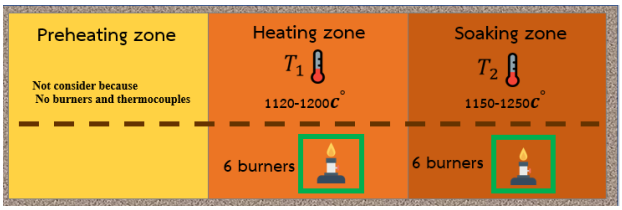

Figure 1. Reheating furnace Pusher type [4].

The process of reheating furnace pusher type divided into 3 processes which are the iron rolling process, which will be working during 08.00 a.m. – 06.30 p.m. After that, it will be reheating furnace process consume time during 06.30 p.m. – 09.00 p.m. In 09.00 p.m. – 09.30 p.m., it is accelerating process for the steel ready for the iron rolling. The process is shown in figure 2.

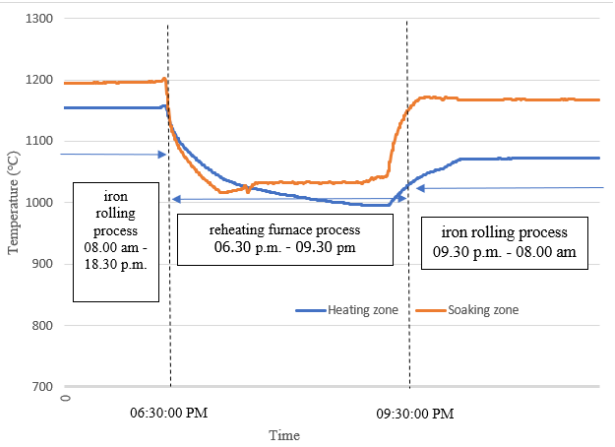

Figure 2. The process of reheating furnace pusher type.

The problem is that the temperature inside the reheating furnace overheats before 09.30 p.m. that causes energy consumption. In 2010 Srisertpol J. et. al. studied the mathematical model in the state-space model of reheating furnace walking hearth type to design open or close burners with the desire heating curve up. In 2012 Pongam T. et al used genetic algorithm to estimate the parameter of the reheating furnace from fuel flow rate and temperature response. In 2018 Silaon S. and Wongsrisai S. applied the mathematical model of reheating furnace pusher type and simulated the system of reheating furnace to find the setting temperature in soaking zone. The result was that the appropriate temperature of the soaking zone should be 950 □ to 1150 □ at 9.30 pm. The reheating furnace pusher type has been used for a long time which affects the temperature control within the reheating furnace and the parameters used in the mathematical model to control the temperature have been a change. In this work, we study the mathematical model of reheating furnace pusher type and applied Levenberg Marquardt algorithm and Nelder - Mead algorithm to estimate the parameters according to the actual temperatures to compare the performance in reheating furnace process.

2. MATHEMATICAL MODEL AND METHODS

The mathematical model used in this work based on the basic heat transfer theory S. Silaon and S. Wongsrisai was applied the mathematical model[4] to the furnace as shown in figure 3.

Zone 1 – Heating zone

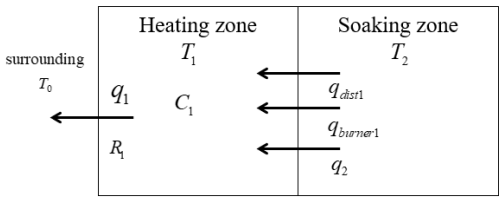

Figure 3. The thermal system at heating zone.

The mathematical model described the thermal system at heating zone can be written as equation (1)

$$C_1 \frac{dT_1}{dt} = q_2 + q_{dist1} - q_1 + q_{burner1}. \quad (1)$$

Mathematical formula for the thermal resistance of heat flow rate between heating zone and surrounding can be written in equation (2)

$$q_1 = (T_1 - T_0)\frac{1}{R_1}. \quad (2)$$

And the thermal resistance of heat flow rate between heating zone and soaking zone can be described in equation (3)

$$q_2 = (T_2 - T_1)\frac{1}{R_2}. \quad (3)$$

The equation of combustion is shown in equation (4)

$$q_{burner1} = N_1 vLHV, \quad (4)$$

where

C_1 is thermal capacitance at zone 1,

q_1 is heat flow rate at zone 1,

q_2 is heat flow rate at zone 2,

q_{dist1} is disturbance of heat flow rate at zone 1,

$q_{burner1}$ is the heat flow rate of combustion at zone 1,

R_1 is thermal resistance at zone 1,
R_2 is thermal resistance at zone 2,
T_1 is temperature at zone 1,
T_2 is temperature at zone 2.
N_1 number of burners that open in zone 1,
v is volume flow rate, and
LHV is lower heating value.

Zone 2 – Soaking zone

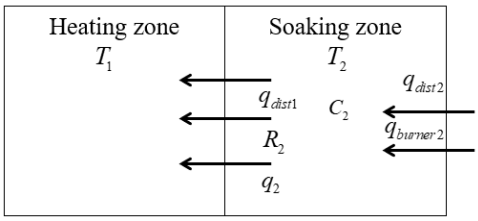

Figure 4. The thermal system at soaking zone.

The mathematical model described the thermal system at soaking zone can be written as equation (5)

$$C_2 \frac{dT_2}{dt} = q_{dist2} + q_{burner2} - q_2. \qquad (5)$$

And the equation of combustion is shown in the equation (6)

$$q_{burner2} = N_2 vLHV, \qquad (6)$$

where
C_2 is thermal capacitance at zone 2,
q_{dist2} is disturbance of heat flow rate at zone 2,
$q_{burner2}$ is the heat flow rate of combustion at zone 2,
N_2 number of burners that open in zone 2.

We simplify the equation (1) and equation (5) as follows

$$\frac{dT_1}{dt} = bT_2 - (a+b)T_1 + aT_0 + m \qquad (7)$$

$$\frac{dT_2}{dt} = cT_1 - cT_2 + n, \qquad (8)$$

where

$$a = \frac{1}{C_1R_1}, b = \frac{1}{C_1R_2}, c = \frac{1}{C_2R_2}, m = N_1 vLHV + q_{dist1},$$
$$n = N_2 vLHV + q_{dist2}.$$

In practice we cannot find the parameters that are a, b, c, m and n , so we have to compute the parameters by using optimization technique. We estimate the above parameters by using Nonlinear least square method – Levenberg Marquardt algorithm and pattern search method – Nelder-Mead algorithm. The objective function is to minimize the sum of residual errors of temperature between data and model as shown in equation (9)

$$e_w = \sum_{i=1}^{N} \left[T_w(i) - \tilde{T}_w(i) \right]^2, \qquad (9)$$

where N is total number of data, w is number in each zone that is w = 1, 2. T_w is actual temperature from the reheating furnace and $\tilde{T}_w$ is the temperature from mathematical model of reheating furnace.

2.1 Levenberg Marquardt algorithm [5,8]

Levenberg Marquardt algorithm is used to solve nonlinear least squares problems. The Levenberg Marquardt algorithm is a modified Gauss-Newton method to avoid the Hessian matrix as singular matrix. This method is a combination of two methods: the gradient descent and the Gauss-Newton. From equation (9), we get

$$\text{Minimize } g(z) = \sum_{t=1}^{N} \left[T_w(z_t) - \tilde{T}_w(z_t) \right]^2.$$

Let $z_k = [a_k, b_k, c_k, m_k, n_k]^t$ where k is the number of iteration update by the algorithm as follow,

$$z_{k+1} = z_k + s_k$$
$$s_k = -(J^T(z_k)J(z_k) + \lambda_k I)^{-1} J(z_k) g(z_k) \qquad (10)$$

where J is Jacobian matrix of objective function.

In equation (10) the value λ is a positive value named the damping parameter. If the λ is a large value, the Levenberg Marquardt algorithm is the gradient descent method. This is a good strategy when the current solution is far from the minimum. On the other hand, if λ is a small value, the Levenberg Marquardt algorithm is the Gauss-Newton method. This is a desired behavior for the final steps of the algorithm since, near the minimum, the convergence of the Gauss-Newton method can be almost quadratic. So, λ affects the length and direction of the solution. Consequently, the λ adjustment of the details is as follows, if λ improve objective function then the step(s_k) is applied and λ is divided by a constant (with general). On the other hand, if increases of the cost function, the step is rejected and is multiplied by . This is the basic strategy for updating the damping parameter. The algorithm of the Levenberg Marquardt algorithm is shown in figure 5.

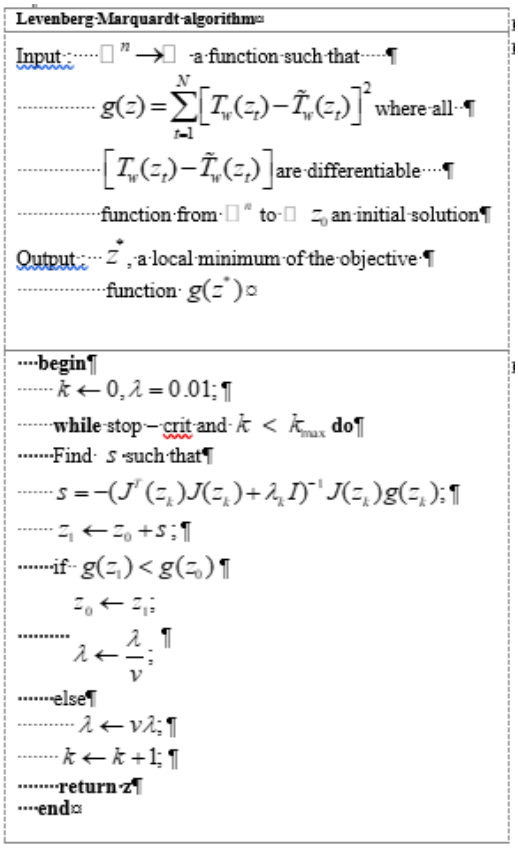

Figure 5. The Levenberg Marquardt algorithm [8]

The stopping criteria of the algorithm will stop as follow conditions:

- The number of iteration actualized by the algorithm attains the maximum iteration. The maximum iteration is 100 iterations.
- The function tolerance or parameter tolerance is 1×10^{-3}

2.2 The Nelder - Mead algorithm [6,8]

The Nelder-Mead method is a heuristic optimization technique to solve unconstrained optimization problem. This algorithm is based on the iterative update of a simplex. The method relies on the comparison of function values at the n+1 vertices of a general simplex (polytope of dimension n+1). As instance, one dimensional simplex is a line, in two dimensions, the simplex is a triangle and in three dimensions, it is a tetrahedron. The algorithm progresses iteratively while replacing the worst vertex (with the highest cost value) by another projected point.

The projected point is determined by one of the following operators: reflection, expansion and contraction. Constants α, γ and β are the reflection, expansion and contraction coefficients respectively. So, we want to minimize the function as follow,

$$\text{Minimize } g(x)=\sum_{t=1}^{N}\left[T_w(x_t)-\tilde{T}_t(x_t)\right]^2$$

Let x_0 be an initial solution where $x_0=[a_0,b_0,c_0,m_0,n_0]$, h be the index of the 'worst vertex' where $x_h=[a_h,b_h,c_h,m_h,n_h]$ and l be the index of the 'best vertex' where $x_l=[a_l,b_l,c_l,m_l,n_l]$.

The transform of the Nelder - Mead algorithm can show in figure 6.

Nelder - Mead search algorithm

Input : $f:\mathbb{R}^n \to \mathbb{R}$ the cost function

x_0 an initial solution

Output : x^*, a local minimum of the cost function $g(x)$

begin

$k \leftarrow 0,\ \alpha = 1, \gamma = 2, \beta = \frac{1}{2}$;

while stop-crit **and** $(k < k_{max})$ **do**

$h \leftarrow \arg\max_i g(x_i)$;

$l \leftarrow \arg\min_i g(x_i)$;

$x' \leftarrow (1+\alpha)\bar{x} - \alpha x_h$;

if $g(x') < g(x_l)$ **then**

$x'' \leftarrow (1-\gamma)\bar{x} - \gamma\bar{x}$;

if $g(x'') < g(x_l)$ **then**

$x_h \leftarrow x''$;

else

$x_h \leftarrow x'$;

else if $g(x') > g(x_k), \forall k \neq h$ **then**

if $g(x') \leq g(x_h)$ **then**

$x_h \leftarrow x'$;

$x'' \leftarrow \beta x_h + (1-\beta)\bar{x}$;

if $g(x'') > g(x_h)$ **then**

$x_k \leftarrow \frac{x_k + x_l}{2}$;

else

$x_h \leftarrow x''$;

else

$x_h \leftarrow x'$;

$k \leftarrow k+1$;

return x_l

end

Figure 6. The Nelder - Mead search algorithm [8].

3. RESULTS AND DISCUSSION

The experiment was divided into 3 experiments with different initialization which are result1 with $T_1(0) = 932, T_2(0) = 1052$, result2 with $T_1(0) = 934, T_2(0) = 1055$,and result3 with $T_1(0) = 936, T_2(0) = 1053$. We will estimate the parameter by using non-linear least squares method – Levenberg Marquardt algorithm and Nelder - Mead algorithm with 3 datasets calculated by MATLAB Simulink on ASUS Intel Core(TM) i7-6700HQ CPU @ 2.60 GHz 2.59 GHz. The error is calculated by using the formula $\sqrt{\frac{1}{N}\sum_{i=1}^{N}\left(T_w(i) - \tilde{T}_w(i)\right)^2}$. The result can be shown in the Table 1.

Table 1. The parameters and error from Levenberg Marquardt algorithm and Nelder – Mead search method

PARAMETERS	NON – LINEAR LEAST SQUARE - LEVENBERG MARQUARDT ALGORITHM			PATTERN SEARCH NELDER – MEAD SEARCH METHOD		
	RESULT1	RESULT2	RESULT3	RESULT1	RESULT2	RESULT3
a	0.0825	0.14272	0.20282	0.085049	0.14328	0.20832
b	0.06929	0.58145	0.50403	0.073484	0.58247	0.53754
c	0.19734	0.38333	0.3369	0.19773	0.38226	0.34214
m	11.485	8.0874	19.659	11.772	8.1498	19.671
n	6.0162	10.68	9.4608	6.0268	10.652	9.5926
Error in zone 1	1.0742	3.5210	2.4703	1.0884	3.5254	2.4542
Error in zone 2	2.7279	5.3613	4.7919	2.7199	5.3575	4.8087
Time (seconds)	109	103	78	1079	1409	1329
Number of iteration	9	9	9	21	21	31

The temperature response in Heating zone and Soaking zone between the measurement temperature and the temperature response by using Levenberg Marquardt algorithm and The Nelder - Mead algorithm is shown in figure 7 and figure 8, respectively.

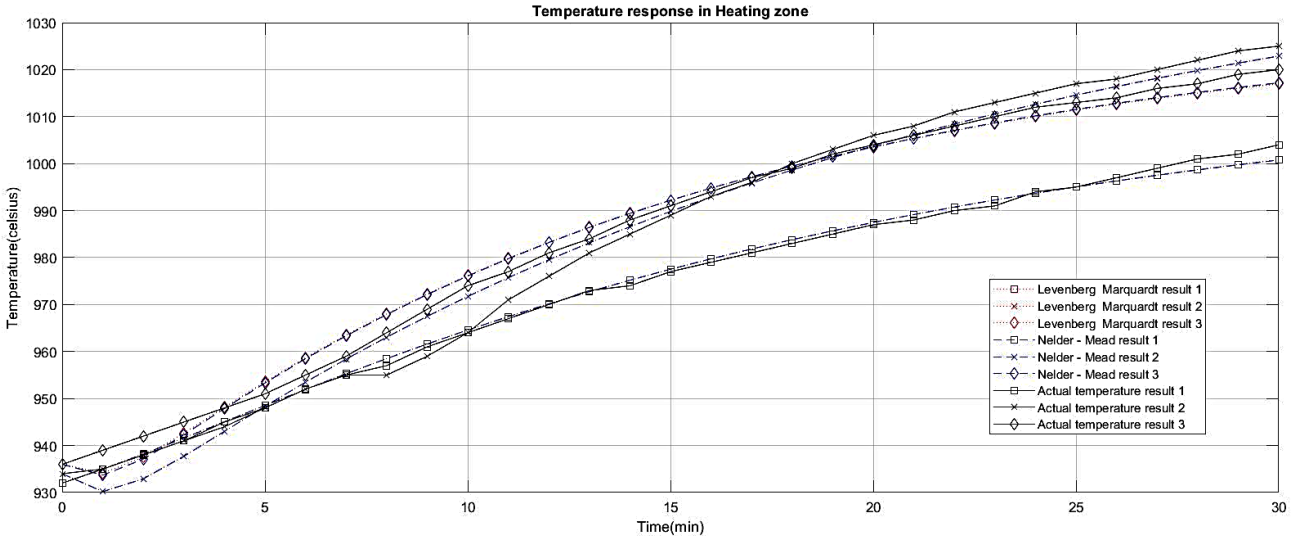

Figure 7. Temperature response in heating zone in each results.

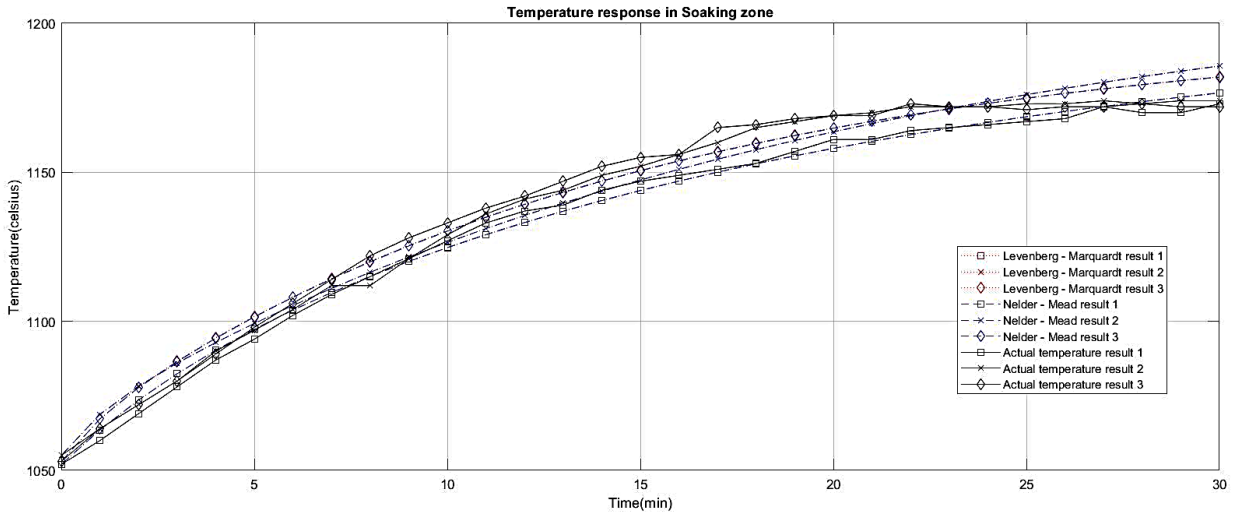

Figure 8. Temperature response in soaking zone in each results.

The results show that the temperature response obtained from the Levenberg Marquardt algorithm and the Nelder - Mead algorithm is slightly different. The number of iteration and the time of calculation of the Levenberg Marquardt algorithm are less than the Nelder - Mead algorithm. Due to the Levenberg Marquardt algorithm need to compute the derivative of the objective function to find the direction search in an orderly way with the principle of finding. Meanwhile, the Nelder-Mead algorithm does not need to compute the derivative of the objective function for the direction search because the Nelder - Mead algorithm uses random search direction.

4. CONCLUSIONS

In this work, we demonstrate the parameter estimation method of reheating furnace pusher type by using the Levenberg Marquardt algorithm and the Nelder - Mead algorithm to compare the response temperature from the mathematical model. The results show that the mathematical model of reheating furnace pusher type from the response temperature provide slightly different the response temperature. The Levenberg Marquardt algorithm is efficient in the calculations to fast converge to the optimal solution.

5. ACKNOWLEDGMENTS

The authors would like to thank the Science Achievement Scholarship of Thailand (SAST) and department of Mathematics, Faculty of Science, King Mongkut's University of Technology Thonburi for the support of research.

6. REFERENCES

[1] Iron and Steel Institute of Thailand. Energy Efficiency Assessment of Reheating Furnace 2010; 6

[2] J. Srisertpol, S. Tantrairatn, P. Tragrunwong, and V. Khomphis , Temperature control for reheating furnace walking hearth type in heating curve up process. World Scientific and Engineering Academy and Society 2010;464-9.

[3] T. Pongam, J. Srisertpol and V. Khomphis, Manufacturing process identification for the reheating furnace walking hearth type using genetic algorithm, International Journal of Modeling and Optimization, 2012:2:114-8.

[4] S. Silaon and S. Wongsrisai. Temperature Control for Reheating Furnace in Heating Curve Up Process at On Peak [dissertation] Thailand: King Mongkut's University of Technology Thonburi; 2018.

[5] D. Ramadasan, M. Chevaldonné, and T. Chateau. Lma: A generic and efficient implementation of the levenberg– marquardt algorithm. Software: Practice and Experience 2017.

[6] S. Singer and J. Nelder. Nelder-Mead algorithm. Scholarpedia 2009;4:2928.

[7] A. K. Al- Othman and K. M. El- Nagger. Application of pattern search method to power system security constrained economic dispatch, World Academy of Science, Engineering and technology 25 2007;28-33.

[8] F. Brunet. Contributions to Parametric Image Registration and 3D Surface Reconstruction [dissertation] Dept. Computer Science Universite d'Auvergne 2010:30-4

CreTech 2020
8th International Conference on Creative Technology
Multidisciplinary
to Drive Economy and Social
http://utkcretech.rmutk.ac.th

Effects of Trailing Edge Modification on the Performance of the S1223 Airfoil

Supakit Worasinchai[1*]

[1]Renewable Energy Laboratory, Materials for Energy Research Group,
National Metal and Materials Technology Center, Pathum Thani, Thailand, 12120
*Corresponding author. E-mail: supakitw@mtec.or.th

ABSTRACT

The paper presents wind tunnel investigations of the effects of trailing edge modification on the performance characteristics of the S1223 airfoil. The investigation was examined through the measurement of static surface pressure, lift, and drag coefficients at three different Reynolds numbers of 62,000, 83,000, and 133,000. The investigation revealed that the trailing edge modification basically reduces the adverse pressure gradient on the suction surface and increases the static surface pressure on the pressure side. This leads to a higher pressure difference, contributing to a higher lift coefficient. With a less severe pressure recovery on the suction surface, the stall is postponed to a higher incidence angle. Nevertheless, the modification also induces a drag penalty, causing a reduction in performance. At the lowest Reynolds number investigated, while the maximum lift coefficient was 1.2 at a stall angle of 12^o, the modification increased the lift coefficient to 1.663 at a stall angle of 20^o. The lift-to-drag ratio however decreased from 7.65 to 6.6 at the incidence angle of zero and continued over the incidence range. The investigation of the lift-to-drag ratio indicates that the drag penalty is less pronounced when the operating Reynolds number is significantly high. At the highest Reynolds number the lift-to-drag ratio increased to a maximum value of 28.1 compared to that of 7.52 in the S1223 case.

Keywords: S1223 airfoil, Trailing edge modification, Performance characteristics, Low Reynolds number

1. INTRODUCTION

The airfoil performance is one of the crucial parameters in the turbomachinery design. In wind turbine application, it plays an important role in converting kinetic energy in the wind stream to mechanical energy which is further transmitted to a generator to produce electricity. A suitable design or selection of the airfoil section is then critical and possess a significant impact on the overall performance of the wind turbine [1].

The Darrieus vertical axis wind turbine has a potential in electricity generation as its performance is comparable to the horizontal axis wind turbine counterpart [2-3]. Performance analysis of this type of turbine by Worasinchai et al [4] had indicated that the operation of the airfoil when rotates around its vertical axis is analogous to the flapping mechanism that birds employ to fly. It is then interesting to examine how a bird-like airfoil behaves as it might be beneficial in improving the performance of this type of turbine.

The S1223 airfoil is a high-lift airfoil section that was designed by Selig and Guglielmo [5]. It was designed by employing both concave pressure recovery and aft-load to create large pressure difference between suction and pressure surface. This results in a highly

cambered airfoil with a sharp trailing edge (Fig 1). Its thickness and camber are 12.1% and 8.7%, respectively A measurement of bird wings by Liu et al has shown that its shape is closely resemble with a seagull wing [6].

Figure 1. Seagull wing and the S1223 airfoil

Performance testing of this airfoil was conducted by Selig [5] at a Reynolds number of 200,000 had shown that the airfoil exhibits a high lift value of 2.2 which is 30% higher than the Fx63-127 airfoil. Experiments also show that the s1223 airfoil exhibits a severe adverse pressure gradient and its performance is expected to degrade when operating at lower Reynolds numbers. This behavior is however not considered to be appropriate in the Darrieus wind turbine application as the turbine operates with a wide range of Reynolds number and incidence angle. A small modification might be applied to overcome this characteristics.

Apart from designing a new airfoil, it is common to make a small modification to the existing airfoil to improve its performance. One of the available modifications is trailing edge modification proposed by Standish and van Dam [7]. The modification will make the airfoil trailing edge blunt by adding thickness which is defined as thickness-to-chord ratio (t/c) (Fig. 2). The additional thickness is then added on either sides of the camber line to obtain the blunt trailing edge version of the airfoil. A number of testing on this blunt modification has indicated that the t/c ratio should not be too high or a degradation of the performance might be expected [8-9].

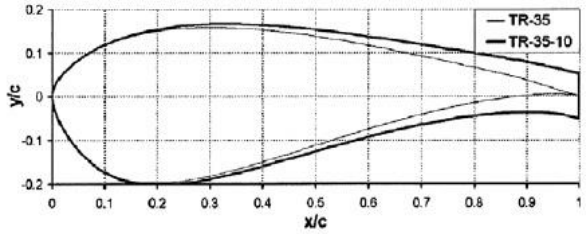

Figure 2. Blunt trailing edge modification [8]

This paper investigates the feasibility of applying the blunt trailing edge modification to the S1223 to improve its performance at three low Reynolds numbers through wind tunnel measurements of pressure, lift, and drag coefficients. The investigations are made at three different Reynolds numbers of 62,000, 83,000, and 133,000 which is a normal operating Reynolds number range of the small urban wind turbines [10].

2. THE AIRFOIL MODELS

The S1223 airfoil model was fabricated from fullcure 720 material by rapid prototyping technique, resulting in a high surface precision (±0.1mm). It has a chord of 110mm and a span of 457mm to fit with the tunnel test section. The model was equipped with a stud that spans over the entire model. One end of this stud was connected to an electronic force balance (Fig. 3).

The model also has a number of holes which are connected to a series of tube on the other end. These tubes were then connected to a scannivalve and a pressure transducer.

Figure 3. Airfoil model

The t/c ratio of the blunt trailing edge modification was chosen to be 5% t/c and its shaped is depicted in Figure 4. It was fabricated using the same technique. It is noted as S1223B in this study.

Figure 4. S1223B

3. WIND TUNNEL AND MEASUREMENT

The wind tunnel employed in this testing is a jet type tunnel. It has a square cross-section of 457 x 457mm (Fig. 5). It also has solid sides but open top and bottom to avoid blockage effects when testing at high incidence angles [10].

Figure 5. Wind tunnel and force balance

The airfoil model was attached to the test section at the middle. Its shaft was attached to a force balance that used to measure lift and drag forces. On the other end, a series of tubes are connected to a scannivalve and a pressure transducer to measure static surface pressure over the airfoil surface (Fig. 6).

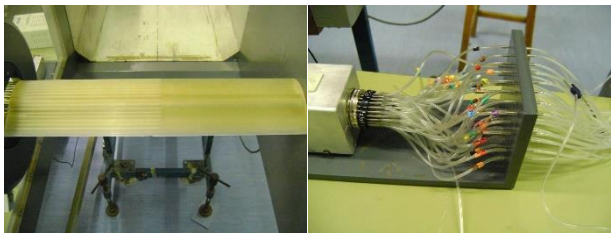

Figure 6. Surface pressure measurement

In testing, the wind tunnel was controlled by an inverter to set fequency and wind speed. The tested wind speeds were 9, 12, and 20 m/s, resulting in Reynolds number of 62,000, 83,000, and 133,000 which is an operating Reynolds number range in small urban wind turbine applications. In force measurements, the airfoils was set at an incidence angle of 0^o and then increased every 2^o up to an incidence angle of 30^o as suggested by [5].

A computer-based system was used to record all pressure and force signals via an NI USB-6218 ADC consisting of 16 channels with a resolution of 16 bits. This device has a sample rate of up to 250 kS/s.

4. RESULTS AND DISCUSSION

4.1 The S1223 Performance

Lift and drag coefficients of the S1223 is presented in Figure 7. It can be seen from the figure that the airfoil exhibits high lift properties and the highest lift coefficient is 1.644 at the Reynolds number of 133,000 and stalls at an incidence angle of 20. As the Reynolds number decreases, the maximum lift coefficient is reduced and stall will occur at a lower incidence angle. At the lowest tested Reynolds number of 62,000, the maximum lift is 1.2 and stall occurs at 12°.

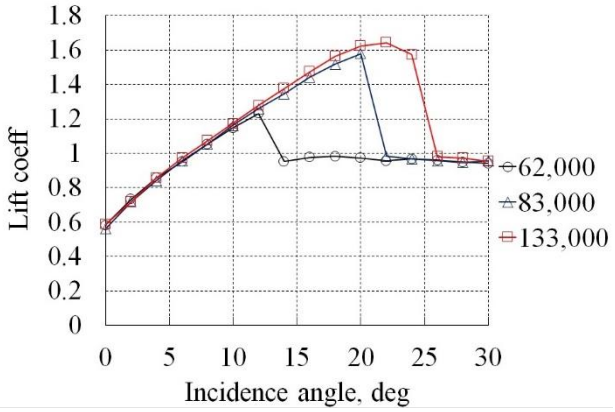

Figure 7. Lift coefficients

Surface pressure measurements reveal that the S1223 demonstrates the presence of the laminar separation bubble (Figure 8). It can be observed that the bubble progresses upstream with increasing incidence angle and the stall is caused by bubble bursting, leading to an abrupt stall.

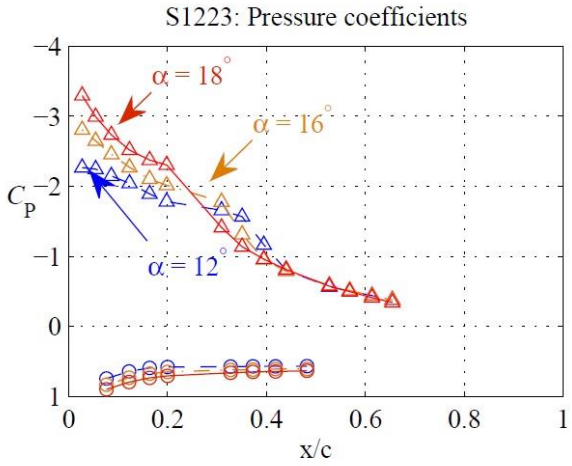

Figure 8. Surface pressure coefficients: S1223

In terms of drag, the S1223 airfoil exhibits a relatively high drag at a zero incidence angle (approximately 0.07). The drag increases with the increasing incidence angle and the drag coefficient will be around 0.55 at the incidence angle of 30° (Fig. 9).

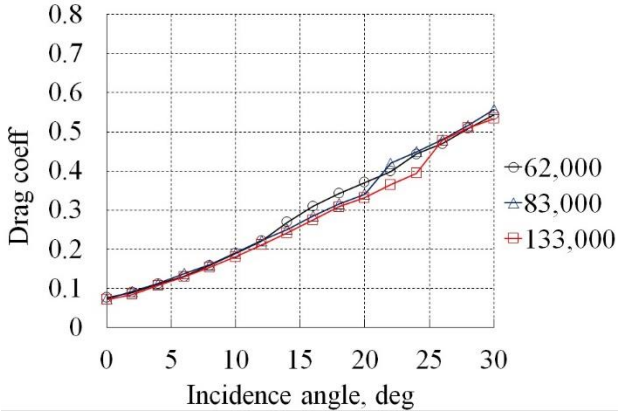

Figure 9. Drag coefficients

4.2 The S1223B performance

Lift coefficients of the S1223B airfoil are presented in Figure 10. It can be seen that lift coefficients of this airfoil is less sensitive to Reynolds number change. The maximum values of lift coefficients are 1.663, 1.755, and 1.756 at Reynolds number of 62,000, 83,000, and

133,000, respectively. The stall incidences angles are 20º, 22º, 22º.

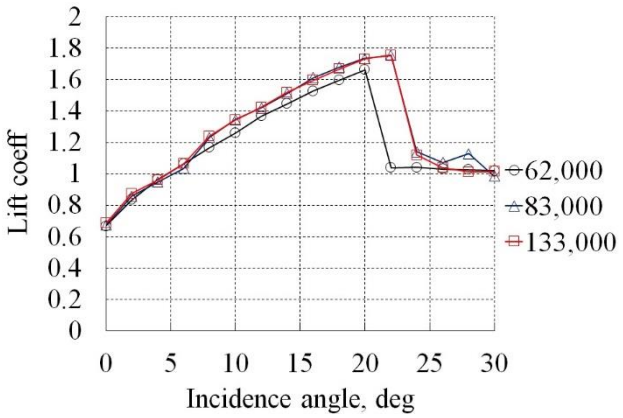

Figure 10. Lift coefficients: S1223B

Static pressure measurements reveal that this modification alters the flow on both suction and pressure surfaces (Fig. 11 and 12). It can be observed that the S1223B exhibit a lower suction peak at the leading edge. With the trailing modification, the adverse pressure gradient is less severe and the separation bubble occurs further downstream.

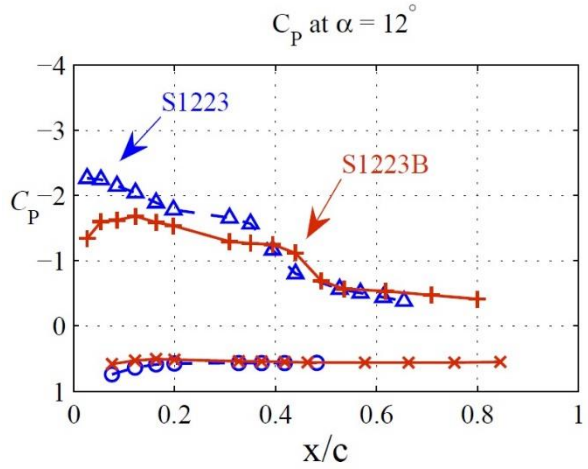

Figure 11. Surface pressure coefficients at an incidence angle of 12º

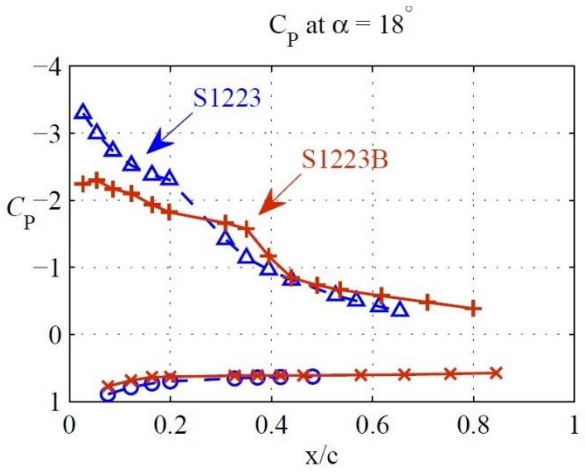

Figure 12. Surface pressure coefficients at an incidence angle of 18º

In terms of drag, the S1223B airfoil exhibits the same pattern as seen in the S1223 case with a small increase in base drag (approximately 0.10) (Fig. 13). This drag increases with increasing incidence angle and the drag coefficient will reach a value of 0.54 at the incidence angle of 30º. It is interesting to note however that, at the highest Reynolds number of 133,000, the drag coefficient decreases when the incidence angle is lower than 8º.

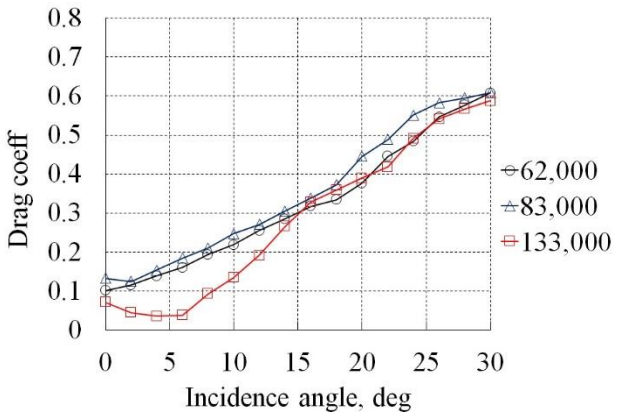

Figure 13. Drag coefficients: S1223B

A comparison of lift-to-drag ratios of both airfoils shows that, although the modification will increase the lift value of the airfoil, the drag coefficient also increases and the lift-to-drag ratio will not always beneficial. At the low Reynolds number of 62,000, the S1223B exhibits a lower lift-to-drag ratio at low incidence angle range between 0^o to 10^o. After this point, the lift-to-drag ratio of the S1223B is higher than that of the S1223 and this is mainly because of its high lift property. In contrast, the effect of trailing edge modification provide a benefit at a high Reynolds number of 133,000. At this Reynolds number, the flow has a higher kinetic energy to overcome the blunt trailing edge and instead of generating vortex the flow will bend over the trailing edge just like the flow observed for a Gurney flap [10].

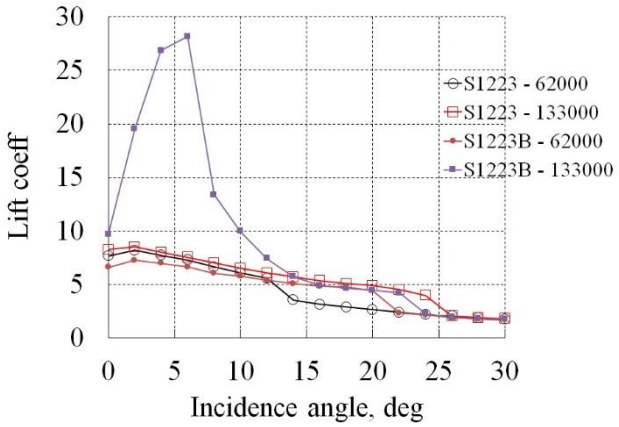

Figure 13. Lift-to-drag coefficients

4.3 The underlying flow physics

The underlying flow physics of this beneficial behavior is anticipated to be similar to that which is observed for a Gurney flap and on an inverted strip (Fig. 15). The Gurney flap is a short flat plate attached to the trailing edge on the pressure side of the airfoil. The inverted strip is basically the Gurney flap that is attached on the suction side.

Basically, the addition of the Gurney flap will induce the flow to accelerate over the suction surface and to decelerate on the pressure surface, causing a downward deflection (flow turning) at the trailing edge (it is also viewed as an effective camber as it shifts wake deficit to lie downward) (Fig. 15). The addition of an inverted strip on the suction side will result in an opposite effect and will produce an upward deflection.

The blunt trailing edge modification which adds thickness symmetrically to the camber line can then be viewed as an addition of both the Gurney flap and the strip on both surfaces and this effectively decelerates the flow on both sides (as indicated by the reduction of pressure peak on the both surfaces (at around 0.1c, Fig. 11).

The addition of the thickness also reduces the adverse pressure gradient that the flow has to overcome on the suction side. The flow then separates further downstream (0.3c in comparison to 0.2c for the S1223 case at the incidence angle of 12°, Fig. 11). This modification also produces a larger pressure difference between suction and pressure surfaces near the trailing edge (from 0.5c to 1c). The presence of a separation bubble and its movement towards the leading edge when the incidence is increased indicates that the stall is caused by bubble bursting.

With this flow behavior, the blunt trailing edge modification will always increase the base drag of the airfoil and lift-to-drag ratio will not always increase. The true benefit of applying the modification will happen when the t/c ratio is not too large at the required operating Reynolds number range. For this study, a further reduction of the t/c ratio would be more beneficial if it has to be applied for the Darrieus wind turbine that operates at low rotational speeds where its operating Reynolds number is comparatively low.

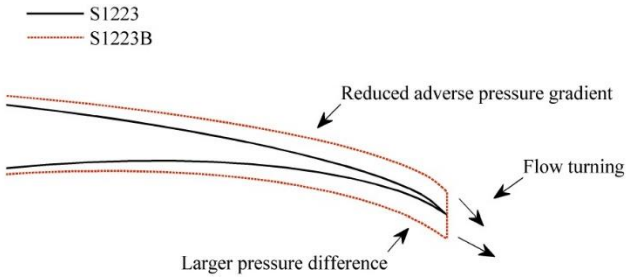

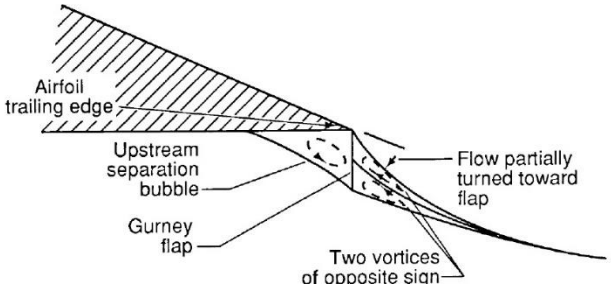

Figure 15. Flow physics

5. SUMMARY

The effect of trailing edge modification on the performance of the S1223 airfoil section was investigated in this paper and the following conclusions are drawn:

5.1 The blunt trailing edge modification affects the flow over the airfoil and alters surface pressure on both suction and pressure surfaces. A formation of the laminar bubble then occurs downstream.

5.2 The modification leads to a less severe pressure recovery on the suction surface and the presence of the separation is moved further downstream, leading to a delay of stall.

5.3 It also increases the pressure on the pressure side, creating a large pressure difference and hence a higher lift value. The high lift values increase at all Reynolds number investigated. At the highest Reynolds number of 133,000, the lift coefficient is increased to 1.756 and the stall occurs at an incidence angle of 22°, compared to those of 1.64 and 20°, respectively.

5.4 With the less severe pressure recovery generated by the modification, the S1223B airfoil is less sensitive to Reynolds number change.

5.5 The modification makes the S1223B blunter and its base drag is increased over the incidence range.

5.6 In terms of the lift-to-drag ratio, the modification will not significantly improve the airfoil performance at the low Reynolds number as the base drag is high. A more benefit occurs at a higher Reynolds at which the lift-to-drag ratio of the S1223B section increases up to a value of 28.1 compared to that of 7.52 of the S1223 section.

6. REFERENCES

[1] Tangler JL, Somers DM. NREL Airfoil Families for HAWTs. National Renewable Energy Laboratory, NREL/TP-422-7109, JAN 1995.

[2] Sheldahl RE. Comparison of field and wind-tunnel Darrieus wind-turbine data. SAND80-2469, Sandia National Laboratory, 1980.

[3] Sheldahl RE, Blackwell BF. Free-air performance tests of a 5-metre-diameter Darrieus turbine, SAND-77-1063, Sandia National Laboratory, 1977.

[4] Worasinchai S, Ingram GL, Dominy, RG. The Physics of H-Darrieus Turbines Self-Starting Capability: Flapping-Wing Perspective. ASME Turbo Expo 2012.

[5] Selig MS, Guglielmo JJ. High-Lift Low Reynolds Number Airfoil Design J Aircraft 1997; 34(1):72-79.

[6] Liu T, Kuykendall K, Rhew R, Jones S. Avian Wings. Proceedings of the 24th AIAA Aerodynamic Measurement Technology and Ground Testing Conference 2004.

[7] Standish KJ, van Dam CP. Aerodynamic Analysis of Blunt Trailing Edge Airfoils. ASME J Solar Energy Engineering, 2003, 125:479-487.

[8] van Dam CP, Kahn, DL. Trailing Edge Modifications for Flatback Airfoils. SAND2008-1781, 2008.

[9] Baker JP, Mayda EA, van Dam CP. Experimental Analysis of Thick Blunt Trailing- Edge Wind Turbine Airfoils. ASME J Solar Energy Engineering, 2006, 34(1):72-79.

[10] Worasinchai S. Small Wind Turbine Starting Behaviour. PhD Thesis, School of Engineering and Computing Sciences, Durham University, 2012.

CreTech 2020
8th International Conference on Creative Technology
Multidisciplinary
to Drive Economy and Social
http://utkcretech.rmutk.ac.th

Simulation applied modeling for solving layout design

Suphatra Kritwattanakorn[1*], Phacharadit Paengchit[1], Tinno Kwandee[1]

[1] Department of Production Engineering, Faculty of Technical Education.
Rajamangala University of Technology Krungthep, Thailand.
*Corresponding author. Tel: 0 2287 9600 (7056), E-mail: suphatra.k@mail.rmutk.ac.th.

ABSTRACT

Currently, the industry has many processes related to the production system because each product has complex parts or components, materials and methods of production. The basic technique principally used in improving manufacturing competitiveness is layout management. Therefore, this paper investigates problem into industrial workstation design and layout in manufacturing process. The format of the station consists of several workstations and rectangular shape is fixed width and length to make feasible work. The objective of a facility layout problem has been to minimize total distances of the manufacturing system. Genetic algorithm (GA) was used in this study, that are used to solving the layout for manufacturing effectiveness while simulation serves as a system performance evaluation tool. The paper illustrates the performance of the algorithm and show that genetic algorithm provides accurate results in minimizing total distances. Finally, the results showed that the total machine layout distance can be reduced from 38.45 meter to 19.62 meter.

Keywords: Genetic Algorithm (GA), Machine Layout, Facility Layout

1. INTRODUCTION

An industry has processing lines and sometimes various products. Each product has its own operational steps, workstations, and conditions, which is different from others. Manufacturing system has to be managed for maximizing efficiency. The workstations are arranged to suit operations. Therefore, the arrangement of devices and machines is one of the basic requirements in designing a flexible manufacturing system. A proper design of such a system will result in smooth operations and reduced total distances. This kind of activity was called facility layout problem or machine layout problem. A number of parameters involved and sequences of operations make this problem intrinsically difficult.

Genetic algorithm (GA) is an adaptive heuristic search algorithm based on the ideas of natural selection and genetics evolution. Solutions of problems can be searched and exploited randomly within a known space [4]. GA is not a new tool for machine layout problems. It has been applied broadly. Datta, Amaral, and Figueira [1] used it for arranging a number of facilities on a line with minimum cost which this problem was called single row facility layout problem (SRFLP). Facilities sizes of 60 to 80 had been arranged effectively. Sadrzadeh [2] also utilized GA to solve the facility layout problem (FLP) in a manufacturing system. Matrix encoding technique was used for the chromosomes, facilities were grouped, thus, total material handling cost of multi-line layout problem with the multi-products had been minimized. The proposed method can competently obtain the better solutions than CRAFT (Computerized relative allocation of

facilities technique) algorithm and the entropy-based algorithm. However, Srinivas et al [3] pondered that the solutions obtained from using GA may be influenced by various parameters such as, population size, number of generations, crossover rate, mutation rate, and the length of the block to be exchanged between parents to generate offspring's. Therefore, they suggested an approach called the sensitivity analysis to guideline to select the GA parameters. As a result, the quality of GA solutions can be practically improved.

There are many tools used for solving problems with GA. It was found that the most popular method is using MATLAB for a large layout. However, the source code of genetic algorithm is slightly difficult to apply and develop from the view of unskillful users who need to layout machines. Therefore, this study decided to utilize Microsoft Excel (MS Excel) to solve the problems. MS Excel spreadsheets are widely used and relatively easy to understand. The objective of this study was to solve facility layout problems in a limited working area by minimizing total distance of material handlings of a multi lines and multiproduct manufacturing system. The sets of solutions had been examined by adapting sensitivity analysis method.

2. METHODS

Genetic algorithm (GA) is a technique based on biological principles of evolution and it is an alternative useful tool for optimization. In this layout problem, machines in a manufacturing system will be the genes in a chromosome; the chromosome represents a layout in a specific area. A certain layout will have a total distance different from other layouts. Total distances calculated from the sum of distances of material handlings of all products. GA method starts with creating initial populations (initial chromosomes) by randomization. Later processes in GA approach consist of 2 processes: crossover and mutation. These are to create the new populations – the offspring. The new chromosomes will be created by selecting two chromosomes in the initial populations to be parents of later chromosomes. By mating parents called crossover process, there will be 2 new chromosomes. Another process to create the offspring is the mutation process. It can be done by choosing 2 genes in a chromosome of the initial populations and switch their positions. GA then is started over again at crossover and mutation processes. The processes will be stopped at a certain number of runs or optimized solution is found. GA helps generating possible solutions called population. Results calculated from each member of population are compared in order to find potential answers leading to optimization.

2.1 Initialization

Before starting GA, parameters involved should be encoded. Generally, the codes are in the forms of binary values (0, 1), alphabetical characters (A, B, C), or Arabic numbers (1, 2, and 3). In this study, the strings of genes were established as the characters. For example, in the assembly line of Furniture production, eight machines have been presented in a row (Fig. 1). The number of genes in chromosomes is equal to the number of machines

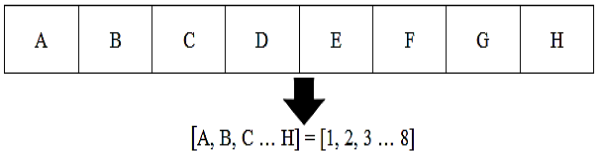

Figure 1. Coding of Genes.

All the machines have rectangular shape with different sizes and have been arranged in a limited area of working (length, L and width, W). It was assumed that the machines can be accessed from any directions. The distance

between a pair of machines was calculated from the centers of the machines. Besides, any machine was taken as there is a fixed gap (g) between each other [5], so there will be enough space for handling materials. Machine layout as in a row will be placed into the plan size L x W from left to right and up as shown in Fig. 2. Therefore, column width of the layout is referred to the biggest size of the machine in that column (Ci). Initial population is selected by randomization.

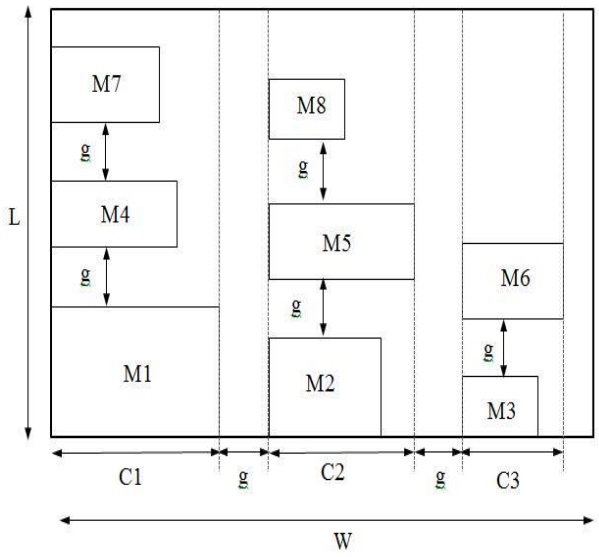

Figure 2. Machine Layout.

2.2 Selection

The chromosomes of the initial population are selected to be parents by the selection method. There are several methods of selection but one of the most popular is Roulette Wheel Selection (RWS) [6] which was also used in the study. An appropriate chromosome parents for the new population will be selected. In this purpose, minimizing total distances for machine layout problem was the aim. The objective function of this machine layout problem can be defined as following:

$$Z = \sum_{j=1}^{M}\sum_{i=1}^{M} f_{ij}d_{ij} \qquad (1)$$

Where M is the number of machines in layout problem fij is the frequency of trips between machines i to j dij is the distance between machines i to j

The value of the fitness function in the population can be calculated according to equation (1). Then rearrange of workstations process will start without time consideration in production scheduling. During execution of GA, the values fij has been unchanged because it was assumed that all products were required at the same amount. The value of dij based on the sizes of machines and layout and the total distance was calculated from equation (2).

Total distance = □ (**P1**+**P2**+**P3**) (2)

When P is the production routing, the sequences of operations of each products have been presented in Table 1.

2.3 Crossover

Crossover is the process to create new individual's representation from parts of population (see Fig. 3). The crossover process can be carried by randomly selecting point to be crossed from parent chromosomes. According to sensitivity analysis, layout designer specifies crossover probability (Pc) of genes. The cutting sections are exchanged to create new chromosomes called offspring.

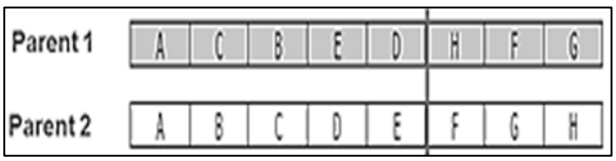

Next Step

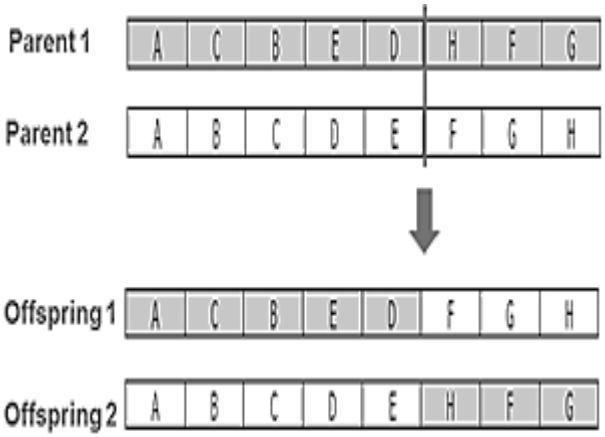

Figure 3.:Crossover process.

Two parents then were replaced by the offspring chromosomes. The total distances of all feasible chromosomes were computed. Then, if the offspring chromosomes deliver better solution than their parents, they will be move to the mutation process. Otherwise, new run will be start.

2.4 Mutation

Mutation process is changing structure of chromosomes by switching genes (Fig. 4). This is a genetic operator used to maintain genetic diversity from one generation in population of chromosomes to the next. The two positions are randomly selected and genes are swapped at these positions. According to sensitivity analysis, users specify mutation probability (P_m).

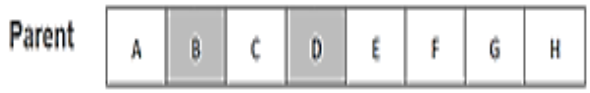

Next step **Random point**

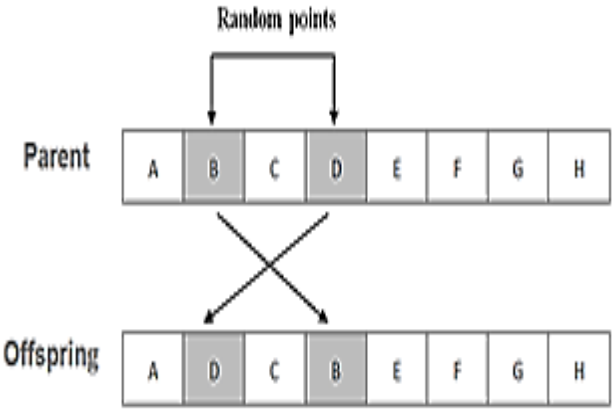

Figure 4. Mutation Process

3. RESULTS AND DISCUSSION

The proposed genetic algorithm method was used in order to layout machines for the assembly lines of particular sub-assemblies of furniture production in the area of 10m x 10m. Eight machines were consisted in the problem for analysis. The part lists and the production data suggested that there were 3 products with different production routings which were shown in Table 1. Production routings of products no.1, 2, 3 (P1, P2, P3) follow the routes of {A, B, C, D}, {A, E, F, G} and {A, H}, consequently. The sizes of the machines were presented in Table 2. Any machine was taken as there is a fixed gap of 1 m between each other. Initial layouts were set at 10 arrangements (population size = 10) by randomization. The problem was solved by programming VBA in Microsoft Excel 2010.

The intended method had been illustrated. The operation of the proposed GA was analyzed by comparing its result with those of current machine layout and Critical Path Method (CPM) [7]. The CPM of the activities was shown in Fig. 5.

Table 1: Part list and production data of the products.

Product	Production routing
1	A-B-C-D
2	A-E-F-G
3	A-H

Table 2: Dimensions of the machines.

Machine	Dimensions	
	Length (m)	Width (m)
A	2.00	2.00
B	1.30	1.35
C	1.35	1.25
D	1.35	1.30
E	1.22	1.25
F	1.00	1.00
G	1.22	1.25
H	1.20	1.22

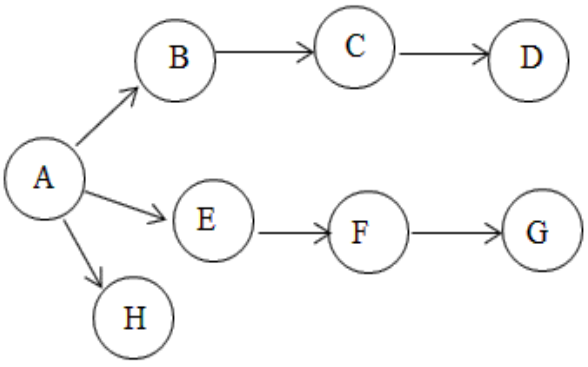

Figure 5. Network of critical path method (CPM).

Srinivas et al [3] suggested that for a small layout problem, Pc and Pm should be 0.7 and 0.4 respectively. However, for this example, it was found that the mutation probability, Pm would be 0.1. The reason was higher mutation probability cause higher chance of genes to be selected and switched. As a result, the order of the machine operation was messed up and the solution obtained was not practicable. On the other hand, crossover probability Pc affected only little because genes were selected as a set

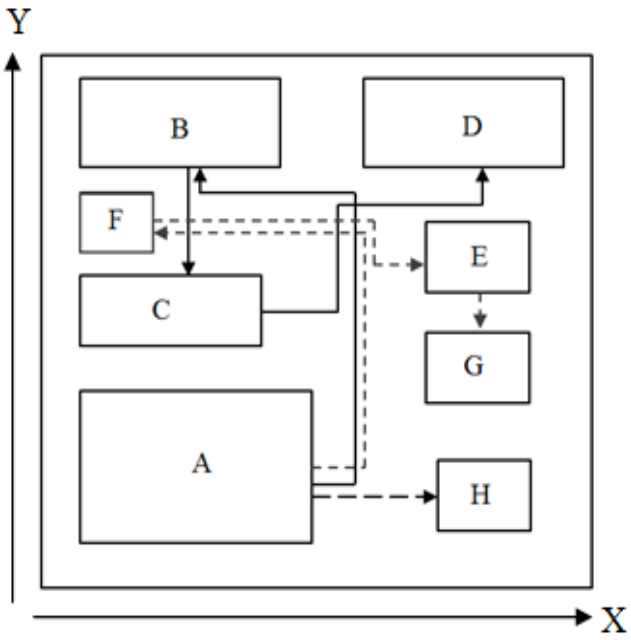

Figure 6.: Machine Layout before Improvement.

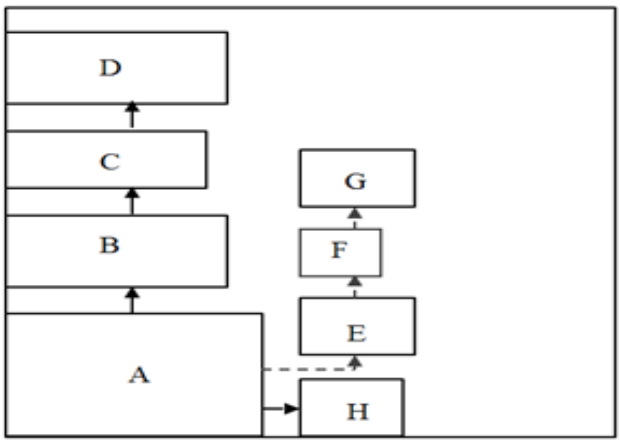

Figure 7. Machine Layout after Improvement by Using GA.

Table 3: Comparison between the different approach

Method	Total distance (m)
Current machine layouts	38.45
Critical path method (CPM)	20.88
Genetic algorithm (GA)	**19.62**

Fig. 6 and Fig. 7 show the layout before improvement and the one obtained by using the proposed GA. The comparison of the total distances calculated from different approaches was shown in Table 3. The results show that the proposed GA generated the best solution. The total distance was reduced to 19.62 m.

4. CONCLUSIONS

Multi-line layout problems can be solved by applying the proposed genetic algorithm method. The results shown that machines can be laid out in the plane region as well as total distances between them were minimized. A case study has been shown. The performance of the proposed genetic algorithm method was analyzed by comparing its result with the solution obtained by using critical path method. The total distances of the case study had been reduced from 38.45 m to 19.62 m using the proposed model and 20.88 m by critical path method. 48.97% distance had been shortened. Therefore, it can be suggested that applying modified genetic algorithm is suitable for solving facilities layout problem. Sensitivity analysis was proved a useful tool; however, their parameters affected greatly on whether the solutions will be practicable. For the future plan, other practical objectives or conditions should be encountered such as cost function likewise the directions of entering into the machines.

5. ACKNOWLEDGMENTS

This research was supported by Research and Development Institute (RDI), Rajamangala University of Technology Krungthep

6. REFERENCES

[1] D. Datta, A.R.S. Amaral and J.R. Figueira, "Single row facility layout problem using a permutation-based genetic algorithm," European Journal of Operational Research, Vol.213, No.2, pp.388-394, 2011.

[2] Amir Sadrzadeh, "A genetic algorithm with the heuristic procedure to solve the multi-line layout problem," Computers & Industrial Engineering Vol. 62, pp. 1055–1064, 2012.

[3] C. Srinivas, Reddyb B. Ramgopal, K. Ramji and R. Naveend, "Sensitivity Analysis to Determine the Parameters of Genetic Algorithm for Machine Layout," Procedia Materials Science Vol. 6, pp. 866–876, 2014.

[4] H.J. Holland, "Adaptation in Natural and Artificial Systems," University of Michigan Ann Arbor, 1975.

[5] P. Pongcharoen, "Scheduling Mixed-Model Production on Multiple Assembly Lines with Shared Resources Using Genetic Algorithms," International Journal of Production Economics, Vol. 78, No. 3, pp. 311-322, 2002.

[6] R. Kumar, "Blending Roulette Wheel Selection & Rank Selection in Genetic Algorithms," International Journal of Machine Learning and Computing, Vol.2, No. 4, pp. 365-371, 2012.

[7] Kelley J., Walker M. "The Origins of CPM A Personal History," PMNET work, Vol.3, No.2, pp.7-

CreTech 2020
8th International Conference on Creative Technology
Multidisciplinary
to Drive Economy and Social
http://utkcretech.rmutk.ac.th

Improvement of Mechanical Properties for ASME SA-192 Steel Finned Tubes Using Wire Arc Spraying

Montri Sangsuriyun[1*], Prayoon Surin[1] and Krittee Eidhed[2]

[1] Department of Advanced Manufacturing Technology, Faculty of Engineering, Pathumwan Institute of Technology, Bangkok, Thailand
[2] Faculty of Engineering, King Mongkut's University of Technology North Bangkok,Bangkok, Thailand
*Corresponding author. E-mail: montri.sang@npu.ac.th

ABSTRACT

The objectives of this study were to improve the hardness of ASME SA-192 steel finned tubes using the wire arc spraying process with TH450 Chrome Nickel amorphous. The cooling rates of specimens sintered at 300, 600 and 900°C were determined and compared between the cooling rates of noncoated and coated specimens using independent t-test. The results showed no difference in the cooling rates between noncoated and coated specimens (p-value > 0.05), and it can be, therefore concluded that wire arc spray coating did not affect the cooling rate. The tensile tests of specimens were then conducted, and it was found that all of Chrome Nickel amorphous-coated specimens showed high surface hardness resulting in higher tensile stress. After the noncoated specimens that did not meet the ultimate tensile strength (UTS) standard (FT-2 and FT-3) were coated, the strength of both specimens increased and met the UTS standard from 417 and 426 MPa to 666 and 882 MPa, respectively. Therefore, spray coating with Chrome Nickel amorphous is a suitable technique for industrial applications that require higher hardness and can reduce maintenance costs.

Keywords: Spray coating, ASME SA-192 steel, mechanical properties, cooling of finned tube

1. INTRODUCTION

For more than a decade, ASME SA-192 carbon steel tube has been used in industrial plants, power plants, canned food industry, oil refineries and other industries as the finned tube heat exchanger, especially in oil refineries where such steel has been used to heat crude oil. It is also used as a device to reduce the temperature of gas oil, including a device used for heat recovery in order to increase the efficiency of the production process, to reduce costs and to protect the environment [1-2]. The problems encountered in the use of ASME SA-192 carbon steel tube in various applications are such as the damage of boiler tube caused by caustic corrosion, acid corrosion, oxygen pitting, hydrogen damage, stress corrosion cracking (SCC), waterside corrosion fatigue, fireside corrosion fatigue, fireside corrosion in the superheaters, water wall fireside corrosion, high-temperature oxidation, short-term overheating, long-term overheating, graphitization, dissimilar metal weld, erosion and mechanical fatigue [3]. Besides, the prolonged exposure of carbon and low alloy steel to a temperature exceeding 427°C can lead to microstructural degradation of materials such as creep cavitation, carbide coarsening, and graphitization in rare cases. In general, graphitization is a result of the decomposition of pearlite (iron carbide) into the equilibrium iron graphite structure. It can severely reduce the toughness of steel when the graphite particles or

nodules are formed in the plane in a continuous manner. Graphitization can result in the premature failure of pressure boundary components, including high energy piping systems and boiler tubes. Failure due to graphitization is still a concern in aged carbon and carbon-molybdenum steel, both in weldments and base metal [4]. So, thermal spray coating has been developed as a technology for producing high-quality materials on various surfaces, which depends on the deposition of molten or semi-molten materials used to form coating [5]. In the oil rigs and other chemical industries, ASME SA-192 finned steel tube has been used, and it has been found that the environment in these industries can accelerate the corrosion. Therefore, the authors aim to develop the surface spray coating process in order to increase the service life by using wire arc spraying method. In the wire arc spraying apparatus, two wires are used as electrodes in an electrical circuit. These two wires are fed from each side of the spray gun, and the end of each wire touches each other in front of the spray gun, as shown in Figure 1.

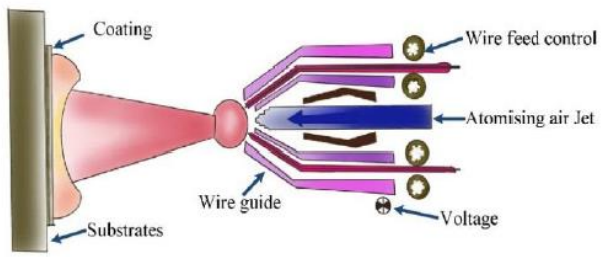

Figure 1 Wire arc spray coating [6].

Once electricity is applied through the wires, an electric arcing appears at the wire ends in front of the spray gun. The heat released from arcing increases and the wire ends is continuously heated to the melting point of the wire material. At the same time, high-pressure air or gas stream is applied at the wire ends from the back of the spray gun.

This air or gas stream must have sufficient pressure to tear the molten wire material off the wire ends into molten aerosols which will then travel into the air or gas stream until these aerosols hit the surface of the specimen and harden and form a coating layer [7-8]. According to a previous study focusing on the optimization of high-frequency resistance welding process using mechanical properties of SA-192 steel finned tube, the welding parameters which are current (A), voltage (kV) and frequency (rpm) correlate with the heat input. The mechanical property testing reveals that the ultimate tensile stress does not always result in the highest strength compared to the fatigue test. The welding parameters affect the melting process and optimum weld width and weld depth which is a result of HAZ of the specimen [9]. In this study, the spray coating technique was used to improve the properties of heat resistant ASTM SA-192 steel finned tube in order to improve the service life and mechanical properties.

2. MATERIALS AND METHODS

2.1 Materials and specimen preparation

In this study, finned tube heat exchanger made of ASTM SA-192 high-carbon steel was investigated. The properties of ASTM SA-192 high-carbon steel are shown in Table 1.

Table 1 Chemical composition and mechanical properties of ASTM SA-192 steel.

Material	Chemical Composition (%)				
ASTM SA-192	**C**	**Mn**	**Si**	**P**	**S**
	0.06-0.18	0.27-0.63	□0.25	□0.034	□0.035
	Mechanical Properties (MPa)				
	Tensile Strength (MPa)	Yield Strength (MPa)	Elongation (%)		
	□325	□180	□35		

The specimens used in this study were prepared in accordance with the finned tube production standard [10] as shown in Figure 2 with a tube diameter of 34.5±1 mm and tube wall thickness of 4 mm and the fin was 16±1 mm high and 1 mm thick.

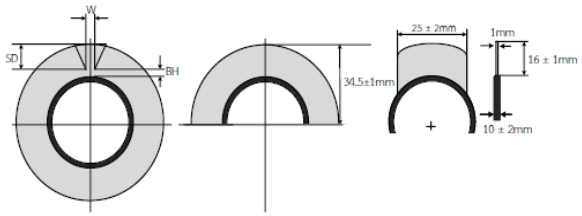

Figure 2 Dimensions of the finned tube specimen.

2.2 Wire arc spray coating

In wire arc spray coating, rust stains on the specimen surface must be removed by sandblasting and then wiped clean. After that, the specimens were spray- coated with TH205 Nickel Aluminum and TH450 Chrome Nickel amorphous with optimum spray parameters [11] as shown in Table 2. In electric arc spray coating, voltage and current can be adjusted, and the value of the current is automatically connected to wire feed rate, e.g. when the current increases, the wire feed rate will increase simultaneously [12-13] as shown in Figure 3.

Figure 3 Arc spray coating machine model AH-20A.

Table 2 Control parameters used in the wire arc spray experiment

No.	Parameter	Default value	Unit
1.	Air compressor, 20 HP/15 KW, model AH 20A	8	bar
2.	Voltage	37.5	V
3.	Electric current flowing through a conductor	19.6	A
4.	Temperature up to	926.67	°C

2.3 Cooling efficiency test

The cooling efficiency test of all seven specimens, noncoated and coated with TH450 Chrome Nickel amorphous was conducted by burning the ASTM SA-192 steel specimens at high temperature in furnace (Nabertherm: model LH/LF), from 30°C to 300, 600 and 900°C, respectively. The specimens were then burned for another 45 minutes. After the burning process completed, Transmitter METER (model TH205) was used to measured and recorded the specimen temperature at 5 minutes interval in order to observe the cooling rate of both finned tube specimens in triplicate as shown in Figure 4.

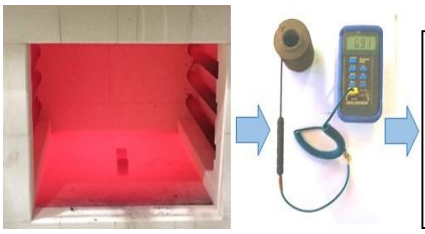

Figure 4 Burning in furnace and measurement of cooling rate of the finned tube.

2.4 Micro Vickers Hardness Tester

The hardness test of all seven specimens, both noncoated and coated with TH450 Chrome Nickel amorphous was performed. Before the hardness test, the ASTM SA-192 specimen surface must be polished using 180-200 grit sandpaper and then finished using a felt cloth and 0.3-0.1 µm alumina powder.

The specimens were then etched with the mixture ratio/proportion of nitric acid in alcohol (10: 90) to expose the microstructure of the specimens. After these pretreatment steps, the hardness test of all seven specimens was performed with 0.98 kg compression load using Micro Vickers Hardness tester model (HV-1000) [14]. The results were expressed as $HV_{0.5}$. The test points for hardness test are shown in Fig. 6.

2.5 Tensile Strength Test

Tensile strength test of specimens was then performed at a constant extension rate until failure. The tensile test was performed at Disp of 0.500 mm/min, 1.00 kN/s or 10 MPa/s load and 0.0500 mm/s extension speed in triplicate per treatment in which the standard ultimate tensile strength (UTS) must be higher than UTS of the fin (350 MPa) [15]. In other words, the fracture must occur at the fin.

3. RESULTS

3.1 Temperature against time for cooling of finned tube

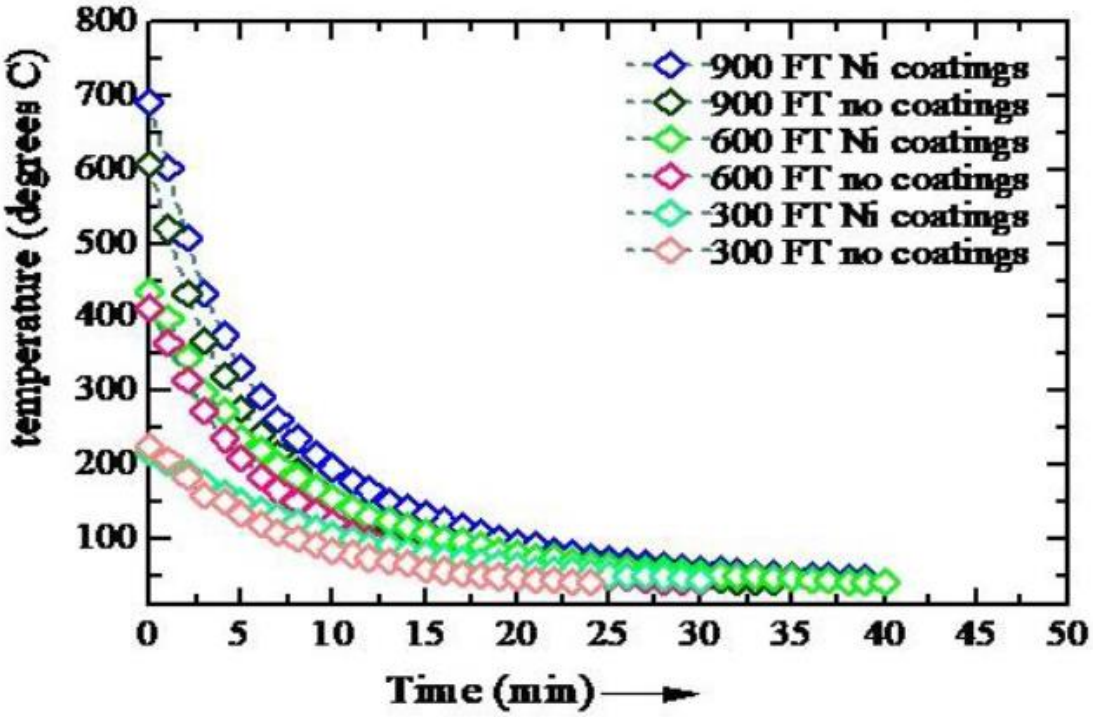

Figure 5 Graph of temperature against time for cooling of finned tube (NiC is Ni Coated and NonC is Noncoated).

Table 3 Descriptive statistics.

Heat	Coating Type	N	Mean	Std. Deviation
300°C	Noncoated	25	92.4400	54.58867
	Ni Coated	31	92.3871	53.87930
600°C	Noncoated	31	122.7742	101.30341
	Ni Coated	41	124.9756	101.53213
900°C	Noncoated	35	147.7429	101.30341
	Ni Coated	41	161.4390	101.53213

Table 4 Independent samples t-test.

Heat	t	df	Sig. (2-tailed)
300°C	.004	54	.997
600°C	-.091	70	.928
900°C	-.394	74	.694

Figure 5 shows the comparison of temperatures in the cooling process of ASTM SA-192 steel finned tube specimens, both noncoated and TH450 Chrome Nickel amorphous-coated specimens. Specimens in experiment 1 were removed from the furnace at 900°C, and the temperatures of both specimens sharply decreased. In this experiment, the average temperature of the noncoated specimens removed from the furnace was 605°C, while an average temperature of the coated specimens removed from the furnace was 691°C. It was found that the noncoated and coated specimens took 34 and 43 minutes, respectively to cool down to 38°C. For experiment 2, specimens were removed from the furnace at 600°C, and it was also found that the temperatures of both specimens rapidly decreased. An average temperature of the noncoated specimens removed from the furnace was 433°C, while an average temperature of the coated specimens removed from the furnace was 411°C. It was found that the noncoated and coated specimens took 33 and 42 minutes, respectively to cool down to 38°C. For experiment 3, specimens were removed from the furnace at 300°C, and it was found that the temperatures of both specimens slightly decreased. An average temperature of the noncoated specimens removed from the furnace was 218°C, while and an average temperature of the coated specimens removed from the furnace was 225°C. It was found that coated and noncoated specimens took 28 and 24 minutes, respectively to cool down to 38°C. The cooling rates during 1-15 minutes were relatively high. Arc spray coating with Chrome Nickel amorphous at high temperature affected the cooling rates, while arch spray coating at low temperature resulted in no difference in cooling rates. However, the independent t-test results as shown in Table 3 showing the comparison of average temperatures in the cooling process of noncoated and TH450 Chrome Nickel amorphous-coated ASTM SA-192 steel finned tube specimens sintered at 300, 600 and 900°C showed no difference in the cooling rates between noncoated and coated specimens at a significance level of 0.05 in Table 4.

3.2 Comparison between the hardness noncoated and Ni-coated ASTM SA-192 steel finned tube specimens

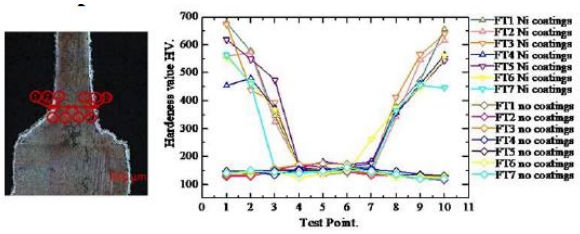

Figure 6. The test points (a) and comparison of the hardness of noncoated and Ni- coated specimens (b).

Arc spray coating of ASTM SA-192 steel specimens resulted in high hardness values at point 1-3 and pointed 8-10. These areas were arc spray- coated with Chrome Nickel amorphous, and the surface of these areas, therefore, showed high hardness in the range of 400-650HV since all seven specimens were spray- coated simultaneously. However, the heat-affected zone (HAZ) was observed between the coating layer, and the tuned point of the specimen was affected by the heat resulting in higher hardness compared to the heat-affected zone and decrease in hardness values at point 4-7 in range of 131-155 $HV_{0.5}$ as shown in Figure 6.

3.3 Comparison between the tensile properties of noncoated and TH450 Chrome Nickel amorphous-coated finned tube specimens

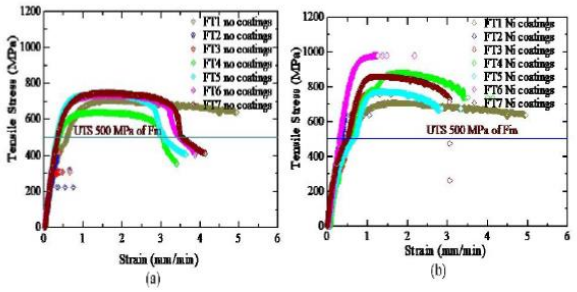

Figure 7 Comparison of Strain-Strength of noncoated specimens (a) and TH450 Chrome Nickel amorphous-coated specimens (b).

According to Figure 7 (a), the tensile stress of noncoated specimens FT-1, FT-4, FT-5, FT-6 and FT-7 was 621, 640, 740, 739 and 749 MPa, respectively. It was also found that the adjustment of current, voltage and frequency in the welding process resulted in optimum melting and weld depth for all five specimens. The tensile stress of these specimens met the UTS standard of not less than 325 MPa, and the fracture must occur at the fin. FT-2 and FT-3 showed the tensile stress of 417 and 426 MPa, respectively, and the fracture was observed between the fin and tube. These specimens, therefore, did not meet the UTS standard.

According to Figure 7 (b), the Chrome Nickel amorphous- coated specimens showed high surface hardness in the range of 400-650HV since all seven specimens were spray- coated simultaneously, as shown in Figure 6. The tensile stress of FT-1, FT-2, FT-3, FT-4, FT-5, FT-6 and FT-7 was 705, 666, 768, 882, 776, 982 and 863 MPa which met the UTS standard, respectively.

4. CONCLUSIONS

4.1 Cooling rates at 600°C □ 900°C of the ASTM SA-192 steel finned tubes spray-coated with Chrome Nickel amorphous were high, and no difference was observed, while no difference in cooling rates was observed between both specimens at 40°C □ 300°C. The independent t-test of the specimens sintered at 300, 600 and 900°C showed no difference in the cooling rates between noncoated and coated specimens at a significance level of 0.05.

4.2 Arc spray coating of ASTM SA-192 steel finned tubes with Chrome Nickel amorphous increased the surface hardness values of specimens. After the deterioration of the coating layer, the specimen can be re-sprayed for many times. In addition, this process

increased the tensile strength compared to that of the noncoated specimen.

4.3 Noncoated specimens, FT-2 and FT-3 did not meet the ultimate tensile strength (UTS) standard. Arc spray coating with Chrome Nickel amorphous increased tensile stress of these specimens from 417 and 426 MPa to 666 and 882 MPa, respectively, which met the UTS standard.

5. DISCUSSION

5.1 The results showed in this study were only obtained from the experiments of ASTM SA-192 steel finned tubes coated by wire arc spraying technique which may be applied to other materials. However, for accuracy, the experiments should be conducted before applying this technique to other materials.

5.2 According to the hardness test, it was found that as the thickness of the coated specimen increased the hardness of specimen increased, then the hardness was gradually stable and eventually decreased. The results may be different when the hardness test is conducted using other methods.

5.3 The results shown above indicate that the coating can increase the tensile stress. However, further study should be conducted in the humid and corrosive environments to determine the suitability of the properties of coating materials to be further used with the finned tube.

6. REFERENCES

[1] Lebele-Alawa BT, Egwanwo V. Numerical analysis of the heat transfer in heat exchangers. IJAST 2012; 2:60-4.

[2] Kocurek R, Adamiec J. Manufacturing technologies of finned tubes. ADMS 2013; 13:26-35.

[3] Kumar A, Sapra PK. Boiler tubes failure: Causes and remedies a case study of a fertilizer plant. IJET 2013; 4:132-5.

[4] Foulds JR, Viswanathan R. Graphitization of steels in elevated-temperature service. J MATER ENG PERFORM 2001; 10:484-92.

[5] Chandler H. Heat treater's guide: practices and procedures for irons and steels. 2nd ed. Ohio: ASM international; 1994.

[6] Sangsuriyun M, Sangsuriyun S. Study of mechanical properties of AISI S45C steel using arc spray coating. Proceedings of the 2nd Conference on Innovation Engineering and Technology for Economy and Society; 2018 Dec 16; Kasem Bundit University, Romklao Campus. Bangkok; 2018.

[7] Chauhan M, Kala H, Joshi A. A review on Investigation of different Thermal Spraying process. Pauri- Garhwal, India: Department of Mechanical Engineering, Govind Ballabh Pant Engineering College Ghurdauri; 184.

[8] Yang K, Liu M, Zhou K, Deng C. Recent developments in the research of splat formation process in thermal spraying. J MATER 2013; 1-14.

[9] Sangsuriyun M, Surin P, Eidhed K. Optimization of high-frequency resistance welding process using mechanical property of finned tube SA-192 steel. ARPN J Eng Appl Sci 2020; 15: 607-12.

[10] Tulsa Fin Tube Inc. International standard for dimensions, tolerances and tests of high frequency resistance welded fins [Internet]. 1990 [cited 2014 Feb 3]. Available from: https://tulsafintube.com/wp-content/uploads/2015/03/International-Standard-for-High-Frequency-Welded-Fins-Download.pdf

[11] Moreau C, Gougeon P, Lamontagne M, Lacasse V, Vaudreuil G, Cielo P, et al. Thermal spray industrial applications. Proceedings of the 7th Thermal Spray Conference; 1994 June; Boston, MA. ASM International Materials Park; 1994. p. 431-7.

[12] Jandin G, Liao H, Feng ZQ, Coddet C. Correlations between operating conditions, microstructure and mechanical properties of twin wire arc sprayed steel coatings. MAT SCI ENG A- STRUCT 2003; 349:298-305.

[13] Saravanan P, Selvarajan V Joshi V, Sundarajan G. Experimental design and performanceanalysis of alumina coatings deposited by a detonation spray process. J PHYS D APPL PHYS 2001; 34:131-140.

[14] Gane N, Cox JM. The micro-hardness of metals at very low loads. Philos Mag 1970; 22:0881-91.

[15] ASTM Subcommittee D20. 10 on Mechanical Properties. Standard test method for tensile properties of thin plastic sheeting. American Society for Testing and Materials. 1995.

CreTech 2020
8th International Conference on Creative Technology
Multidisciplinary
to Drive Economy and Social
http://utkcretech.rmutk.ac.th

Effect of Deposition Time on the Structure of TiCrN Nanocomposite Thin Films Deposited by Reactive DC Magnetron Sputtering from Mosaic Target

Siriwat Alaksanasuwan[1,2], Adisorn Buranawong[1,2], Nirun Witit-anun[1,2*]

[1]Department of Physics, Faculty of Science, Burapha University, Chonburi 20131, Thailand.
[2]Thailand Center of Excellence in Physics (ThEP), MHESI, Bangkok 10400, Thailand.
*Corresponding author. E-mail: nirun@buu.ac.th

ABSTRACT

In this research work, the influence of the deposition time on the crystal structural, surface morphology and chemical composition of titanium chromium nitride (TiCrN) thin films has been successfully investigated. The TiCrN thin films were deposited on Si substrate using reactive DC magnetron sputtering from a mosaic Ti-Cr target. The crystal structural, microstructure, surface morphology and chemical composition were studied using X-ray diffraction (XRD), field-emission scanning electron microscopy (FE-SEM) and energy dispersive spectroscopy (EDS), respectively. The results showed that the as-deposited thin films were formed as a (Ti,Cr)N solid solution. The crystal structure from X-ray diffraction pattern of TiCrN thin films with different deposition time shows the presence of (111) (200) and (220) plane orientations. The as-deposited thin films exhibited a nanostructure with crystallite size in the range of 43.8-56.9 nm. The lattice constants were ranging from 4.160 to 4.167 Å. The film's thickness increased from 148 nm to 461 nm with increasing in the deposition time. The chemical composition of the films varied with the film thickness. The as-deposited TiCrN thin films showed compact columnar and dense morphology as a result of changed the deposition time.

Keywords: TiCrN thin films, reactive DC sputtering, mosaic target, the deposition time

1. INTRODUCTION

In the last decade, surface engineering is the most important and urgent technology for the new industrial development, especially on improving the surface properties of machinery parts, such as cutting and forming tools. One is the tribology properties of the surface materials, which must have high hardness, low friction and wear rate for a wide range of the working environments. Transition metal nitride hard coating is one of the most promising materials used to enhance the surface tribology properties of industrial parts. Thus, these coatings have acceptable for conventional materials to extend the lifespan of tools.

The single-transition metal nitride coating such as titanium nitride (TiN) and chromium nitride (CrN) is known as the first generation of the hard coating for machining tools and industrial parts [1]. Generally, these transition metal nitrides coating (sometimes called binary nitrides hard coating) possess higher hardness than normal high-speed steel and cemented carbide. However, the mechanical properties of these coating or thin films are easily degraded by thermal oxidation at high-temperatures [2]. So, in order to overcome the limitations of this hard-coating, the new types of ternary nitride hard coating or thin films have been developed by

adding some element in the structure of the binary nitrides hard coatings, such as TiAlN, TiZrN, TiVN, and TiCrN [3]. Among these coatings, the ternary of TiCrN thin films have been attracted more attention due to its outstanding properties with high hardness (25-38 GPa), low friction coefficient, good wear resistance, good chemical stability and high-temperature oxidation at above 700 °C [4-5].

Typically, there have been many methods to synthesize the TiCrN thin films such as evaporation [6], ion beam assisted deposition [7], ion plating [8], and magnetron sputtering [9]. Among these techniques, the magnetron sputtering method is the most suitable one due to the low-temperature process, the use of non-toxic gases and the simple process [10-11]. In the case of the magnetron sputtering method, for deposited a ternary hard coating, various sputtering targets can be used such as multi-target, alloy target, and mosaic targets. Even though the multi- target sputtering makes it possible to control the composition of the as-deposited thin films by varying the sputtering power of each cathode, but this method cannot be used in actual manufacturing due to its complexity at an industrial scale. Therefore, the tendency in the ternary nitride hard coating deposition is to develop the process or the new method of sputtering from a single target, such as an alloy target or a mosaic target [12].

However, it is well known that the physical and chemical properties of the thin film prepared by the sputtering method depend strongly on the deposition parameters such as total pressure, gas flow rate, sputtering power, external heating, and voltage biasing. So, the effect of deposition parameters on the structure of the as-deposited thin films still important to investigate. Nowadays, the studies of the TiCrN thin film deposition by the reactive sputtering technique have been focused on the effects of the deposition parameters on the structure and properties of the TiCrN thin films. However, investigations of the TiCrN thin film deposition from the mosaic target are still limited.

In this work, the TiCrN thin films were synthesized by the reactive DC unbalanced magnetron sputtering technique using a mosaic target at room temperature, without external heating and biasing. The characteristics of the as-deposited thin films such as the crystalline structure, surface morphology, microstructure, and chemical composition were investigated as a function of the film thickness.

2. MATERIALS AND METHODS

2.1 Thin Films Preparation

TiCrN thin films were deposited on Si substrate by reactive DC magnetron sputtering technique from a mosaic target. The Ti-Cr mosaic target styled, used in this work, is made by embedding chromium rods (99.99%) into the high sputtering rate area of metal titanium (99.97%) disk, with a diameter of 54 mm and thickness of 3 mm thick as shown in Figure 1. Pure Ar (99.999%) and N_2 (99.999%) were used as the sputtering and reactive gases, respectively. Before deposition, the coating chamber was evacuated to a base pressure of 5×10^{-5} mbar. Previous to the deposition of the process of thin films, the pre-sputtering stage was start-up by ion bombardment from Ar^+ ions, which sputtered on the target to eliminate the surface impurities under a shutter shielding in about 5 min. The TiCrN films were deposited at different deposition time, process variable, of 15, 30 and 45 min, while the deposition parameters such as Ar and N_2 gas flow rate, sputtering power, substrate-target distances, substrate temperature, and working pressure were constant. The deposition parameters are summarized in Table 1.

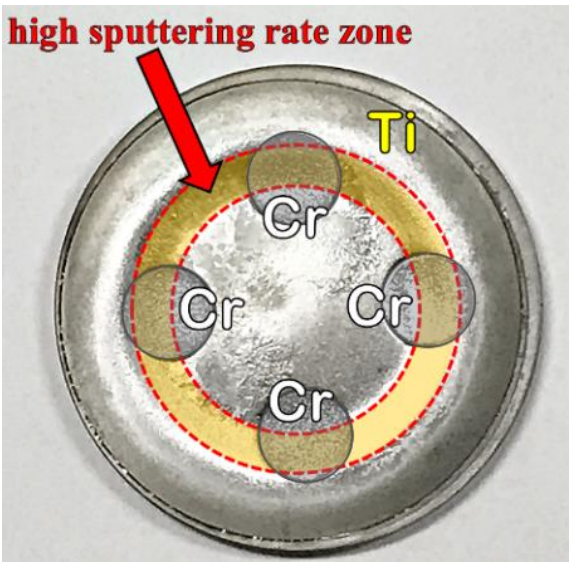

Figure 1. The Ti-Cr mosaic target.

Table 1. The thin film deposition parameters.

Parameters	Details
Sputtering target	Ti-Cr mosaic target
Substrate temperature	room temperature
Substrate-target distances	15 cm
Base pressure	5.0×10^{-5} mbar
Working pressure	5.0×10^{-3} mbar
Sputtering power	310 W
Flow rate of Ar	16 sccm
Flow rate of N_2	6 sccm
Deposition time	15, 30, 45 min

2.2 Thin Films Characterization

The crystal structures and crystal size of the TiCrN thin films were characterized by X-ray diffraction (XRD: BRUKER D8) using CuKα radiation ($\lambda = 0.154$ nm). The XRD patterns acquire in a 2θ continuous scan mode, scanning speed of 2°/min, and the grazing incidence angle of 3°. The phases of films were determined by Bragg's law and compared with the Joint Committee on Powder Diffraction Standard (JCPDS) files. The crystallite size calculated by using Scherrer's equation from the FWHM data acquired from XRD pattern. The microstructure and film thickness were investigated by Field Emission Scanning Electron Microscope (FE-SEM: Hitashi s4700). The chemical composition of the as-deposited films determines by Energy Dispersive X-ray spectroscopy (EDS: EDAX), which equipped on Scanning Electron Microscopy (SEM: LEO 1450VP).

3. RESULTS AND DISCUSSION

3.1 Crystal Structure

The crystal structures of the as-deposited TiCrN thin films prepared on Si (100) wafers at different deposition time in the range of 15 to 45 min, were investigated by XRD technique. The X-ray diffraction patterns were shown in Figure 2. The lines at a diffraction angle (2θ values) of standard TiN (JCPDS No. 87-0633) and CrN (JCPDS films No. 77-0047) with (111), (200), and (220) plane are shown for comparison purposes. The results exhibited a low crystallinity of deposited films for 15 min. After that, for a higher deposition time of 30 min, it was found that the films were shown a strong (111) reflection plane which was higher compared to the (200) plane and (220) planes. The results showed a preferred orientation (111) plane of deposited films. Whereas, at the highest deposited films of 45 min, the diffraction peaks were very similar to previous condition of deposition time (15 and 30 min). It was found that the highest crystallinity at all planes was performed. The results still showed a preferred orientation (111) plane of deposited films and the intensity of XRD peaks were grown up with increasing deposition time. These results can be explained by the fact that the thickness of films increased with increasing deposition time. This process led to the upward intensity of XRD peak of deposited films.

In addition, the XRD peak position of the as-deposited films laid between the standard 2θ peak of TiN and CrN. This result suggested that the as-deposited thin films in this work formed a solid solution of (Ti,Cr)N with the fcc NaCl phase. A solid solution of the TiCrN films formed whereby the Ti atoms were substituted

by Cr atoms in the TiN structure. Since the atomic radius of Cr atom (0.1249 nm) is smaller than that of Ti atom (0.1445 nm) [13]. In fact, this phenomenon was found in various researchers. They also reported the fcc NaCl phase in (Ti,Cr)N thin film prepared by the sputtering method [4,9,11,13]. The data for the calculated crystallite size and the lattice constants of the as-deposited films are shown in Table 2. It was indicated that the crystal sizes of the as-deposited films were rather constant, ranging from 43.8 to 55.6 nm. Furthermore, the lattice constants of films calculate from all of the diffraction peaks for the film deposited at various deposition time were rather constant in the range of 4.162 to 4.167 Å. It can confirm that the as-deposited thin film in this study was formed as the solid solution of (Ti,Cr)N and it also supports as the crystal structure obtained from the XRD result.

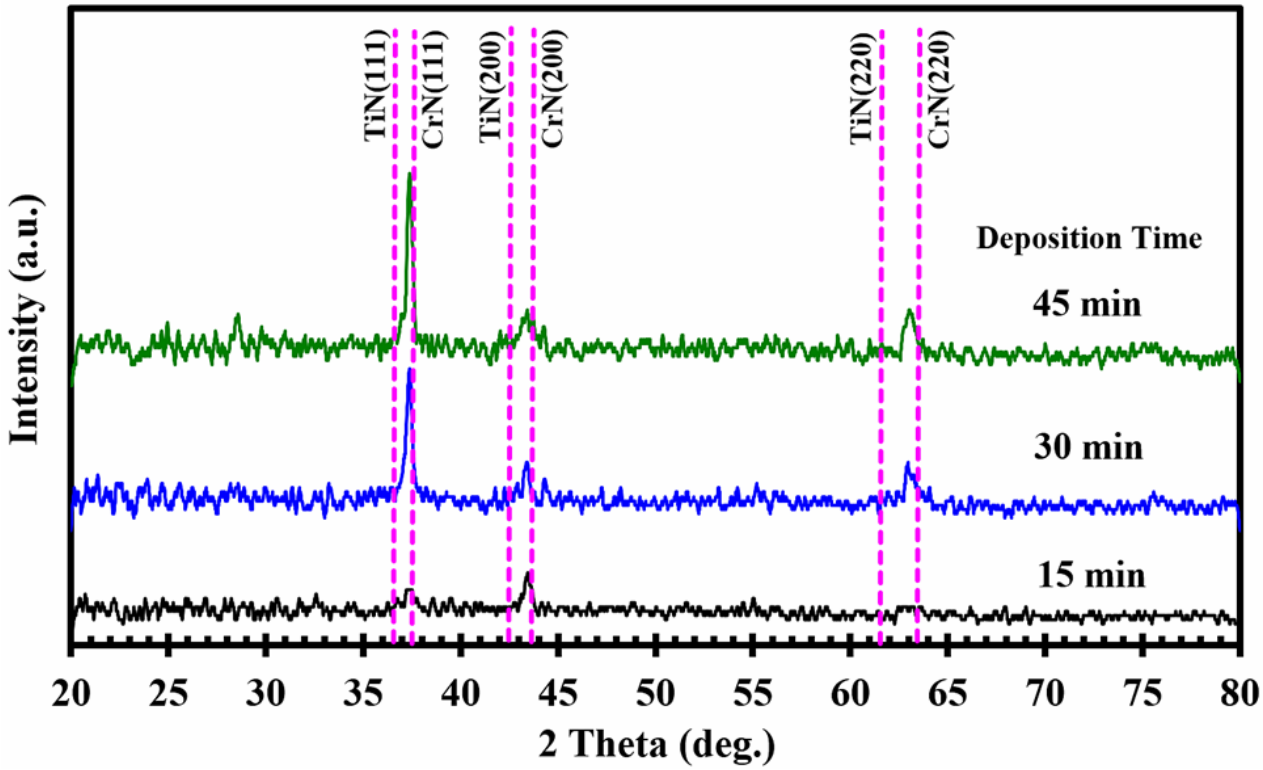

Figure 2. XRD patterns of TiCrN thin films.

Table 2. Some properties of the TiCrN thin films with different deposition time.

Dep. Time (min)	Thickness (nm)	Crystallite size (nm)			Lattice constants (Å)			$Ti_{1-x}Cr_xN_y$		
		(111)	(200)	(220)	(111)	(200)	(220)	1-x	x	y
15	148	47.9	43.8	-	4.162	4.160	-	0.30	0.70	2.40
30	273	54.1	56.9	47.8	4.163	4.167	4.165	0.29	0.71	1.85
45	461	55.9	50.3	49.1	4.163	4.162	4.165	0.28	0.72	1.51

It was revealed that the lattice constant of the TiCrN films was progressively increased with increasing the nitrogen gas flow rates as shown in Figure 4. Moreover, the lattice constants of the as-deposited thin films were in the range of 4.144 to 4.181 Å, between that of CrN (4.148 Å; JCPDS 77-0047) and TiN (4.238 Å; JCPDS No. 87-0633), which confirms that the atoms of chromium have completely incorporated into the TiN structure.

The crystal sizes of the as-deposited TiCrN thin films, in this work, calculated from FWHM of XRD spectra using the Scherrer's equation were less than 45 nm, which in the range of 33.3 to 42.7 nm, as shown in Table 2.

3.2 Chemical Composition

In this work, the chemical composition of the as-deposited TiCrN thin films was measured from EDS technique as shown in Table 2 which expressed the concentration of Ti, Cr and N as the function of the deposition time. It was indicated that as the nitrogen content of the films reduced from 70.63 to 60.21 at.% with increasing of the deposition time from 15 to 45 min. Oppositely, the titanium and chromium content increased from 8.68 to 11.31 at.% and 20.70 to 28.48 at.%, respectively.

Moreover, it also shows the ratio x of chromium content in TiCrN thin films defined as $x = Cr/(Ti+Cr)$ and thin film composition $Ti_{1-x}Cr_xN_y$ as a function of the deposition time. It was found that the ratio x of chromium content is rather constant in the range of 0.70 to 0.72. The film composition of varied deposition time was $Ti_{0.30}Cr_{0.70}N_{2.40}$, $Ti_{0.29}Cr_{0.71}N_{1.85}$, and $Ti_{0.28}Cr_{0.72}N_{1.51}$, respectively. In addition, the ratio y of nitrogen content in TiCrN thin films defined as $y = N/(Ti+Cr)$ for all samples was more than 1. It reveals that all the as-deposited TiCrN thin films in this study were over stoichiometry.

3.3 Microstructure

The microstructure and the cross-sectional of the TiCrN thin films deposited at different total pressure in this work are shown in Figure 3. It can be seen that the small grain and smooth surface were obtained at a deposition time of 15 min (Figure 3(a)). The morphology of the as-deposited thin films was generally composed of uncountable grains like an island with different sizes randomly dispersed on the surface and these were enlarged with increasing the deposition time. Furthermore, for the deposition time of 30 min (Figure 3(b)) and 45 min (Figure 3(c)), the morphology was mainly composed of many large grains like an island with different sizes distributed randomly on films surface. The thicknesses of films which measured from cross-section analysis as a function of deposition time were listed in Table 2. It revealed that films deposited at 15 min have the lowest thickness of 148 nm. The increased thickness to 273 nm was investigated for the deposition time of 30 min. The gradual increase of thickness to 431 nm was found for the film prepared at a deposition time of 45 min. This result was owed to a few deposited atoms which sputtered from the target reach to the surface of substrate. It was achieved for short deposition time hence the low thickness. The deposited atoms were more adsorbed on the surface after arriving at the substrate through the longer deposition time therefore, the thickness was enlarged. In addition, the deposition rate of the films, in this work, constantly increased from 4.9, 9.1 and 14.4 nm/min with increasing of the deposition time from 15, 30 and 45 min, respectively.

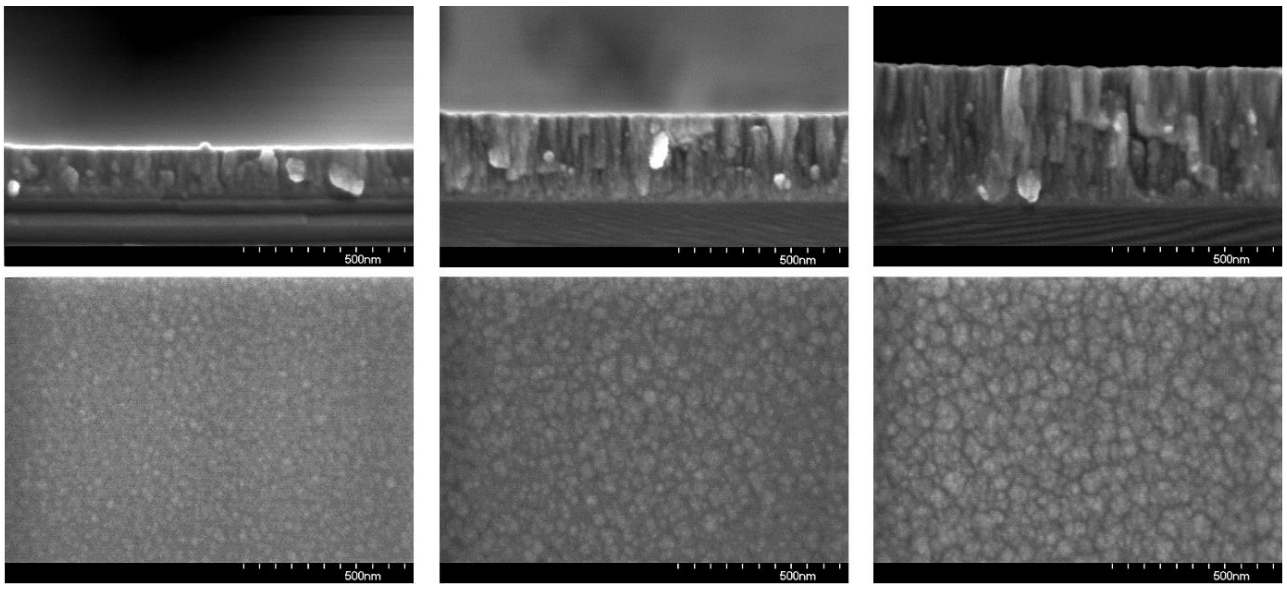

(a) (b) (c)

Figure 3. FE-SEM micrograph of TiCrN thin films deposited at difference deposition times; (a) 15 min, (b) 30 min, (c) 45 min.

The cross-sectional SEM micrographs of the as deposited TiCrN thin films were also showed in Figure 3. The dense microstructure in which no void between grains was identified from the thin film deposited at 15 min as shown in Figure 3(a). When deposition time reach to 30 min, the porous columnar structure which contains short columnar grains exhibited throughout the film thickness (Figure 3(b)). It can be seen that the film composes of long columnar grain with grain boundaries were slightly observed for the film deposited at 45 min (Figure 3(c)). The cross-section observation apparently reveals the film perform columnar form which corresponds to Zone T in the structure Thornton's zone model. Additionally, the fracture of grain boundary located through columnar grains related to the low density of film and strength of boundary bonding between grains is weak.

4. CONCLUSIONS

In this research work, the ternary nitride nanostructured TiCrN films were successfully deposited on Si(100) substrates by reactive DC magnetron sputtering technique using a Ti-Cr mosaic target at room temperature without external heating and biasing to the substrate. The crystal structure, surface morphology and chemical composition were studied using X-ray diffraction (GIXRD), field-emission scanning electron microscopy (FE-SEM) and energy dispersive spectroscopy (EDS), respectively. The results showed that the as-deposited thin films formed solid solutions of (Ti,Cr)N with the fcc phase at all the deposition times. It was found that increasing the deposition times caused the films thickness to increase. X-ray diffraction pattern of TiCrN films with different deposition time shows the preferred orientations of (111) (200) and (220).

The as-deposited films shown a nanostructure with crystallite size in a range of 43.8 to 56.9 nm. The lattice constants were ranging from 4.160 to 4.167 Å. The chemical composition of the films varied with the film thickness. The N content of the films reduced, whereas the Ti and Cr content increased with increasing the deposition time. The thin film composition of varied deposition time were $Ti_{0.30}Cr_{0.70}N_{2.40}$, $Ti_{0.29}Cr_{0.71}N_{1.85}$, and $Ti_{0.28}Cr_{0.72}N_{1.51}$, respectively. The as-deposited TiCrN thin films showed compact columnar and dense morphology as a result of changed the film thickness.

5. REFERENCES

[1] Wang WL, Zhang RQ, Liao KJ, Sun YW, Wang BB. Nucleation and Growth of Diamond Films on Aluminum Nitride by Hot Filament Chemical Vapor Deposition. Diamond and Related Materials 2000; 9:1660-1663.

[2] Xue CL, Chang SL, Ye Z, Hua T, Guo WL, Chao CM. Tribological Properties of the Ti-Al-N Thin Films with Different Components Fabricated by Double- Targeted Co-Sputtering. Applied Surface Science 2010; 256:4272-4279.

[3] Witit-anun N, Buranawong A. Effect of Deposition Time on Structure of TiAlN Thin Films Deposited by Reactive DC Magnetron Co- Sputtering. Applied Mechanics and Materials 2017; 866:318-321.

[4] Witit-anun N, Teekhaboot A. Effect of Ti Sputtering Current on Structure of TiCrN Thin Films Prepared by Reactive DC Magnetron Co-Sputtering, Key Engineering Materials 2016; 675-676:181-184.

[5] Chen SY, Luoa DF, Zhao GB. Investigation of the properties of $Ti_xCr_{1-x}N$ coatings prepared by cathodic arc deposition. Physics Procedia 2013; 50:163-168.

[6] Wolfe DE, Gabriel BM, Reedy MW. Nanolayer (Ti,Cr)N coatings for hard particle erosion resistance. Surface and Coating Technology 2011; 205:4569-4576.

[7] Budzynski P, Sielanko J, Surowiec Z, Tarkowski P. Properties of (Ti,Cr)N and (Al,Cr)N thin films prepared by ion beam assisted deposition. Vacuum 2009; 83:186-189.

[8] Lee DB. TEM study on oxidized TiCrN coatings ion-plated on a steel substrate. Surface and Coating Technology 2003; 173:81-86.

[9] Paksunchai C, Denchitcharoen S, Chaiyakun S, Limsuwan P. Effect of Sputtering Current on Structure and Morphology of $(Ti_{1-x}Cr_x)N$ Thin Films Deposited by Reactive Unbalanced Magnetron Co- sputtering. Procedia Engineering 2012; 32:875-881.

[10] Shum PW, Li KY, Shen YG. Improvement of high-speed turning performance of Ti–Al–N coatings by using a pretreatment of high-energy ion implantation. Surface and Coatings Technology 2004; 198:414-419.

[11] Thampi A, Bendavid A, Subramanian B. Nanostructured TiCrN thin films by Pulsed Magnetron Sputtering for cutting tool applications. Ceramics International 2016; 42:9940-9948.

[12] Golosov DA, Melnikov SN, Dostanko AP. Calculation of the elemental composition of thin films deposited by magnetron sputtering of mosaic targets. Surface Engineering and Applied Electrochemistry 2012; 48:52-59.

[13] Paksunchai C, Denchitcharoen S, Chaiyakun S, Limsuwan P. Growth and characterization of nanostructured TiCrN films prepared by DC magnetron cosputtering, Journal of Nanomaterials 2014; Advance online publication. DOI:10.1155/2014/609482.

CreTech 2020
8th International Conference on Creative Technology
Multidisciplinary to Drive Economy and Social
http://utkcretech.rmutk.ac.th

Molecular Classification of Cassava Bacterial Blight, Xanthomonas axonopodis pv. manihotis in Thailand

Chotiros Phaisomboon[1], Nattaya Srisawad[1], Supajit Sraphet[1], Kanokporn Triwitayakorn[1*]

[1]Institute of Molecular Biosciences, Mahidol University, Thailand
*Corresponding author. E-mail: kanokporn.tri@mahidol.ac.th

ABSTRACT

Cassava is one of the important crops as a world's source of carbohydrate. It is used as a staple food in many countries in the tropical zone. Several Limitation that affect to cassava production including cassava bacterial blight (CBB). CBB caused by gram-negative bacteria *Xanthomonas axonopodis* pv. *manihotis* (*Xam*). To control this disease, variations of *Xam* should be studied. There are variable numbers of tandem repeat (VNTRs) in bacteria genome that have the potential to classify in strain levels. The collection of 16 *Xam* isolates since 1983 to 2017 from four provinces in Thailand was used to determine with 22 variable numbers of tandem repeat (VNTR). Four groups with high similarity were observed. Interestingly, those groups showed no relationship with their collected locations. This might be due to transporting for cassava stem for propagation. Moreover, we found that some VNTR regions have the potential for application in the detection of *Xam* in Thailand in the future.

Keywords: Variable numbers of tandem repeat, Polymerase chain reaction, Cassava bacterial blight

1. INTRODUCTION

Cassava (*Manihot esculenta* Crantz) is a perennial shrub belonging to the Euphorbiaceae family. Its starchy storage root is one of the carbohydrate sources in the world. Cassava is used as a staple food in many tropical countries of Africa, Asia, and Latin America. Moreover, cassava starch has been used as raw materials for bioethanol production. Cassava is one of the important crops in Thailand. In 2017, Thailand had produced 30.5 million tons of cassava and exported with a value of 72.7 billion Baht. However, several diseases have resulted in decreasing in cassava production. One of the most common diseases of cassava is cassava bacterial blight (CBB) caused by a gram-negative bacteria *Xanthomonas axonopodis* pv. *manihotis* (Xam). This bacteria is a foliar and vascular pathogen that infects the plant through stomata and wounds [1]. Inside the plant tissue, *Xam* colonizes in the intercellular space or the xylem vessels and then spreads systemically within the plant [2]. *Xam* dispersal is stimulated by wind-driven rain splash [3]. The symptoms of CBB are shown as angular leaf spotting, water-soaked, blighted leaves, wilting, gum exudation, vascular necrosis, and dieback [4]. CBB can affect cassava losing up to 80% [5]. In Thailand, it has been reported of *Xam* distribution in Rayong, Nakhonratchasima, Kamphaengphet, and Prachinburi provinces from 1983 until nowadays.

In this study, we aim to classify *Xam* isolates collecting in Thailand based on a variable number of tandem repeat (VNTRs).

VNTRs are short nucleotide sequences (20–100 bp) where have a high mutation rate and vary in copy numbers in bacterial genomes. They arise through DNA strand slippage during DNA replication [6]. Polymerase chain reaction (PCR) classification based on the VNTR loci is a method for molecular typing of bacteria at the strain levels [7]. To date, there are VNTR typing in Ralstonia solanacearum in potato [8], *X. arboricola* for walnut blight [9] and *X. oryzae* pv. *oryzicola* in rice [10]. In *Xam*, VNTR primers have also been developed [11]. To control this disease, understanding in the variations of bacteria is also important. Therefore, this project focuses on the classification of variations of *Xam* in Thailand based on VNTR regions by using the PCR technique.

2. MATERIALS AND METHODS

Bacterial culture and DNA extraction: Total 16 isolates of *Xam* from four provinces in Thailand including Nakhon Ratchasima, Kamphaeng Phet, Rayong and Prachinburi. Those bacterias were collected by plant pathologists from the department of agriculture, Thailand during 1983-2017 (Figure 1) were used in this study. Bacteria was cultured on YPGA (0.5 % yeast extract, 0.5 % peptone, 0.5 % glucose and 1.5 % agar) for 2 days before transferred to NYG (0.3% yeast extract, 0.5% peptone, 2% glycerol) broth for another 2 days at 28 °C under constant shaking. The genomic DNA of each isolate was extracted by CTAB method according to Bart et al., 2012 [12]. Briefly, cultures in NYGB were centrifuged to obtain bacterial cells at 10,000 rpm for 5 minutes. Then cells were lysed in SDS/CTAB extraction buffer before mixed with chloroform:isoamylalcohol (24:1) extraction. DNA was precipitated in isopropanol and washed with 70% ethanol. DNA pellet was collected and dissolved with RNase-sterilized distilled water. DNA quantity and quality were assessed by a combination of nanodrop and agarose gel electrophoresis.

PCR amplification and acrylamide gel electrophoresis using VNTR primers: Genomic DNA of *Xam* was amplified by PCR using 22 pairs of VNTR primers according to Arrieta-Ortiz *et al.*, 2013 [11]. PCR reactions were performed in a final volume of 25 µl containing 12.5 ng genomic DNA, 2.5 mM MgCl2, 100 nM PCR primers, 0.1 mM dNTP and 1 unit of *Taq* DNA polymerase (Vivantis). All reactions were run for 35 cycles, consisting an initial denaturation step of 3 min at 95 °C of, 20 sec at 95 °C, 30 sec at 52–58 °C (depending on the primer pairs), and 30–60 sec at 72 °C and a final extension step of 10 min at 72 °C. Genotyping was analyzed by 5% (w/v) polyacrylamide gel electrophoresis. The PCR products were electrophoresed at 1100 V until the PCR product moved to the appropriate positions indicated by loading dyes which related to the size of PCR product. Gel visualization was carried out by silver staining as described by Benbouza et al., 2006 [13]. Genotypic data were subjected to construct the phylogenic tree construction.

Genotyping data analysis: The genetic distance was calculated for distance- based clustering by Dice similarity index [14]. Then the distance tree was constructed by UPGMA (unweighted pair group method with arithmetic mean) and 100 for boot- strapping using Past3 1.0. Principal coordinates analysis (PCoA) was constructed by using the same genotypic data by Dice similarity index in Past3 1.0. Moreover, the distance heatmap of the same data set was constructed by RStudio 1.1.463.

3. RESULTS AND DISCUSSION

Genomic DNA samples of sixteen isolates of Thai's *Xam* were amplified and genotyped by

22 VNTR primer pairs. The acrylamide gel electrophoresis was performed to separate the PCR products. Amplified DNA bands were scored as a dominant type of present or absent at a particular level. The distance tree and the distance reciprocal comparison heatmap were constructed using those genotypic data (figure 2). The distance tree (figure 2A) representing the ancestor of *Xam* isolates was determined and classified into four clades. The biggest clade was clade number 2 which had 9 members and the solitary clade which was clade 3 only has *Xam*D as the member. When focused on each clade, there were different members origins in the same clade. Besides reciprocal comparison (figure 2B), some clades as *Xam*A, *Xam*C, and *Xam*G showed high similarity even those 3 isolates were collected from two different locations. Moreover, comparing between *Xam*51 and *Xam*716, the results also showed high similarity even these two isolates were from different locations and time collections. To clarify the results, the same distance data were used to construct the Principal coordinates plot (figure 3). The clustering from PCoA showed no relationship between a cluster and *Xam* origins that similar to the study of *Xam* in Colombia. Trujillo et al., 2014 [15] used five VNTR primer pairs to classify 101 *Xam* isolates from four locations in the Eastern Plain of Colombia. Their results also showed no relationship between distinct groups and the collected locations. Moreover, [16] focused on the population structure of *Xam* in the Caribbean region of Columbia by AFLP markers. Total 247 isolates from five locations which collected in 2008, 2009 and 2010 were used to study. Their results indicated that the cluster composed of isolates from the different collected locations. It is possible that similar *Xam* genetic were found in different locations might be due to transferring of stem cuttings as the propagation method of cassava from locations to others. In Thailand, planting materials for cassava propagation has traded between provinces which cause migration of *Xam*.

Isolate name	Collected year	Location (province)
A	2014	Nakhon Ratchasima
B	2014	Kamphaeng Phet
C	2014	Nakhon Ratchasima
D	2014	Rayong
E	2014	Kamphaeng Phet
F	2014	Kamphaeng Phet
G	2014	Kamphaeng Phet
H	2014	Rayong
PR1	2017	Prachinburi
PR2	2017	Prachinburi
PR3	2017	Prachinburi
51	1983	Rayong
535	1986	Prachinburi
716	1987	Nakhon Ratchasima
1460	1997	Rayong
2491	2014	Nakhon Ratchasima

Figure 1. Detail of 16 *Xam* isolates in this study including isolate name, collected year and location.

In terms of molecular technique, VNTR has been applied to study in *Xam* from Arrieta-Ortiz *et al.*, 2013 [11] which used *Xam* from 9 countries in their experiment. Then Trujillo *et al.*, 2014 [15] selected the top five high HGDI from the first one to study in Columbia. In this study, all of primer from [11] were utilized. Then data were subjected to calculated Hunter- Gaston discriminatory index (HGDI) [17] based on genotypic data of each VNTR locus. The most polymorphic was locus XaG1_29 (HGDI = 0.917) which could distinguish as 8 haplotypes. However, there were nine loci showed monomorphic (Table 1). The results of each experiment were compared in table 1. There were differences of HGDI numbers in the same VNTR loci, an indication some variations of the region in different *Xam* origins. Some VNTR loci were still high in every experiment indicating that this region was highly variable or had differences in isolate levels. Interestingly, some loci showed some differences from others

previous studies. For example when compared two loci from [11] and [15] (including XaG1_02 and XaG1_67) which showed a high HGDI score, but showed monomorphic (HGDI = 0) in this study. These results might cause by differentiation in that region that is conserved in the country. Moreover, XaG1_67 was proposed as a detection primer specific of *Xam* in Ghana [18] but also found in Thailand. Previously, [19] proposed the detection primers as XV/XK pair which were designed specifically for Transcription activator-like region. Whereas, this TAL region contains a high copy number of repetitive sequences [20] where more deletion or DNA slippage rate might occur in the replication process. When that primer were used to amplify in our sixteen isolates in this study, the results showed that some isolate had low amplification and differences in PCR product sizes (figure5). Therefore XaG1_67 had the potential to be a detecting primer which specific in Thailand's *Xam*.

4. CONCLUSION

We have classified 16 isolates of Thailand's *Xam* as four groups. Those groups show no relationship between the groups and the isolate's origins. When comparing differences in the VNTR regions by HGDI value, there are some differences in Thailand and Columbia. Those regions might be a conserve in a particular country. The results indicated that XaG1_67 VNTR locus that showed conserve in our samples might be able to develop as detecting primer for *Xam* in Thailand. However, additional *Xam* isolates should be included to confirm the constancy of this region.

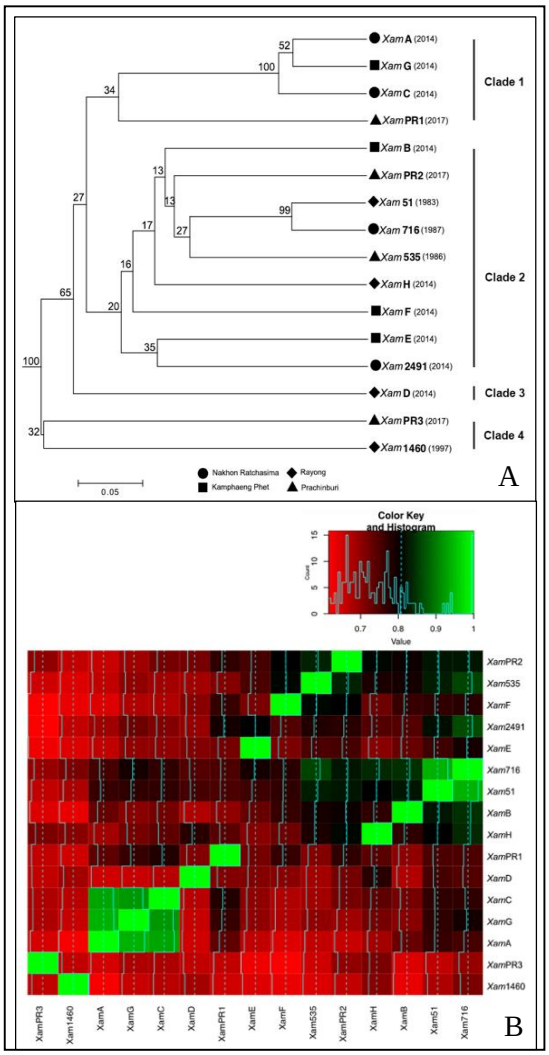

Figure 2. Phylogenetic tree of 16 *Xam* isolates. (A) Phylogenetic is constructed by Dice similarity coefficient include bootstrap values (from 100 replicates) at branch point and each isolate is indicated with shape according to collecting location.
(B) Heatmap of reciprocal Dice similarity coefficient.

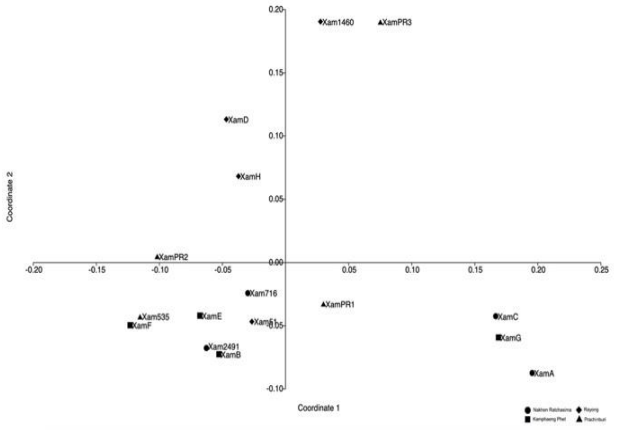

Figure 3. Principal coordinate analysis (PCoA) scatter plot (1st and 2nd axis) of sixteen *Xam* isolates. Distance matrix calculated using Dice similarity index [14] to construct PCoA by using Past3 (hammer, harper and ryan 2001). Transformation exponent c=2; similarity index: user distance; eigenvalue scale.

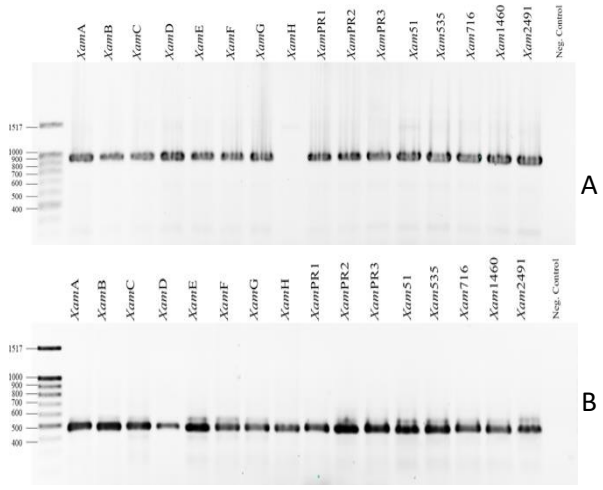

Figure 4. PCR product of sixteen *Xam* isolates on 1% agarose gel stained with ethidium bromide. A) XV/XK primer pair, B) XaG1_67 primer pair. Sterilized distilled water was used instead of DNA sample in PCR reaction as the negative control.

Table 1. Hunter-Gaston discriminatory index of each VNTR loci from Arrieta-Ortiz et al., 2013, Trujillo et al., 2014 and this study.

VNTR locus	HGDI score [11]	HGDI score [15]	HGDI score (from this study)
XaG1_02	0.894	0.7019	0.000
XaG1_12	0.635	-	0.867
XaG1_29	0.854	0.858	0.917
XaG1_58	0.658	-	0.667
XaG1_65	0.670	-	0.575
XaG1_67	0.900	0.8428	0.000
XaG1_70	0.773	-	0.675
XaG1_71	0.778	-	0.783
XaG1_72	0.710	-	0.242
XaG1_73	0.903	0.797	0.900
XaG2_50	0.774	-	0.717
XaG1_101	0.618	-	0.517
XaG1_105	0.694	-	0.517
XaG1_108	0.306	-	0.000
XaG1_110	0.523	-	0.000
XaG2_37	0.476	-	0.000
XaG2_52	0.839	0.5873	0.233
XaG2_55	0.146	-	0.000
XaG2_106	0.170	-	0.000
XaG2_109	0.486	-	0.125
XaG2_116	0.089	-	0.000
XaG2_117	0.031	-	0.000

5. ACKNOWLEDGEMENTS

For all of Xam isolates were identified and given from Dr. Nuttima Kositcharoenkul and Mr. Rungsi Charaensatapon as plant pathologist from Plant Protection Research and Development office, Field Crops Research Institute in Department of Agriculture,Thailand. Chotiros Phaisomboon, received scholarship from Development and Promotion of Science and Technology Talents Project (DPST), Thailand.

6. REFERENCES

[1] Gudesblat, E.G., S.P. Torres, and A.A. Vojnov, Stomata and pathogens warfare at the gates. Plant Signaling & Behavior, 2009. 4(12): p. 1114- 1116.

[2] Buttner, D. and U. Bonas, Regulation and secretion of Xanthomonas virulence factors. FEMS Microbiol Rev, 2010. 34(2): p. 107-33.

[3] Bock, C.H., P.E. Parker, and T.R. Gottwald, Effect of simulated wind- driven rain on duration and distance of dispersal of *Xanthomonas axonopodis* pv. citri from canker-infected citrus trees. Plant Dis, 2005. 89(1): p. 71-80.

[4] Wydra, K., A. Banito, and K.E. Kpémoua, Characterization of resistance of cassava genotypes to bacterial blight by evaluation of leaf and systemic symptoms in relation to yield in different ecozones. Euphytica, 2007. 155: p. 337-348.

[5] Lozano, J. C., Cassava bacterial blight a manageable disease. Plant Disease, 1986. 70(12): p. 1089-1093.

[6] Pitt, T. L. and M. R. Bare, Medical Microbiology. 18 ed. Classification, identification and typing of micro-organisms. 2012, London, UK: Churchill Livingstone.

[7] Vergnaud, G. and C. Pourcel, Multiple locus variable number of tandem repeats analysis. Methods Mol Biol, 2009. 551: p. 141-58.

[8] Parkinson, N., et al., Application of variable-number tandem-repeat typing to discriminate *Ralstonia solanacearum* strains associated with Englishwatercourses and disease outbreaks. Appl Environ Microbiol, 2013. 79(19): p. 6016-22.

[9] Essakhi, S., et al., Phylogenetic and Variable-Number Tandem-Repeat Analyses Identify Nonpathogenic *Xanthomonas arboricola* Lineages Lacking the Canonical Type III Secretion System. Appl Environ Microbiol, 2015. 81(16): p. 5395-410.

[10] Zhao, S., et al., Development of a variable number of tandem repeats typing scheme for the bacterial rice pathogen *Xanthomonas oryzae* pv. *oryzicola*. Phytopathology, 2012. 102(10): p. 948-56.

[11] Arrieta-Ortiz, M.L., et al., Genomic survey of pathogenicity determinants and VNTR markers in the cassava bacterial pathogen Xanthomonasaxonopodis pv. Manihotis strain CIO151. PLoS One, 2013. 8(11): p. e79704.

[12] Bart, R., et al., High-throughput genomic sequencing of cassava bacterial blight strains identifies conserved effectors to target for durable resistance. Proc Natl Acad Sci U S A, 2012. 109(28): p. E1972-9.

[13] Benbouza, H., et al., Optimization of a reliable, Fast, Cheap and sensitive silver staining method to detect SSR markers in polyacrylamidegels. Biotechnol. Agron. Soc. Environ., 2006. 10(2): p. 77-81.

[14] Dice, R. L., Measures of the amount of ecologic association between species. Ecology, 1945. 26(3): p. 297-302.

[15] Trujillo, C.A., et al., Population typing of the causal agent of cassava bacterial blight in the Eastern Plains of Colombia using two types of molecular markers. BMC Microbiology, 2014. 14: p. 161.

[16] Trujillo, C.A., et al., A complex population structure of the cassava pathogen *Xanthomonas axonopodis* pv. *manihotis* in recent years in the Caribbean Region of Colombia. Microb Ecol, 2014. 68(1): p. 155-67.

[17] Hunter, P. and M. Gaston, Numerical index of the discriminatory ability of typing systems: an application of Simpson' s index of diversity. J Clin Microbiol, 1988. 26: p. 2465–2466.

[18] Abdulai, M., et al., Detection of *Xanthomonas axonopodis* pv. *manihotis*, the causal agent of cassava bacterial blight diseases in cassava (*Manihot esculenta*) in Ghana by polymerase chain reaction. Eur J Plant Pathol, 2018. 150: p. 471-484.

[19] Verdier, V. , Detection of the cassava bacterial blight pathogen, *Xanthomonas axonopodis* pv. *manihotis*, by polymerase chain reaction. Plant Disease, 1998. 82: p. 79-83.

[20] Castiblanco, L. F. , et al. , TALE1 from *Xanthomonas axonopodis* pv. *manihotis* acts as a transcriptional activator in plant cells and is important for pathogenicity in cassava plants. Mol Plant Pathol, 2013. 14(1): p. 84-95.

CreTech 2020
8th International Conference on Creative Technology
Multidisciplinary
to Drive Economy and Social
http://utkcretech.rmutk.ac.th

The reduction of free fatty acid in coconut oil by using montmorillonite K-30 as the heterogeneous catalyst for biodiesel production

Siraprapa Chaleechat[1], Siriruk Maliruk[1], Piyanuch Nakpong[1*]

[1] Department of Chemistry, Rajamangala University of Technology Krungthep, Thailand
[*]Corresponding author. Email: piyanuch.n@mail.rmutk.ac.th

ABSTRACT

High free fatty acid (FFA) coconut oil is one of the attractive feedstocks for low cost biodiesel production, but the high FFA is the big obstacle for the commonly used production process (alkali-catalyzed transesterification). In this present study, the two-step acid-catalyzed esterification with methanol by using montmorillonite K-30 as the heterogeneous catalyst is employed for the reduction of FFA in coconut oil. The effects of four important variables, such as methanol amounts (20-50% v/v), catalyst amounts (0-11% w/v of oil), reaction temperatures 32-60 °C), and reaction times (0.5-3 h) on the esterification reaction were also investigated. The initial value of FFA content in coconut oil is 4.97% w/w and it was reduced to 2.53% w/w (49.09% conversion) in the first step with 50% v/v of methanol, 5% w/v of oil of catalyst, 60°C and 2 h. Finally, the FFA content was reduced to 1.37% w/w (45.85% conversion) in the second step under the same condition as used in the first step except for the catalyst amount of 7% w/v of oil. The results from the acid-catalyzed esterification in the first step revealed that the four studied variables had a positive effect on the reaction except when the catalyst amounts in the range of 7-11% w/v of oil were used.

Keywords: Montmorillonite K-30, Free fatty acid, Acid-catalyzed esterification, Coconut oil

1. INTRODUCTION

In the present day, biodiesel is a very important alternative and renewable fuel used in a diesel engine. It is similar to fossil diesel and can be used as pure biodiesel (B100) or mixing with regular diesel (BXX). The demand for biodiesel in Thailand is forecast to increase due to the increasing number of diesel vehicles on Thai transport sector. The use of biodiesel has many advantages such as develop the use of domestic alternative energy, increasing energy security and agriculturist incomes. Due to the higher flash point of biodiesel, it is safer than fossil diesel in the case of a crash, storage and transportation. In addition, it has many environmentally beneficial properties include producing no net output of carbon in the form of carbon dioxide (CO_2), completely non-toxic and biodegradable. In the commercial process, almost all biodiesel is produced from vegetable oil, animal oil/ fats, tallow, and waste cooking oil by alkali-catalyzed transesterification with short chain alcohol. It is the most economical process in which strong alkaline like sodium hydroxide and methanol were often used as catalyst and alcohol, respectively. The transesterification process converts a big molecule of triglyceride into a smaller molecule of fatty acid methyl ester or biodiesel. The alkali-catalyzed transesterification reaction for producing methyl ester is shown in equation 1.

The transesterification process for biodiesel production is one of the sources of glycerol

because the large quantity of glycerol is produced as a coproduct. The glycerol is the valuable chemical used in the cosmetic, pharmaceutical, soap, and chemical industries.

Nowadays, there are many varieties of oil crops which are the base for biodiesel production via the alkali-catalyzed transesterification process. These oil crops include palm, coconut, soybean, cottonseed, corn, rapeseed, canola, mustard, flax, jatropha, roselle, and sunflower. These days, crude palm oil is mainly used in biodiesel production in Thailand. It's well known that oils or fats used as feedstock for the alkali-catalyzed transesterification process must be anhydrous and has low FFA content (less than 1% w/w) [1]. However, these quality feedstocks have a high price which resulted in high biodiesel production cost. For this reason, the lower quality and price of oils with high FFA content were used as feedstocks instead. One of the potential feedstocks is the high FFA coconut oil. Coconut is one of the most important crops of Thailand and the Southern and Eastern regions have the largest planted area of coconut in Thailand. After harvesting, if the coconut is stored in a high humidity environment, the triglyceride of coconut oil is lipase-catalyzed hydrolysis to produce the FFA. This resulted in the increasing of FFA in oil. The low quality of coconut oil containing high FFA is easily available at low price. Therefore, it is the high potential alternative feedstock for biodiesel production. However, this low quality coconut oil cannot be directly used as feedstock in alkali-catalyzed transesterification process due to soap formation during the reaction. The soap is produced from the reaction between FFA and alkaline catalysts. It is the major barrier in biodiesel production which resulted in the decrease of biodiesel yield and increase of operating cost. Thus, the two-step process, acid-catalyzed esterification followed by alkali-catalyzed transesterification is employed. In the first step, coconut oil is pretreated by the acid-catalyzed esterification with methanol for the reduction of FFA content to less than 1% w/w. The esterification between FFA and methanol to produced methyl ester is shown in the equation below.

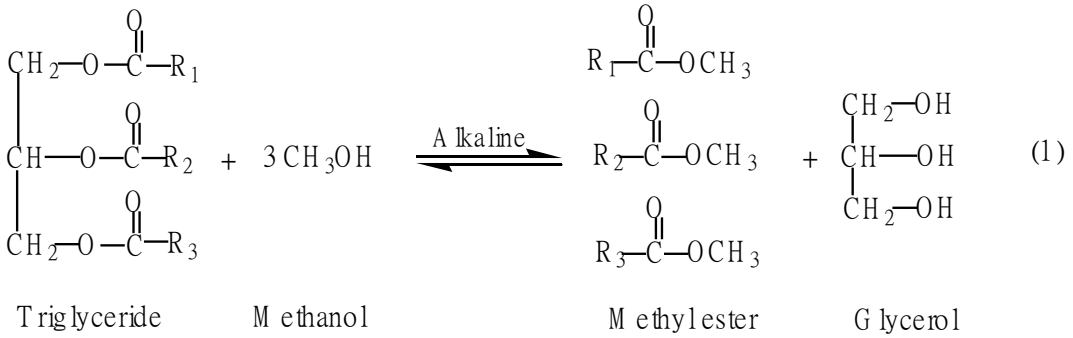

(1)

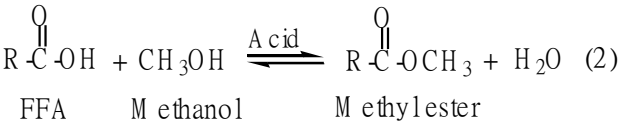

(2)

After that, the coconut oil with low FFA content is subjected to transesterification with methanol in the presence of an alkaline catalyst for converting triglyceride to methyl ester as shown in equation 1. In the esterification step, the most commonly preferred acid catalyst is sulfuric acid which is the homogeneous catalyst. However, using this strong liquid acid has many drawbacks such as corrosion, difficult to recycle, operating at high temperature, toxicity, much water required for product washing, and water treatment system required for a lot of waste water. To avoid these drawbacks, the solid acid catalysts (heterogeneous catalysts) are used to replace the liquid acids. The acid heterogeneous catalysts offer significant advantages of eliminating the environmental

problems, product washing step, corrosion, and toxicity[2]. In addition, these catalysts can be easily separated from the reaction mixture by filtration and some of them can be recycled and reusable. Thus, they recently draw researcher's attention. Several acid heterogeneous catalysts have been proposed to catalyze the esterification of fatty acid and alcohol such as montmorillonite K-10 [3], SO_3H-carbon catalyst derived from glycerol [4] , sulfonated polystyrene compounds (SPS) [5], poly (vinyl alcohol) cross-linked with sulfosuccinic acid (SSA) [6], and sulfonic acid-containing catalyst derived from carbohydrate [7,8]. Recently acid-treated montmorillonite was applied in the catalytic esterification of oleic acid with ethanol. The results revealed that the acid-treated montmorillonite showed promising catalytic activity toward the reaction, with the maximum conversion of oleic acid of 65% at 30 °C [9].

At present, acid-treated montmorillonites can be purchased from a variety of commercial sources and they denoted as K-clays (K-5, K-10, K-20, K-30) [10]. The acid-treated montmorillonites were used for several important reactions both on laboratory and industrial scales as the heterogeneous catalysts [11]. However, no research is reported about using montmorillonite K-30 as a solid acid catalyst for esterification of FFA in vegetable oil with methanol. Hence, in this present research, the study of the reduction of FFA content in coconut oil was done via esterification reaction with methanol by using montmorillonite K-30 as a heterogeneous catalyst. The objectives of this study were: (a) To investigate the optimum reaction conditions for the reduction of FFA in coconut oil, and (b) To study the effects of the important variables on the reaction.

2. MATERIALS AND METHODS

The unrefined coconut oil feedstock was obtained from Sangsook Industry Company Limited, Bangkok,Thailand. Montmorillonite K-30 (in powder form) was purchased from Sigma-Aldrich. Absolute ethanol was purchased from Liquor distillery organization, Bangkok, Thailand. Methanol, sodium hydroxide, potassium hydrogen phthalate, and phenolphthalein were purchased from Ajax Finechem Pty Ltd. All chemicals used in this study such as methanol, absolute ethanol, sodium hydroxide, potassium hydrogen phthalate, and phenolphthalein were analytical reagent grade and used without any pretreatment.

Preparation of coconut oil

Pretreatment of coconut oil was done by heating at 60 ºC and then filtered with Whatman filter paper No.93 to remove impurities. After that, the FFA content in coconut oil was determined by the standard method AOAC Official Method 940.28 (AOAC 2012).

Acid-catalyzed esterification of FFA in coconut oil

In this study, the acid-catalyzed esterification of FFA with methanol by using montmorillonite K-30 as catalyst was conducted to investigate the optimum conditions for the reduction of FFA content in coconut oil. Besides, the effects of important variables on the reaction were also studied. The FFA reduction process composed of two steps. In the first step, the important variables affecting the esterification such as methanol amounts (20, 30, 40, and 50% v/v), catalyst amounts (0, 1, 3, 5, 7, 9, and 11% w/v of oil), reaction temperatures (32, 40, 50, and 60 ºC), and reaction times (0.5, 1, 2, and 3 h) were optimized. In the second step, 6 catalyst amounts of 0, 5, 7, 9, 11, and 13% w/v of oil were used to investigate the optimum conditions for the further reduction of FFA in coconut oil.

The acid-catalyzed esterification reaction was carried out in a laboratory-scale experiment under the atmospheric pressure. First, coconut oil was charged into the 250 mL three-necked flat-bottom flask and heated to the desired temperature under the constant stirring speed by using hotplate with a magnetic stirrer. One neck of the flask was equipped with a reflux condenser which used to

condense the methanol vapor back to the reaction mixture. The two other necks were used for catalyst feeding and equipped with a thermometer. After that, methanol and montmorillonite K-30 were added to the coconut oil and the reaction time was started at this point. After completion of the reaction, the reaction mixture was poured into the separatory funnel and allowed to settle overnight. The reaction mixture was clearly separated into three layers. The top layer was the mixture of residual methanol and water produced from the esterification reaction. The middle layer contained coconut oil, a trace of unreacted methanol, and water whereas the bottom layer was the spent catalyst. The coconut oil layer was separated and subjected to heat at 110 °C to remove methanol and water. Then, the oil product was filtrated with Whatman filter paper No.93 to remove the impurities. Finally, the clear coconut oil product was obtained and the remained FFA in oil was determined by AOAC Official Method 940.28 (AOAC 2012).

3. RESULTS AND DISCUSSION

The coconut oil feedstock obtained from Sangsook Industry Company Limited is an unrefined type. It was viscous liquid with brown in colour. There were some small suspended solids in oil. After pretreatment step, suspended solids were remove by filtration and the clear, viscous, and brown liquid was obtained. The initial FFA content of coconut oil was 4.97% w/w (as lauric acid). The triglyceride of coconut oil composed of three kinds of fatty acid. These included saturated fatty acid, monounsaturated fatty acid, and polyunsaturated fatty acid. The fatty acid composition of coconut oil is shown in table 1.

Therefore, during esterification by using montmorillonite K-30 as a catalyst, the FFAs reacted with methanol to form methyl esters such as methyl laurate, methyl myristate, and methyl oleate as shown in Scheme 1.

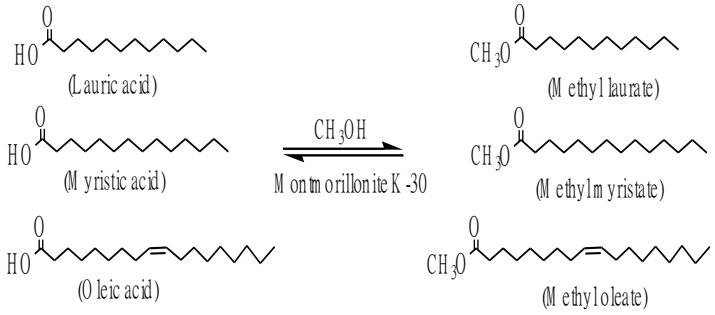

Scheme 1. Acid-catalyzed esterification

Coconut oil is the highest natural source of medium chain fatty acid (lauric acid). Thus, coconut oil biodiesel has a lower viscosity than biodiesel produced from other vegetable oils. Besides, the viscosity of coconut biodiesel was very close to Thai petrodiesel [12].

Table 1. Fatty acid composition of coconut oil [12]

Fatty acid	Structure (xx:y)	Chemical formula	Percentage (%)
Caprylic acid	8:0	$C_8H_{16}O_2$	3.35
Capric acid	10:0	$C_{10}H_{20}O_2$	3.21
Lauric acid	12:0	$C_{12}H_{24}O_2$	32.72
Myristic acid	14:0	$C_{14}H_{28}O_2$	18.38
Palmitic acid	16:0	$C_{16}H_{32}O_2$	13.13
Stearic acid	18:0	$C_{18}H_{36}O_2$	3.60
Oleic acid	18:1	$C_{18}H_{34}O_2$	12.88
Linoleic acid	18:2	$C_{18}H_{32}O_2$	4.35

xx indicates number of carbons.
y indicates number of double bonds in the fatty acids chain.

Acid-catalyzed esterification : Step 1

The effect of methanol amount

The esterification reaction between the FFA and methanol is a reversible reaction and so the excess of methanol must be added to drive the reaction towards the right to ensure the complete reaction. Hence, the effect of methanol amounts of 20, 30, 40, and 50% v/v (1:4, 1:7, 1:11, and 1:17 molar ratio of FFA/methanol, respectively) on the esterification of FFA were studied in the presence of 5% w/v of oil of montmorillonite K-30 at 60 °C for 2 h. The results were shown in Figure 1.

It can be seen clearly from Figure 1 that the methanol amount is one of the important variables that influence the esterification reaction. The increase in the methanol amount from 20-50% v/v consecutively increases the FFA conversion.

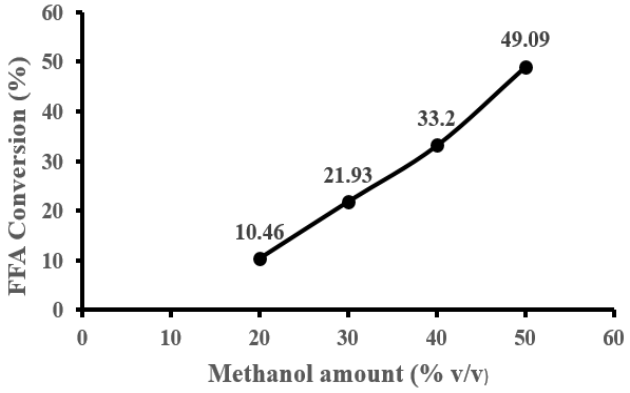

Figure 1. Variation of the FFA conversion with methanol amount.

The highest FFA conversion was reached at the methanol content of 50% v/v (1:17 molar ratio of FFA/methanol) and at this point, the FFA remained in the coconut oil 2.53% w/w. These results can be explained by Le Chatelier's Principle. The equilibrium shifted to the right towards the side of the products when the methanol amount increased. In addition, these results are supported by the collision theory. As the amount of methanol increased, the frequency of successful collisions of the reactants would increase as well. It resulted in the increase of the forward reaction and thus, the more methyl ester product was generated. Moreover, when the excess of methanol was employed, the viscosity of the reaction system was reduced. This resulted in the promotion of the rate of reaction due to the better mixing between coconut oil, methanol, and montmorillonite K-30. Therefore, the optimum methanol amount was 50% v/v.

The effect of catalyst amount

In this research, montmorillonite K-30 was used as a catalyst in the esterification reaction of FFA. Montmorillonite K-30 is one type of the acid-treated montmorillonite clays which pH 2.8-3.8 and surface area ~ 330 m^2/g. Chemical analysis of montmorillonite K-30 is shown in table 2.

The effect of catalyst amount on acid-catalyzed esterification of FFA was studied by varying catalyst amount from 0-11% w/v of oil while the methanol amount, reaction temperature, and reaction time were kept constant at 50% **v/v,** 60 °C, and 2 h, respectively. The results were shown in Figure 2.

Table 2 Chemical analysis of montmorillonite K-30 [10]

Composition	%	Composition	%
SiO_2	80.0	MgO	1.0
Al_2O_3	10.0	Na_2O	0.3
Fe_2O_3	1.8	K_2O	0.5
CaO	0.2	Loss on ignition	6.0

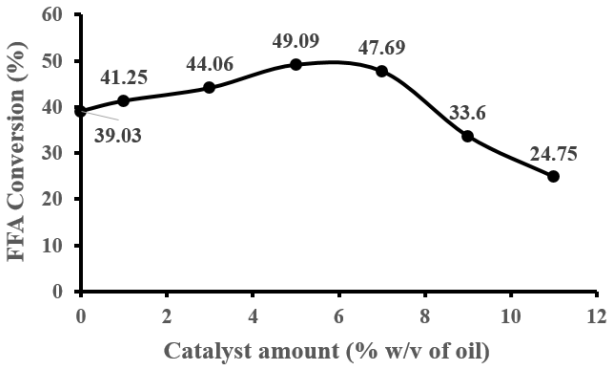

Figure 2. Variation of the FFA conversion with catalyst amount.

The results indicated that the esterification of FFA in coconut oil with methanol could have occurred from the autocatalysis whereby the reaction was catalyzed by the FFA in coconut oil. However, the rate of reaction was slow and only 39.03% FFA conversion was obtained. When the catalyst was used, the rate of reaction was increased. The conversion of FFA increased with the increase of the catalyst amount and the highest conversion was observed with a catalyst amount of 5% w/v of oil. At this point, the lowest FFA

content (2.53% w/w) was obtained. After the catalyst amount of 5% w/v of oil, the conversion of FFA was decreased when the catalyst amount increased. This is due to the using of a high catalyst amount (7-11% w/v of oil) accelerated the rate of reaction which led to the formation of a large amount of water. Thus, according to Le Chatelier's principle, the equilibrium shifted to the left which resulted in the formation of FFA. The 5% w/v of oil of catalyst was found to be optimum because it provided the highest conversion of FFA.

The effect of reaction temperature

The reaction temperature is one of the important variables that affect the reaction rate of the esterification. In this research, the effect of reaction temperature on the esterification of FFA in coconut oil was studied in the range of 32 (room temperature)-60 °C using methanol amount of 50% v/v, catalyst amount of 5% w/v of oil, and reaction time of 2 h. The results were shown in Fig 3.

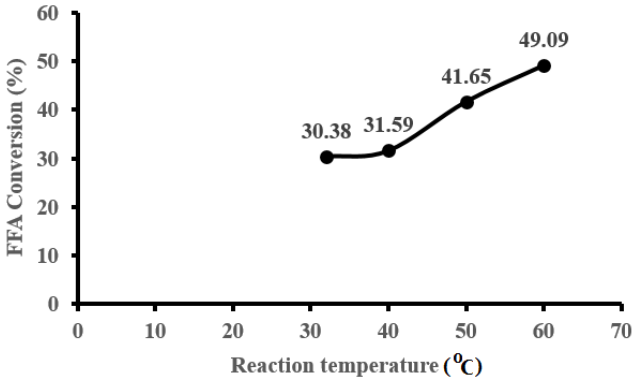

Figure 3. Variation of the FFA conversion with reaction temperature.

As can be seen from Fig 3, montmorillonite K-30-catalyzed esterification of FFA in coconut oil could occur at 32 °C, but the reaction was incomplete. An increase in reaction temperature accelerated the reaction towards the methyl ester formation. Therefore, the FFA conversion was consecutively increased when the temperature increased. This could be explained that esterification is the endothermic reaction [13] in which heat is absorbed in the reaction. When the temperature increased, it caused the forward reaction to occur. This resulted in increasing the amount of methyl ester and decreasing the amount of FFA in oil. In addition, an increase in the reaction temperature increased the kinetic energy of the reactant particles. This resulted in the increase in the number of successful collisions between the molecules of reactants, which led to the increase in rate of FFA conversion. The maximum conversion was reached at 60 °C. Thus, it was the optimum reaction temperature.

The effect of reaction time

The effect of reaction time on the completion of the acid-catalyzed esterification of FFA was studied by varying reaction time from 0.5-3 h. The experiment was carried out by fixing the methanol amount of 50% v/v, catalyst amount of 5% w/v of oil, and reaction temperature of 60 °C. The results were shown in Fig 4.

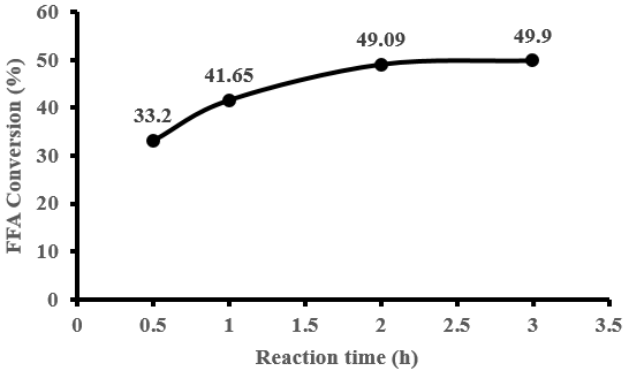

Figure 4. Variation of the FFA conversion with reaction time.

It can be observed that when the short reaction time (0.5 h) was used, the acid-catalyzed esterification of FFA was incomplete. An increase in the reaction time led to more completion of the esterification reaction which resulted in the increase of FFA conversion. From the economic point of view, 2 h. was selected as the optimum reaction time.

Hence, the optimum conditions obtained from the Acid-catalyzed esterification : Step 1 were

methanol amount of 50% v/v, catalyst amount of 5% w/v of oil, reaction temperature of 60 °C and reaction time of 2 h. At these conditions, FFA conversion was 49.09% and the FFA content was reduced from the initial value to 2.53% w/w.

Acid-catalyzed esterification : Step 2

As can be seen that the FFA content in coconut oil was not reduced to less than 1% w/w (limit of FFA content in oil feedstock for alkaline-catalyzed transesterification) by the Acid-catalyzed esterification : Step 1. Hence, further study was performed by using the Acid-catalyzed esterification : Step 2. First, the coconut oil having FFA content of 2.53% w/w was produced by using the optimum conditions of Acid-catalyzed esterification : Step 1. After that, the oil was subjected to further reduction of FFA content by esterification with methanol by using the montmorillonite K-30 as a catalyst. The experiments were conducted by varying the catalyst amount from 0-13% w/v of oil while the methanol amount, reaction temperature, and reaction time were kept constant at 50% v/v, 60 °C, and 2 h, respectively. The results were shown in Figure 5.

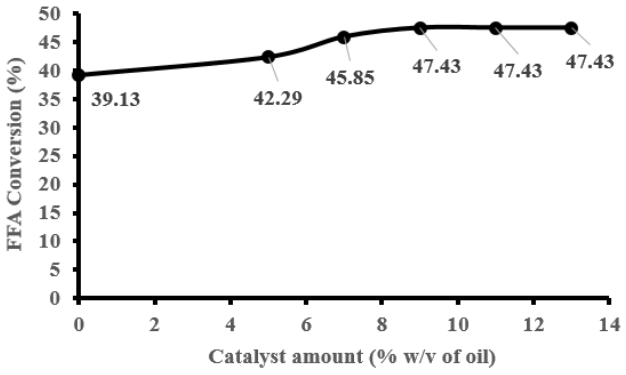

Figure 5. Variation of the FFA conversion with catalyst amount in Acid-catalyzed esterification : Step 2

The results showed that after the Acid-catalyzed esterification : Step 2, the FFA content in coconut oil was not reduced to less than 1% w/w. However, catalyst amounts in the range of 7-11% w/v of oil provided the highest FFA conversion in which the FAA content in oil was 1.33% w/w. From the economic point of view, 7% w/v of oil was selected as the optimum catalyst amount. At this point, the FFA content in coconut oil was reduced from the initial value of 4.97% w/w to 1.37% w/w with the FFA conversion of 47.43%.

4. CONCLUSIONS

In conclusion, this study revealed that the FFA content in coconut oil could be reduced 72.84% from the initial value by the two-step montmorillonite K-30-catalyzed esterification with methanol. In the first step, the FFA content was reduced from the initial value of 4.97 to 2.53% w/w (49.09% FFA conversion) under the optimum conditions of 50% v/v of methanol, 5% w/v of oil of catalyst, 60 °C and 2 h. In the second step, the FFA content was further reduced to 1.37% w/w under the conditions of 50% v/v methanol, 7% w/v of oil of catalyst, 60 °C and 2 h. All of the variables studied in the Acid-catalyzed esterification : Step 1 had a positive effect on the reaction except when the three catalyst amounts of 7, 9, and 11% w/v of oil were used, the negative effect was obtained. Montmorillonite K-30 could be one of the alternative acid heterogeneous catalysts for the reduction of FFA in high FFA containing vegetable oils via acid-catalyzed esterification. However, the FFA content in oils does not exceed 4.97% w/w and the optimum conditions for the reduction of FFA content to less than 1% w/w should be investigated for the future work.

5. ACKNOWLEDGMENTS

The authors wish to thank the Sangsook Industry Company Limited, which provided coconut oil feedstock and Rajamangala University of Technology Krungthep (Bangkok, Thailand) for the financial support.

6. REFERENCES

[1] Johanes BH, Shizuko HH. Biodiesel production from crude Jatropha curcas L. seed oil with a high content of free fatty acids. Bioresource Technology 2008; 99:1716-21.

[2] Lou WY, Zong MH, Duan ZQ. Efficient production of biodiesel from high free fatty acid-containing waste oils using various carbohydrate-derived solid acid catalysts. Bioresource Technology 2008; 99:8752-8.

[3] Kanda LRS, Corazza M L, Zatta L, et al. Kinetics evaluation of the ethyl esterification of long chain fatty acids using commercial montmorillonite K10 as catalyst. Fuel 2017; 193: 265-74.

[4] Prabhavathi Devi BLA, Vijai Kumar Reddy T, Vijaya Lakshmi K, et al. A green recyclable SO_3H-carbon catalyst derived from glycerol for the production of biodiesel from FFA-containing karanja (Pongamia glabra) oil in asinglestep. Bioresource Technology 2014; 153:370-3.

[5] Soldi RA, Oliveira ARS , Ramos LP , et al. Soybean oil and beef tallow alcoholysis by acid heterogeneous catalysis. Applied Catalysis A: General 2009; 361:42-8.

[6] Caetano CER, Guerreiro L, Fonseca IM, et al. Esterification of fatty acids to biodiesel over polymers with sulfonic acid groups. Applied Catalysis A General 2009; 359:41-6.

[7] Mar WW, Somsook E. Sulfonic-functionalized carbon catalyst for esterification of high free fatty acid. Procedia Engineering 2012; 32: 212-8.

[8] Chen G, Fang B. Preparation of solid acid catalyst from glucose- starch mixture for biodiesel production. Bioresource Technology 2011; 102:2635-40.

[9] Nascimento AR, Alves JABLR, Freitas Melo MA, et al. Effect of the acid treatment of montmorillonite clay in the oleic acid esterification reaction. Materials Research 2015; 18:283-287.

[10] Flessner U, Jones DJ, Rozière J, et al. A study of the surface acidity of acid-treated montmorillonite clay catalysts. Journal of Molecular Catalysis A: Chemical 2001; 168: 247–56.

[11] Ayouba M, Ullaha S, Inayatd A, et al. Process optimization for biodiesel production from waste frying oil over montmorillonite clay K-30. Procedia Engineering 2016; 148:742-9.

[12] Nakpong P, Wootthikanokkhan S. High free fatty acid coconut oil as a potential feedstock for biodiesel production in Thailand. Renewable Energy 2010; 35:1682-7.

[13] Yaakob AQ, Bhatia S. Esterification of palmitic acid with methanol in the presence of macroporous ion exchange resin as catalyst. IIUM Engineering Journal 2004; 5:35-51.

CreTech 2020
8th International Conference on Creative Technology
Multidisciplinary to Drive Economy and Social
http://utkcretech.rmutk.ac.th

Hydrogen sulfide gas sensor based on Cadmium and Zinc ferrite nanoparticles

Pranrawee Sukhan[1]*, Chaikarn Liewhiran[2,3]

[1] Program in Materials Science, Faculty of Science, Maejo University, Chiang Mai, 50290, Thailand.
[2] Departments of Physics and Materials Science, Faculty of Science, Chiang Mai University, Chiang Mai, 50200, Thailand
[3] Center of Excellence in Materials Science and technology, Chiang Mai University, Chiang Mai, 50200, Thailand
*Corresponding author. E-mail: tamaekong.nittaya@gmail.com

ABSTRACT

Cadmium and zinc ferrite nanoparticles were prepared by co-precipitation. The crystal structure and morphology of the samples characterized by mean of X-ray diffraction (XRD), transmission electron microscope (TEM). The corresponding X-ray diffraction peaks confirm the formation of cubic spinel structure of $CdFe_2O_4$ and $ZnFe_2O_4$. The $CdFe_2O_4$ and $ZnFe_2O_4$ nanoparticles show spherical nanostructures with the average size of 22 and 23, respectively. The gas sensing properties of the samples were also investigated. The results reveal that the $CdFe_2O_4$, can increase efficiency sensitivity to hydrogen sulfide gas up to 12 at 10 ppm. The gas response was investigated in the temperature of 350°C toward hydrogen sulfide gas concentrations.

Keywords:Cadmium, Zinc ferrite, Nanoparticles, Hydrogen sulfide.

1. INTRODUCTION

Spinel-type oxide with a formula of AB_2O_4 is important complex oxide in gas-sensing materials. The literature has reported $CdFe_2O_4$ sensor to show a high response to dilute CH_3SH and ethanol. The response of $CdFe_2O_4$ sensor prepared by chemical precipitation method was more than 20 to 100 ppm ethanol at 300ºC. And the Ag doped $CdFe_2O_4$ sensor prepared by sol–gel response was 39.18 to 45 mol.L^{-1} (about 1000 ppm) ethanol at 330ºC [1]. In this study, $CdFe_2O_4$ powder was prepared by sol-gel method, and its response to 100 ppm ethanol was 55 at 250ºC.

Many works on spinel ferrites for gas sensor application have been carried out [2–4]. Among spinel ferrites, spinel zinc ferrite ($ZnFe_2O_4$), a typical normal spinel with Zn^{2+} ions distributed on the tetrahedral Asites and Fe^{3+} ions located on the octahedral B-sites, is a promising material for detecting gases because of its good chemical and thermal stability, low toxicity, high specific surface area and excellent selectivity [5–8]. The gas-sensing properties of sensors based on pure $ZnFe_2O_4$ to acetone gas have been investigated. It is reported that the response to acetone vapor (50,000 ppm) of sensor based on $ZnFe_2O_4$ prepared by sol–gel method is 8 at 550 °C [8]. Sensors based on $ZnFe_2O_4$ materials with other nanostructures, such as nanoparticles, nanospheres and nanosheets have been investigated with many gases, including H_2S gas [9–13]. For instance, Zhou et al. [14] reported that gas sensors based on porous $ZnFe_2O_4$ nanospheres synthesized by solvothermal methods exhibit high response of 11.8 to 30 ppm acetone at 200 °C but low response of 1.6 to H_2S at the same concentration and temperature.

2. MATERIALS AND METHODS

2.1 Particles synthesis and characterization

The $CdFe_2O_4$ and $ZnFe_2O_4$ were prepared as follows. The nitrate of Cd or Zn and iron were dissolved in water at the designated molar ratio Cd/Feor Zn/Fe (1:2). To this solution, a 6 M NaOH solution was added at 70°C under stirring for aging for 1 h, the resulting precipitate (hydroxides) was collected by centrifugation, washed thoroughly with distilled water to adjust the pH neutral and dried at 120°C. Finally, the precursor was calcined twice at 400°C for 1 h and 600°C for 2 h to form the $CdFe_2O_4$ and $ZnFe_2O_4$.

The samples were characterized by X-ray diffraction (XRD, Rigaku, TTRAXIII diffractometer), scanning electron microscopy (SEM, JEOL JSM-6335F), energy-dispersive x-ray spectroscopy (EDS) and transmission electron microscopy (TEM).

2.2 Preparation of thick films and sensing test

Paste for sensing film fabrication was prepared by mixing the nanoparticles into an organic solution composed of ethyl cellulose and α-terpineol, which acted as a vehicle binder and solvent, respectively. The resulting paste was spin-coated on Al_2O_3 substrates with predeposited interdigitated Au electrodes. The films were then annealed at 450°C for 2 h (with heating rate of 2 °C/min) for binder removal. The particle size of films was grown slightly after the films were annealed at 450°C in air. An external NiCr heater was heated by a regulated dc power supply to different operating temperatures. The operating temperature was varied from 200°C to 350°C. The resistances of various sensors were continuously monitored with a computer-controlled system by voltage-amperometric technique with 5 V dc bias and current measurement through a picoammeter. The sensors were characterized towards H_2S in the concentration ranging from 0.5 to 10 ppm. The sensors were exposed to a gas sample for ~5 minutes at each gas concentration and then the air flux was restored for 15 min. The gas sensing behaviors were analyzed in term sensor response defined as the ratio of the original resistance in air to the resistance of a sample upon exposure to the gas for is reducing gas (H_2S).

3. RESULTS AND DISCUSSION

3.1 Characterization

The crystallographic structure of $CdFe_2O_4$ and $ZnFe_2O_4$ nanostructure were characterized by powder XRD (Philips X-ray diffractometer) with a 1.5 kW Cu X-ray source, 2θ range of 10°–60°, scan step of 0.02°. Figure 1. showed the XRD patterns of $CdFe_2O_4$ and $ZnFe_2O_4$nanoparticles. All samples exhibit sharp and pronounced XRD peaks, indicating high degree of crystallinity. The corresponding X-ray diffraction peaks for (111), (220), (311), (422) and (511) planes confirm the formation of cubic spinel structure of $CdFe_2O_4$ (JCPDS Card No. 79–1155) and the corresponding X-ray diffraction peaks for (111), (220), (311), (400), (422) and (511) planes confirm the formation of cubic spinel structure of $ZnFe_2O_4$ (JCPDS Card No. 80–1012).

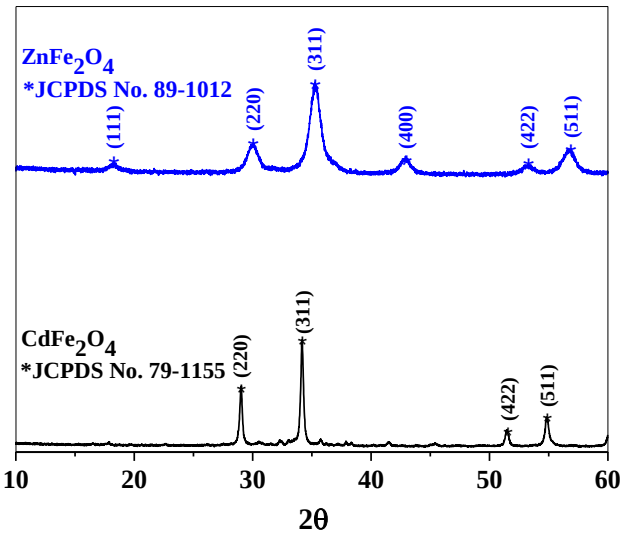

Figure 1. Showed the XRD patterns of $CdFe_2O_4$ and $ZnFe_2O_4$ nanoparticles.

Figure 2. The crystallinity of (a) $CdFe_2O_4$ and(b) $ZnFe_2O_4$nanoparticles were examined by TEM and the selected area electron diffraction (SAED) pattern. The morphology of $CdFe_2O_4$ were spherical and quadrilateral particles with diameter of about 10–20 nm and width of 30–50 nm, length of 30– 50 nm, respectively. For $ZnFe_2O_4$ were spherical particles with diameter of about 10-30 nm.

The corresponding HR-TEM images (right) of samples showed lattice fringes on various nanoparticles whose d-spacings were matched with various planes of the $CdFe_2O_4$ and $ZnFe_2O_4$ phase, in accordance with those observed in the XRD patterns (Figure 1).

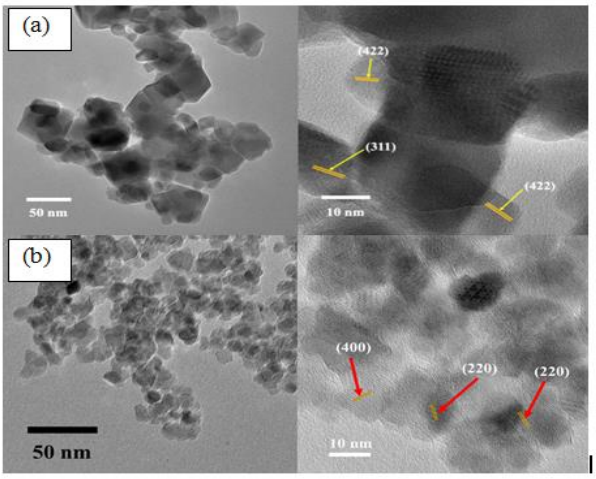

Figure 2.HR-TEM images of (a) $CdFe_2O_4$ and (b) $ZnFe_2O_4$ nanoparticles.

3.2 Gas Sensing Properties

The effect of operating temperature ranging from 200 to 350 °C on the response to 10 ppm hydrogen sulfide (H_2S) of $CdFe_2O_4$ and $ZnFe_2O_4$gas sensors were demonstrated in Figure 3. The responses of all sensors increase monotonically with increasing the operating temperature. In particular, the $CdFe_2O_4$ sensor exhibits the highest response of 12 to 10 ppm H_2S at the operating temperature of 350°C.

The $CdFe_2O_4$ sensing film was smaller band gap energy than $ZnFe_2O_4$ significantly enhances H_2S response. Therefore, the band gap was a major factor determining the electrical conductivity of sensor. The sensor with small band gap significantly enhances electrical conductivity, because of the valence and conduction bands were nearly overlap.

The corresponding sensing characteristics in terms of response time of $CdFe_2O_4$ and $ZnFe_2O_4$ sensors as a function of H_2S concentration showed in second.

In firure 4, the responses of $CdFe_2O_4$ and $ZnFe_2O_4$ sensors were linearly increased with concentration of H_2S were increased. The $CdFe_2O_4$ sensor showed the higher response than $ZnFe_2O_4$ sensors. On the other hand, in term of response time of $CdFe_2O_4$ and $ZnFe_2O_4$ sensors were slightly decreased with concentration of H_2S were increased.

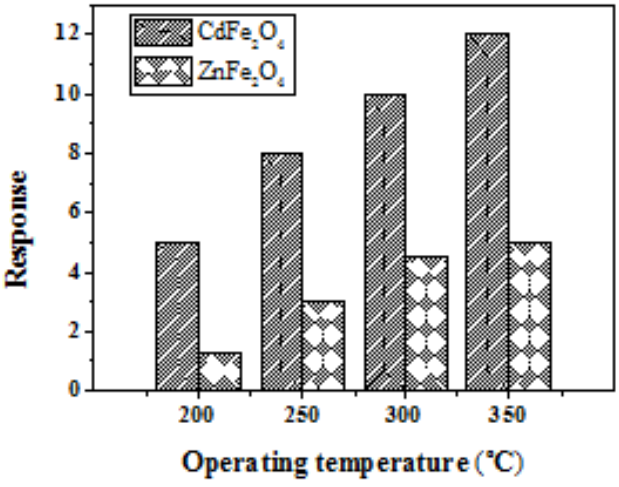

Figure 3. The responses of $CdFe_2O_4$ and $ZnFe_2O_4$ sensors at 200-350 °C to 10 ppm of H_2S.

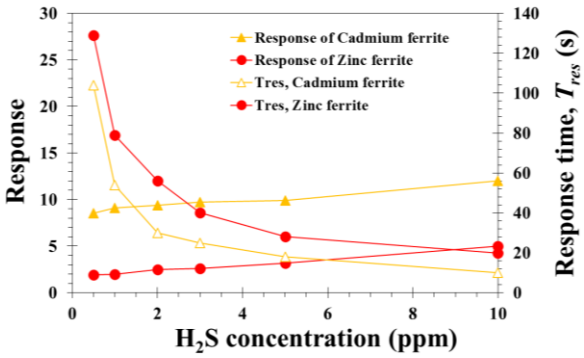

Figure 4. The responses and response time of CdFe2O4 and ZnFe2O4 sensors at 350°C to 0.5-10 ppm of H2S

4. CONCLUSIONS

In conclusion, gas-sensing characteristics of $CdFe_2O_4$ and $ZnFe_2O_4$ nanoparticles were systematically investigated. XRD studies confirmed that the nanoparticles are highly crystalline with the cubic spinel phase of $CdFe_2O_4$ and $ZnFe_2O_4$. Gas-sensing studies showed that $CdFe_2O_4$ nanoparticles sensor can greatly improve the H_2S response.

5. ACKNOWLEDGMENTS

The authors gratefully acknowledge the Program in Materials Science, Faculty of Science, Maejo University. And we wish to thank the Center of Excellence in Materials Science and Technology, Chiang Mai University for financial support under the administration of Materials Science Research Center, Faculty of Science, Chiang Mai University.

6. REFERENCES

[1] Lou X, Liu S, Shi D, Chu W. Ethanol-sensing characteristics of $CdFe_2O_4$ sensor prepared by sol–gel method. Mater Chem Phys 2007; 105:67–70.

[2] Sun Z, Liu L, Zeng Jia D, Pan W. Simple synthesis of $CuFe_2O_4$ nanoparticles as gas-sensing materials. Sens Actuators B 2007; 125:144–148.

[3] Patil JY, Nadargi DY, Gurav JL, Mulla IS, Suryavanshi SS. Synthesis of glycine combusted $NiFe_2O_4$ spinel ferrite: a highly versatile gas sensor. Mater Lett 2014; 124:144–147.

[4] Li Z, Huang Y, Zhang S, Chen W, Kuang Z, Ao D, Liu W, Fu Y. A fast response & recovery H_2S gas sensor based on α-Fe_2O_3 nanoparticles with ppb level detection limit. J Hazard Mater 2015; 300:167–174.

[5] Zhang G, Li C, Cheng F, Chen J. $ZnFe_2O_4$ tubes: synthesis and application to gas sensors with high sensitivity and low-energy consumption. Sens Actuators B 2007; 120:403–410.

[6] Agyemang FO, Kim H. Electrospun $ZnFe_2O_4$-based nanofiber composites with enhanced supercapacitive properties. Mater Sci Eng B 2016; 211:141–148.

[7] Goodarz Naseri M, Saion EB, Kamali A. An overview on nanocrystalline $ZnFe_2O_4$, $MnFe_2O_4$, and $CoFe_2O_4$ synthesized by a thermal treatment method. Nanotechnol. 2012; 2012:1–11.

[8] Li X, Wang C, Guo H, Sun P, Liu F, Liang X, Lu G. Double-shell architectures of $ZnFe_2O_4$ nanosheets on ZnO hollow spheres for high-performance gas sensors. ACS Appl Mater Interfaces 2015; 7:17811–17818.

[9] Zhang Z, Li XL, Ji HM, Zhou YG. Preparation and acetone sensitive characteristics of nano-crystalline $ZnFe_2O_4$ thin films, Materials Science and Technology 2010; 18:23–26.

[10] Cao Y, Jia D, Hu P, Wang R, One-step room-temperature solid-phase synthesis of $ZnFe_2O_4$ nanomaterials and its excellent

gas- sensing property. Ceram Int 2013; 39:2989–2994.

[11] Wu J, Gao D, Sun T, Bi J, Zhao Y, Ning Z, Fan G, Xie Z. Highly selective gas sensing properties of partially inversed spinel zinc ferrite towards H_2S. Sens Actuators B 2016; 235:258–262.

[12] Gopal RCV, Manorama SV, Rao VJ, Reddy CVG. Preparation and characterization of ferrites as gas sensor materials. J Mater Sci Lett 2000; 9:775–778.

[13] Gao XM, Sun Y, Zhu CL, Li CY, Ouyang QY, Chen YJ. Highly sensitive and selective H2S sensor based on porous ZnFe2O4 nanosheets. Sens Actuators B 2014; 193:501–508.

[14] Zhou X, Liu J, Wang C, Sun P, Hu X, Li X, Shimanoe K, Yamazoe N, Lu G. Highly sensitive acetone gas sensor based on porous $ZnFe_2O_4$ nanospheres. Sens Actuators B 2015; 206:577–583.

CreTech 2020
8th International Conference on Creative Technology
Multidisciplinary
to Drive Economy and Social
http://utkcretech.rmutk.ac.th

Development of a computer-controlled nanoparticle generation for inhalation exposure study

Saksith Kulwong [1*]

[1]Department of Industrial Hygiene and Safety, Faculty of Public Health, Burapha University
*Corresponding author. E-mail: saksithkw@hotmail.com

ABSTRACT

Exposures to nanoparticles in the ambient environment have been linked to adverse cardiopulmonary effects. Ambient atmosphere nanoparticles are derived mainly from vehicle combustion or traffic-related emissions. Black carbon is a major component of the soot generated by incomplete fuel combustion. The most appropriate method charactering black carbon is through an inhalation exposure system. There were, however, difficulties in generating nanoparticle with identical size and stable concentration. Therefore, this study developed a controllable nanoparticle generation system suitable for inhalation exposure study. The system was developed and tested for operational performance in generating carbon black in nano-size level, which mostly found in ambient environment. The carbon black nanoparticle number concentration of 5000, 10000, and 25000 particles/cm^3 were generated. Particle diameter modes, number concentrations, size distributions were measured continuously throughout 8 hours. The present system could constantly and repeatedly produce particles with identical size, and size distribution similar to those found in the environment. The control system worked rapidly in achieving 95% of the target concentrations in 5 minutes. In addition, the temperature, pressure, and relative humidity of the exposure chamber could be stably controlled throughout the tested period. The major advantage of this system was the capability of producing monodisperse aerosol particles with desired size, distribution, and concentration that useful for multipurpose nanoparticle inhalation studies.

1. INTRODUCTION

Exposures to ultrafine particles (UFPs, < 100 nm) in ambient air are associated with a board range of adverse health effects including pulmonary and cardiovascular diseases (1), as well as cancer and mortality (2). Because it is small enough to be inhaled and deposited in the lungs, and distributed to secondary organs via the circulation system (1). The ambient atmosphere UFPs are derived mainly from vehicle combustion or traffic- related emissions, and have been identified as particularly relevant to those health effects in humans on both acute and chronic effects (3), (4). Black carbon (BC), a type of ultrafine carbon particle, is a major component of the soot generated by incomplete fuel combustion (5), (6). It is widely used for determination of exposure to diesel soot, which has been classified as a toxic air contaminant and a human carcinogen (7).

One method characterizing ultrafine BC is through an inhalation chamber by using carbon black (CB), since CB is widely used as a model for diesel soot produced by incomplete combustion. A number of inhalation exposure systems have been developed for decades, yet the limitations and challenges are still being reported. For instance, difficulties in aerosolizing and dispersing nanomaterials down to nano-sized level, difficulties in producing stable aerosol concentrations and distribution. Therefore, it is important to develop a

controllable system to generate the aerosol particles for research applications. Herein, this study developed the CB nanoparticle generation and exposure system using computer control, and aimed to meet these following advantages: (1) producing the CB nanoparticle with stable concentration, (2) obtaining the aerosolized CB to the desired size, with identical size distribution, (3) maintaining the concentration of CB at minimal fluctuation of ± 5% throughout the tested period, and (4) minimizing the response time to attain the targeted concentration.

2. MATERIALS AND METHODS

2.1 Experimental setup

The entire experimental setup for nanoparticle generation and exposure system is shown in Figure 1. The system basically consists of an aerosol generation, the particle characterizing section, and the exposure chamber. Compressed air was cleaned by passing through a high efficiency particulate air (HEPA) filter, then regulated by two mass flow controllers (Alicat scientific, MC-10SLPM-D/5M, MC-20SLPM-D/5M).

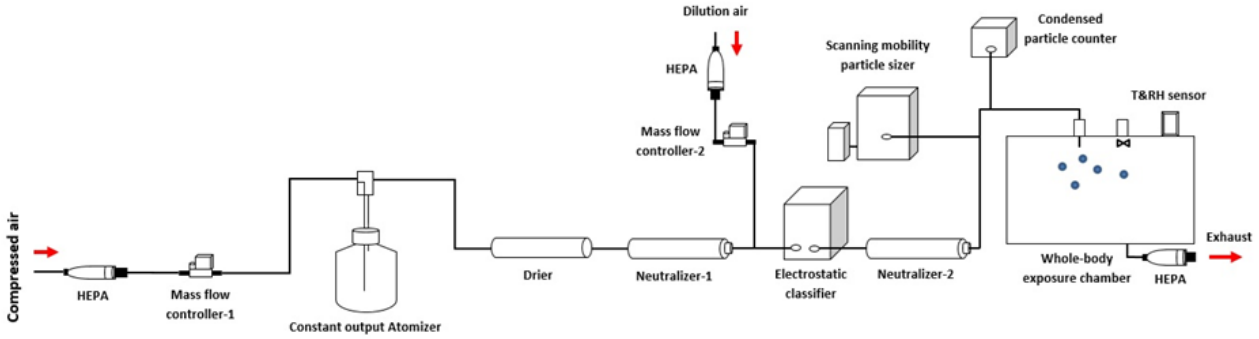

Figure 1. Schematic diagram of monodisperse

The first mass flow controller (MFC-1) was used to supply the air into the atomizer (model 3076, TSI) at a flow rate ranging from 3 to 5 liters per minute (LPM) with a controlled pressure of 30-35 psi, and the second mass flow controller (MFC-2) was used to supply the air to dilute the generated particles with the varied flow rates ranged from 0 to 20 LPM. These two mass flow controllers were put in a feedback loop and automatically controlled by computer LabVIEW program, in maintaining the generated particles at target concentration.

The output particles generated from atomizer were dried by passing through drier column (silica gel). The aerosol particles were then neutralized by neutralizer (3012A, TSI), and the aerosols are now suitable to be classified. Before being classified, the generated particles were diluted by dilution air regulated by MFC- 2, to reach the desired concentration. An electrostatic classifier equipped with the 3085 differential mobility analyzer (DMA) was used as the particle size selector. The selected particles were then neutralized again, and counted by the condensation particle counter (CPC, model 3010, TSI). This CPC is connected with the feedback loop, and used to control the particle number concentration in the exposure chamber. The particle size distributions and real time concentrations at the upstream of exposure chamber were analyzed by scanning mobility particle sizer (SMPS) system (TSI classifier nanoparticle generation and exposure system 3080 equipped with DMA 3081, and CPC 3787 platform). This study, carbon black nanoparticle size of 20 nm was chosen to test because of mimicking the ultrafine black carbon particles

found in the ambient atmosphere described by Yifang Zhu and William C. Hinds (8), (9). A whole-body exposure chamber is used as an inhalation exposure system. The excess particles were exited through chamber outlet that equipped with a HEPA filter at the bottom of the chamber. The temperature and relative humidity of the chamber were continuously monitored by electronic sensor (Vaisala, HMT337).

2.2 CB nanoparticle generator and exposure chamber

The ultrafine CB was purchased from Degussa (Printex-90, 14 nm in diameter with a surface area of 253.9 m^2/g). The CB solution at the concentration of 20 µg/ml in Milli-Q (MQ) water was prepared and used as predator. The solution was prepared by using probe type ultrasonicator (W-250; Branson, Danbury, CT) at high amplitude of 70% for 30 minutes long, to make sure that the particle solution was well- dispersed and homogenized. To stabilize the solution condition at room temperature, the particle solution was placed in a separate container filled with ice at all time of sonication, in order to prevent evaporation of the fluid and particle agglomeration caused by the elevated temperature during the sonication. Then, CB solution was used for atomizer (constant output atomizer; model 3076, TSI). The primary concentration of CB solution is determined based on our previous test regarding the relationship of solution concentrations and particle diameter sizes obtained. The particle solution was contained in the bottle of constant output atomizer (Model 3076) and ready to be generated.

To generate CB monodisperse particles, clean dry compressed air with the control flow rate and pressure of 3- 5 LPM and 30- 35 psi, respectively, was introduced into an atomizer. The solution was drawn into the atomizing section through a vertical passage and was atomized by the jet. Only fine droplets left the atomizer through a fitting at the top (Figure 2), large droplets were removed by impaction on the wall opposite the jet, and excess liquid was drained at the bottom of the atomizer assembly block into the reservoir bottle. Carbon black aerosols were then formed and introduced into the system, and controlled further by LabVIEW program described in previous section.

A 180- L whole- body exposure system (Figure 1.) was designed and constructed out of stainless steel and polycarbonate which capable exposure of 12 rats simultaneously exposed at one time. The chamber measured 20 x 25 x 22 inches allowing generated particles introduced and distributed uniformly to the exposed animals. Each hole and connection in the chamber is sealed with rubber. The carbon black particle is delivered into the chamber from the top center and exited the chamber from the bottom exhausted hole. Additional sampling ports in the chamber permitted the measurement of chamber temperature, relative humidity, and pressure.

2.3 Computer software user interface

The graphical user interface controlling the CB exposure system is implemented using the LabVIEW program. The display of the software interface is shown in Figure 3. A graphical display shown on the lower left of the screen continuously displays the chamber concentration with indicating the target concentration level and ± 5% deviation lines (red and light blue) as the background template. Meanwhile the atomizer pressure regulated pressure with ± 5% deviation lines, were continuously displayed on the upper

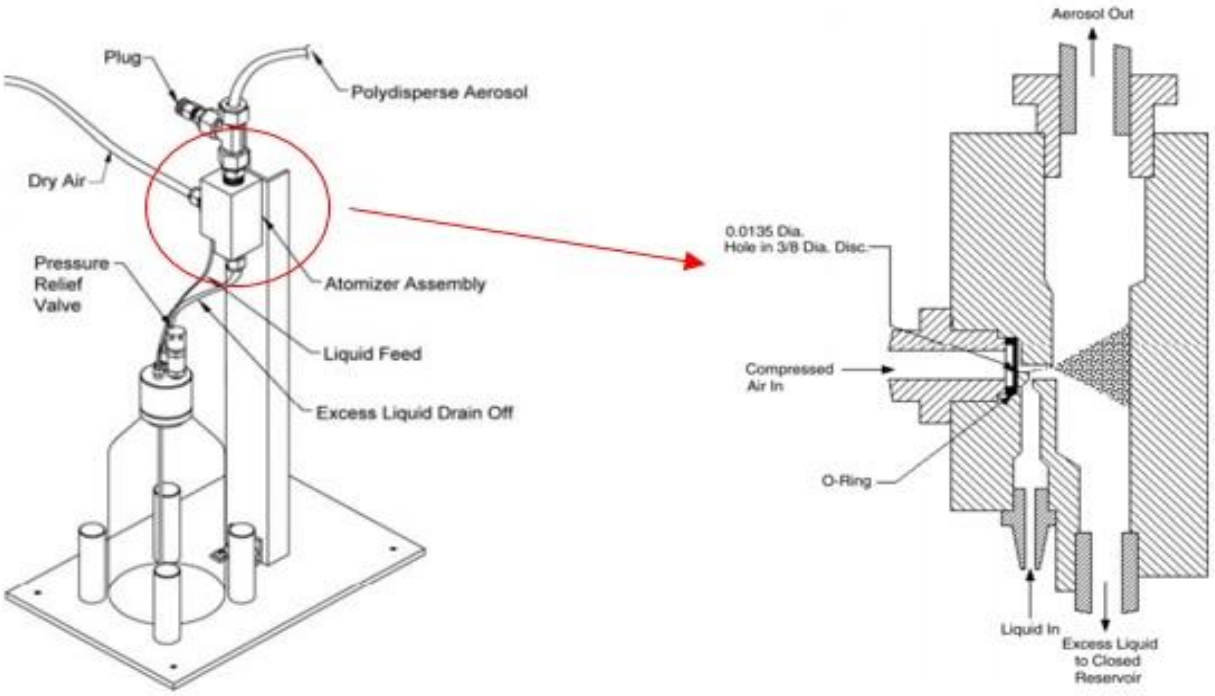

Figure 2. Model 3076 constant output atomizer

right of the screen. There are four column groups placed in a rectangle, the leftmost column displayed the current concentration, mass flow controller (MFC) - 1 and MFC- 2 output, and atomization pressure. The next column includes four user- selected buttons used to specify the communication channels between the particle measuring devices and computer. The third left column provides the channels for data input including of the target generated concentration, maximum airflow regulated by MFC-1 and 2, and atomizer regulated pressure. The last column provides the data input of desired exposure time, and displays of the current and starting time. Four activated buttons in the top of a user interface provide the main control for the particle generation and exposure system including a start (arrow), reset, stop, and pause button. All graphical displays and time are continuously displayed throughout exposure period. Each graphical display is provided the status button at the bottom, and flashing red light is shown up if the concentration or pressure is out of ± 5% limit. The following experimental parameters are automatically saved into the computer at 1- sec intervals: elapsed exposure time (second), atomization pressure (psi), atomization and (TSI incorporated) number concentration (particles/cm3), and exposure chamber temperature (°C) and relative humidity (%). After the exposure time has reached, the program will stop automatically and the data is saved to the designated drive.

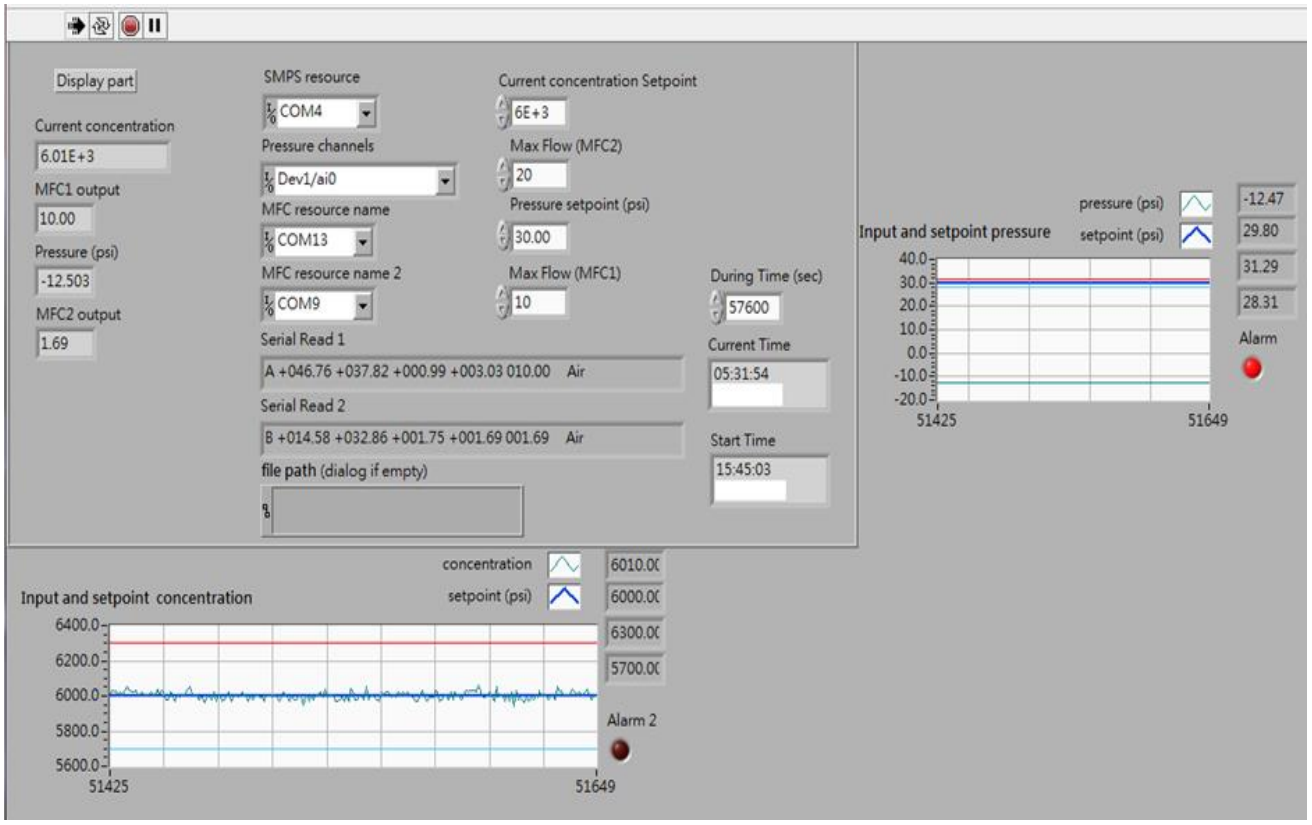

Figure 3. Computer software user interface

2.4. Particle number concentration and stability of the system

To test the performance of the system, the CB particle concentrations of 5000, 10000, and 25000 particles/cm^3 with controlled diameter size of 20 nm were produced. The ultrafine CB solution was used as predator to produce monodispersed CB nanoparticles. The generation and dilution airflows regulated by MFC-1 and 2, respectively, were automatically supplied corresponding to the target number concentration setup in the LabVIEW program. Then, chamber concentration was held constant by the feedback which signaled controlling via the CPC 3010. The number concentration of carbon black particles introduced into the exposure chamber were continuously controlled and monitored throughout 8 hours, herein the stability of computer-controlled system could be confirmed.

2.5 Determination of particle size distribution

The diameter size of generated CB particles was targeted at 20 nm, because of mimicking the black carbon particles found in the ambient environment as mentioned. The CB particle was generated and classified in obtaining the particle with diameter size of 20 nm for all three concentration levels. The particle size distributions were determined using scanning mobility particle sizer (SMPS) system. This analyzing system employed the electrostatic classifier 3080 equipped with 3081 DMA in tandem, and water-based CPC model 3787 for measuring number size distribution of generated particles.

CB nanoparticle in the exposure chamber was measured by the SMPS for 3- min interval throughout the 8-h generation period. The particle diameter mode and geometric standard deviation (GSD) obtained from the cumulative frequency distribution run on TSI aerosol instrument manager (AIM) software were analyzed and used to determine diameter size of generated particles.

2.6. Exposure chamber conditions

The temperature and relative humidity of the exposure chamber were continuously measured throughout 8 hours using a temperature & relative humidity sensor (Vaisala, HMT337). The packs of silica gel were put at the bottom space of the chamber separated from the area of animals' exposure to prevent high relative humidity. The temperature and relative humidity of the exposure chamber were maintained at 22.0 ± 3.0 °C and 30-70%, respectively, as recommended by the organization for economic cooperation and development (OECD).

3. RESULTS

3.1 CB particle number concentration and stability of control regulation

The system was operated totally for 8 hours by computer control, only the short resting time was set in between in order to mimic the real situation when conducting animal exposure. The system was tested on the performance of producing monodisperse CB nanoparticles at diameter size of 20 nm, and the results are shown in Figure 4. Three target number concentrations of CB in the unit of particle number per cubic centimeter (particles/ cm^3) were produced and tested with controlling the variation at ± 5%.

The results showed that the average concentrations of CB nanoparticles generated to the exposure chamber at the first-four hours were controlled at 4,974±316, 9,834± 609, and 24,692±2,321 particles/cm^3 for the target number concentrations of 5,000, 10,000, and 25,000 particles/cm^3, respectively. The results of second-four hours conducted immediately after short resting time revealed similar results for all concentrations as shown in Table 1. Notably, the number concentrations of generated particles were controlled with the fluctuation of less than 10% for the coefficient of variation (CV) at all target concentrations tested (%CV = 6.19-9.43).

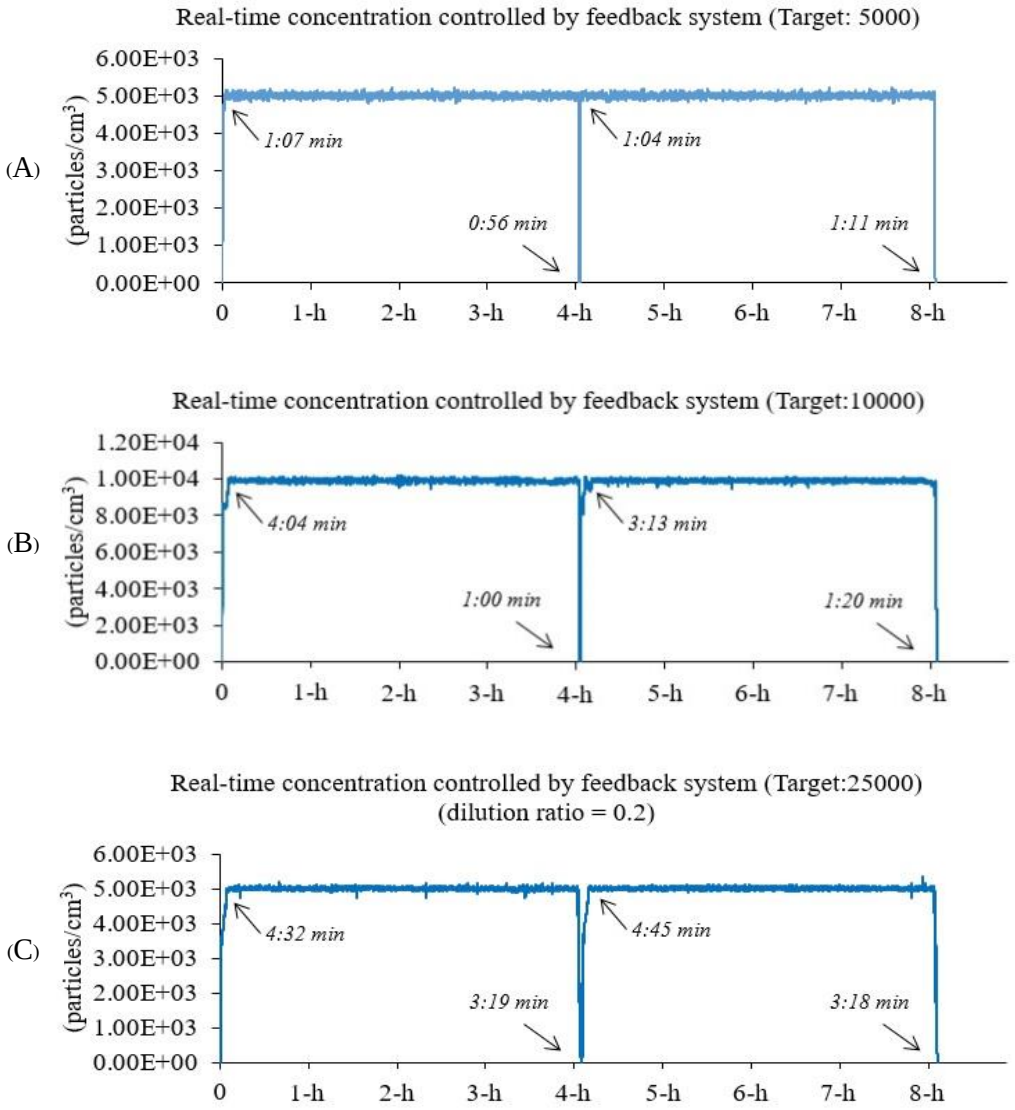

Figure 4. The particle concentration throughout 8-h generated at the target concentration of 5,000 (A), 10,000 (B), and 25,000 particles/cm^3 (C) using feedback system. Inserted time in the graphs indicated the rise time of achieving 95% targeted concentration, and reaching 5% initial concentration.

In addition, the system's stability controlled by feedback system exhibited the rapid rise to the equilibrium particle number concentrations (Figure 4). The rise times required in attaining 95% of the target concentrations varied from 1:04 – 4:45 min. The fall times to reach 5% of initial concentrations varied from 0:56 – 3:19 min. These results showed a good performance of feedback control system in controlling the concentration of CB particles at the stable level, and achieving the equilibrium concentrations rapidly.

Table 1. Mean, standard deviation (SD), and coefficient variation (CV) of particle generation

Time	Target concentration at 5,000 (particles/cm^3)			Target concentration at 10,000 (particles/cm^3)			Target concentration at 25,000 (particles/cm^3)		
	Mean	SD	CV (%)	Mean	SD	CV (%)	Mean	SD	CV (%)
1-4 hr	4,974	316	6.36	9,834	609	6.19	24,692	2,321	9.40
5-8 hr	4,974	323	6.49	9,829	629	6.40	24,711	2,332	9.43

3.2 Particle size distributions of CB

In ideally, the particle size distribution of CB nanoparticle generated to the inhalation chamber should remain constant throughout exposure periods to ensure the reproducibility of the generation system. The particle size distributions of CB for three different concentrations are shown in Figure 5. The size distribution curves indicated normal distribution and they are identical for all three target concentrations.

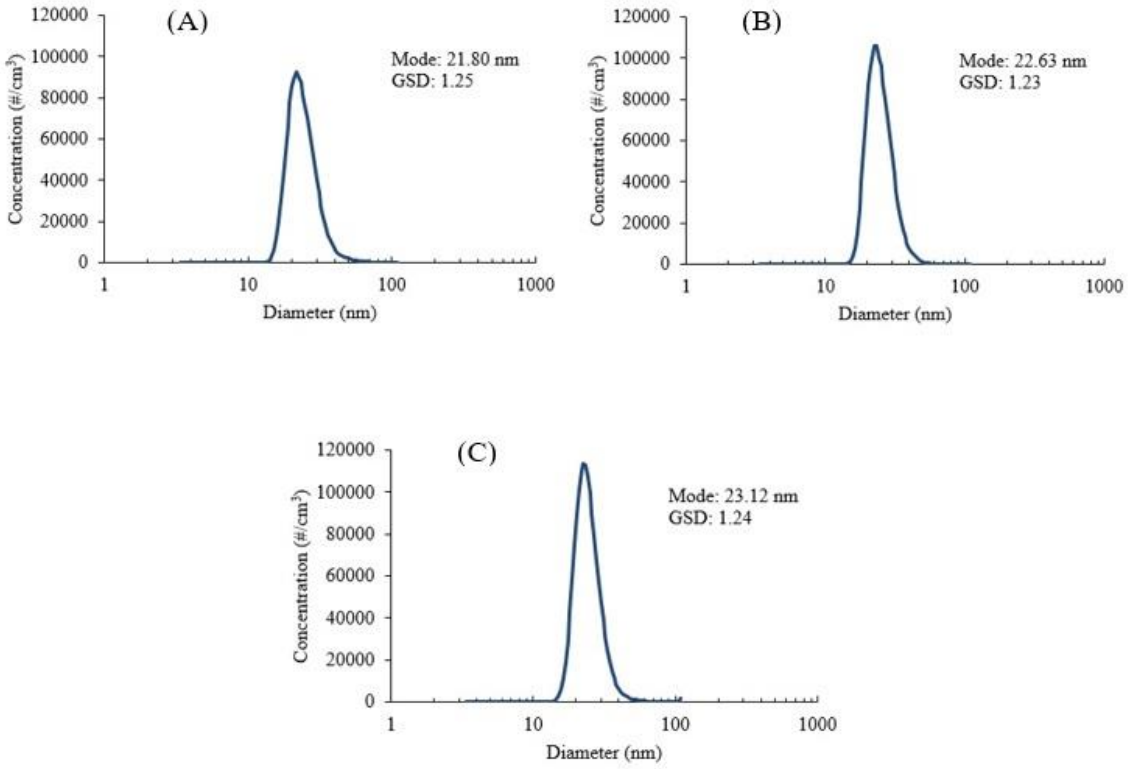

Figure 5. The size distributions of CB particles measured by SMPS throughout 8-h at each target concentration of 5,000 (A), 10,000 (B), and 25,000 particles/cm^3 (C)

The modes and GSD of generated CB particles obtained from SMPS were 21.80 nm (GSD 1.25), 22.63 nm (GSD 1.23), and 23.12 nm (GSD 1.24) for the target concentration of 5000, 10000, and 25000 particles/ cm^3. The results indicated the nano-size level of generated CB particles, and the monodisperse particles confirmed by the GSD (GSD□ 1.25) (10) for all concentration levels.

3.3 Exposure chamber conditions

The average temperature and relative humidity of the exposure chamber were maintained at 24.56 ±0.84 °C, and 48.91 ± 3.83%, respectively, throughout 8-hr generation period as shown in Figure 6. The packs of silica gel put at the space below the area of animals' exposure helped to prevent high relative humidity throughout 8-hr test period. Thus, the results indicated that the environmental conditions of this whole-body inhalation chamber were controlled. The chamber is acceptable by the criterions of the organization for economic cooperation and development (OECD), which recommended that, the temperature and relative humidity of the inhalation chamber should be maintained at 22.0 ± 3.0 °C and 30-70%, respectively.

4. DISCUSSIONS AND CONCLUSIONS

A controllable nanoparticle generation and exposure system was effectively designed. The system consistently generated CB particles throughout the test period, confirming the capability for inhalation studies. The measurement of particle number concentration demonstrated the stability in generating the particles at various concentrations with the fluctuation of less than 10% CV. This value is superior to the recommendation of the OECD, which recommended that no more than ±20% fluctuation for liquid or solid aerosols generation for inhalation studies (11).

Since the OECD test guidelines is the gold standard for the testing of chemicals and periodically reviewed by the scientific committee, and also the animal welfare forum. In considering into the performance of a designed system, the mean equilibrium concentrations of CB particles were achieved in a short time (< 5 min) for all target concentrations, and maintaining the constant levels throughout 8-hr tested period, indicating that the system worked rapidly and appropriately control.

The CB particle size distribution modes measured by the SMPS slightly increased with increasing target concentration, as seen by Figure 5. This is due to increased collision frequency between the aerosol particles upon particle generation. It is expected that higher target concentrations initially result in more agglomeration. However, the characteristics of CB nanoparticles (size distributions, modes, and GSDs) generated by this system mimicked the black carbon particles found in the environment, as described by previous studies (12). Thereby, showing that this system is capable for environmental aerosol particles inhalation study research. Another advantage of this system is the capability in generating the particles at desired size and concentration. This should be very helpful for research applications such as aerosol instrument calibration, filter testing, dose-response inhalation studies, and other experiments for validating models. In addition, this study demonstrated that the temperature, pressure, and relative humidity in the exposure chamber were controlled appropriately in accordance with the OECD guidance, confirming that a designed system can be applied to the inhalation studies.

However, some limitations can also be found in this study such as (1) the presence of small interference peak in the CB solution used, this can affect the GSD and actual concentration of the generated CB, even a little. (2)

A designed system still needs a person whose well-understand the system and parameters to be inputted. Since, those parameters need to be carefully considered at the beginning, then, the system can work continuously without major requirements.

5. ACKNOWLEDGMENTS

This research was partial supported from Faculty of Public Health, Burapha University.

6. REFERENCES

[1] Hubbs, A.F., Mercer, R.R., Benkovic, S.A., Harkema, J., Sriram, K., Schwegler-Berry, D., Goravanahally, M. P., Nurk- iewicz, T. R., Castranova, V. and Sargent, L.M. (2011). Nanotoxicology- a pathologist' s perspective. Toxicol. Pathol., 39, 301-324

[2] Pope, C.A., Dockery, D.W. (2006). Health effects of fine particulate air pollution: lines that connect. Journal of the Air & Waste Management Association 56: 709-742

[3] Hoek, G., Boogaard, H., Knol, A., de Hartog, J., Slottje, P., Ayres, J.G., Borm, P.,Brunekreef, B., Donaldson, K., Forastiere, F., Holgate, S., Kreyling, W.G., Nemery, B., Pekkanen, J., Stone, V., Wichmann, H.E., van der Sluijs, J., 2010. Concentration response functions for ultrafine particles and all-cause mortality and hospital admissions: results of a european expert panel elicitation. Environmental Science & Technology 44, 476-482.

[4] Luke D. Knibbs, Tom Cole- Hunter, Lidia Morawska (2011). A review of commuter exposure to ultrafine particles and its health effects. Atmospheric Environment 45: 2611-2622

[5] Lin, W., Huang, W., Zhu, T., Hu, M., Brunekreef, B., Zhang, Y., Liu, X., Cheng, H., Gehring, U., Li, C. and Tang, X. (2011). Acute respiratory inflammation in children and black carbon in ambient air before and during the 2008 Beijing Olympics. Environ. Health Perspect., 119, 1507-1512.

[6] Tong, H., McGee, J. K., Saxena, R. K., Kodavanti, U.P., Devlin, R.B. and Gilmour, M.I. (2009). Influence of acid functionalization on the cardiopulmonary toxicity of carbon nanotubes and carbon black particles in mice. Toxicol. Appl. Pharmacol., 239, 224-232.

[7] World Health Organization (WHO) (2012). Health effects of Carbon black. WHO Regional Office for Europe Scherfigsvej 8 DK– 2100 Copenhagen, Denmark

[8] Zhu, Y., Hinds, W.C., Kim, S., Sioutas, C. (2002). Concentration and size distribution of ultrafine particles near a major highway, Journal of the Air and Waste Management Association 52: 1032–1042

[9] Zhu, Y., Hinds, W.C., Kim, S., Sioutas, C. (2002). Study of ultrafine particles near a major highway with heavy- duty diesel traffic. Atmospheric Environment 36: 4323–4335

[10] Amit Md. Estiaque Arefin∗, M.H. Masud, Mohammad U. H. Joardder, Md. Shamim Akhter (2017). A monodisperse- aerosol generation system: Design, fabrication andperformance. Particuology 34:118–125

[11] Organisation for Economic Co-operation and Development (OECD) (2009). OECD Environment, Health and Safety Publications Series on the Safety of Manufactured Nanomaterials No 15: Preliminary Review of OECD Test Guidelines for their Applicability to Manufactured Nanomaterials

[12] Cheng YS, Moss OR. 1995. Inhalation exposure systems. In: RO McClellan and RF Henderson, eds. Concepts in Inhalation Toxicology. 2nd ed. Boca Raton, FL: CRC Press, 25-61.

CreTech 2020
8th International Conference on Creative Technology
Multidisciplinary to Drive Economy and Social
http://utkcretech.rmutk.ac.th

Replacing fat with prebiotic in muffin and chilled storage conditions affecting organoleptic characteristics

Nutthaya Srisuvor[1*], Chonthira Sarawong[2], Wipavan Julaya[3]

[1]Subject field of food business Department of food technology and nutrition,
Faculty of home economic technology, Rajamangala University of Technology Krungthep
[2]Subject field of food science and technology, Department of food technology and nutrition,
Faculty of home economic technology, Rajamangala University of Technology Krungthep
[3]Subject field of food product development, Department of food technology and nutrition,
Faculty of home economic technology, Rajamangala University of Technology Krungthep
[*]Corresponding author. E-mail: nuttaya.s@mail.rmutk.ac.th

ABSTRACT

The purposes of this research were to evaluate the types of prebiotics (inulin (IN) and polydextrose (PD) as fat substitutes) affected the sensory properties and study 2 conditions of muffin storage. 1) The mixture of replaced fat with prebiotic was chilled and then baked by an oven (CO) and 2) the mixture of replaced fat with prebiotic was baked, then chilled, and then reheated by a microwave (BCM). The levels of prebiotic at 0, 10, 20, 30, and 40% of fat in each storage condition were assessed by 100 panelists. The IN-CO samples were not significantly different sensory attributes from the CO-control samples except the flavor, and the PD-CO samples were not significantly different sensory attributes from IN-CO samples. The PD-BCM samples were inferior appearance and texture than the BCM-control samples. The CO-muffins with 20 and 30% of PD gave the highest sensory attributes similar to the CO-control samples. The BCM-muffins with 30% of PD were similar to the BCM-control samples. Amount of prebiotic for replacement of fat affected the organoleptic characteristics of muffin. This research was a potential model of chilled muffin storage before baking by replacing fat with PD which their organoleptic characteristics were accepted by consumer.

Keywords: organoleptic characteristics, prebiotic, inulin, polydextrose, muffin

1. INTRODUCTION

Muffin is a bakery which its shelf life is not a long time. It is necessary to use preservatives extending shelf life. Besides, controlling the process of heating and storage are important factors which lead to long storage including its components, moisture and cleanness of production. Mostly bakery products are baked for decrease of moisture contents and water activity to prevent deterioration and extend shelf life, such as cookie, puff, and pie, etc. However, their texture are generally dry and hard. If muffins can be stored in a refrigerator without affecting the organoleptic characteristics, they will have a long shelf life. However, their color, odor, taste, and texture may significantly reduce. Therefore, the researchers interested to study the replacement of fat with prebiotic and the chilled storage of muffin for good sensory features without preservatives.

Inulin (IN) is an indigestible fructose polymer (F_m) or fructose polymer with a glucose molecule (GF_n) which it is isolated from chicory. Polydextrose (PD) is an indigestible glucose polymer which contains some sorbitol and citric acid. It is a relatively high viscosity and gave fat

mouthfeel and creaminess. They are carbohydrate-based fat replacers and also used as a prebiotic. Both fat replacers were often used in high fat food products, i.e., products of dairy, meat, and bakery. They provide 1-1.5 kcal/g of energy. They gave a mouthfeel similar to the full fat or cream, when they were combined with water due to their ability to form a gel. PD also helped absorb moisture well and maintain the freshness and softness of bakery products. IN helped stimulate the immune system, reducing pH and acids after absorption of carbohydrates, and producing vitamins in the body (1, 2, 3, 4, 5, 6). This research needs to study replacement of fat with prebiotic in muffin and chilled storage conditions affecting the sensory qualities. The objectives of this research were to evaluate the impact of incorporation of different the types and amounts of prebiotic and the conditions of muffin storage by chilling mixture before baking and baking the mixture before cold storage and reheating by a microwave affecting sensory quality of muffin.

2. MATERIALS AND METHODS

2.1 Materials

IN (Tienen, Belgium) has the degree of polymerization (DP) 2-60. PD (Danisco, Singagpre Pte Ltd.) has the molecular weight 22,000 Da. Soy protein and xanthan gum were purchased from Chemipan Corporation Co., Ltd. Gluten-free all purpose flour plain (White Wings), double acting formula of baking powder (Unilever Food Solutions), salt (Thai Refined Salt Co., Ltd.), natural cane sugar (Mitr Phol Sugar Co., Ltd.), coconut milk (Thai Agri Food Public Co., Ltd.), rice bran oil (Lam Soon (Thailand) Public Co., Ltd.), and pure corn flour (Continental Food Co., Ltd.) were purchased from supermarket in Bangkok, Thailand.

2.2 Types of prebiotic and storage of muffin

All purpose flour was sieved and other ingredients were weighted following Table 1. All ingredients in each recipe were mixed and poured in molds. Each recipe was divided by 2 parts as following: 1) the mixtures in molds were chilled by a refrigerator (WRN-57HGG3, Korea) (4±1°C, 7 days), then baked by an oven (180°C, 35 min) (CO), and then placed at room temperature for 1 hour and 2) the mixtures in the molds were baked by an oven (GC-1009, Sveba Dahin, Hong Kong) (180°C, 35 min), then placed at room temperature for 1 hour, then chilled at 4±1°C for 7days, and then reheated by a microwave (Samsung, GME711K, South Korean) at 700 W for 30 s (BCM), and then assessed organoleptic properties.

Table 1. Types of prebiotic for replacement of fat in ingredients of muffin

Ingredients (g)	Prebiotics		
	Control	IN	PD
Coconut milk	350	350	350
Rice bran oil	80	60	60
Cane sugar	150	150	150
IN	-	20	-
PD	-	-	20
All purpose flour	355	355	355
Soy protein	20	20	20
Corn flour	8.85	8.85	8.85
Xanthan gum	0.15	0.15	0.15
Baking powder	15	15	15
Salt	1	1	1

From: (7, 8)

2.3 Quantities of prebiotic and storage of muffin

Wheat flour was sieved and all ingredients were weighted as in Table 2. Type of prebiotics was selected according to 2.2 and used for studying in this step. The quantities of prebiotic for replacement of fat in each recipe at 0, 10, 20, 30,

and 40 % of rice bran oil. All ingredients were mixed, put in molds and then divided 2 parts of the experiments as follows:

Table 2. Quantities of prebiotic for replacement of fat in ingredients of muffin

Ingredients (g)	Replacement of fat (%)				
	0	10	20	30	40
Coconut milk	350	350	350	350	350
Rice bran oil	80	72	64	56	48
Cane sugar	150	150	150	150	150
Prebiotic	-	8	16	24	32
Wheat flour	355	355	355	355	355
Soy protein	20	20	20	20	20
Corn flour	8.85	8.85	8.85	8.85	8.85
Xanthan gum	0.15	0.15	0.15	0.15	0.15
Baking powder	15	15	15	15	15
Salt	1	1	1	1	1

From: (7, 8)

1) the mixtures in molds were proceeded by CO and placed at ambient temperature for 1 hour and 2) the mixtures in the molds were proceeded by BCM, and then assessed sensory qualities.

2.4 Assessment of sensory qualities

Sensory qualities were assessed by preference test with 7-point hedonic scales for appearance, color, odor, flavor, taste, texture, and overall liking using 100 panelists in department of food technology and nutrition. Each sample (30 g) was contained in a sealed plastic bag and served at ambient temperature with 3 random digit number (9).

2.5 Analysis of statistics

Randomized Complete Block Design was used for these experiments. Analysis of Variance was analyzed and compared the differences between treatments by Duncan's New Multiple Range Test ($p \leq 0.05$).

3. RESULTS AND DISCUSSION

The sensory evaluations of types of prebiotic (IN and PD) and conditions of storage (CO and BCM) were assessed as in Table 3. The results showed that IN-CO samples were not significantly different sensory attibutes from the control-CO samples except the flavor. The PD-CO samples were no significant difference of all sensory attibutes from IN-CO samples; however, they were lower the appearance, flavor, and texture than the CO-control samples. While the IN-BCM samples were not significantly different all sensory attibutes from the control-BCM samples. In addition, the results showed no significant differences between all samples in color and odor. These indicated that IN- and PD-replaced samples and each condition of heating and storage did not change of color and odor from observation of the consumer. Moreover, the PD-BCM samples were lowest texture scores because PD was more hygroscopic than IN (10). When the baked PD-muffins were chilled in a refrigerator, they could absorp the moisture affecting worse texture. Using types of prebiotic for replacement of rice bran oil in muffin were reported. They showed that the PD-muffins were lower fat and sugar contents than IN-muffins and gave more total dietary fiber contents (no data shown) (11). In addition, a research reported the decrease of the sensory acceptance of bread added with IN (12). Using PD for replacement of fat at 5, 10 and 15 % of wheat flour in pogaca (traditional high-fat bakery product) generally received higher sensory scores than the formulations replaced with IN (13). Thereby this sensory evaluations selected to use PD as a fat replacer for studying the levels of PD in muffin for the next step.

Table 4, the results showed that the levels of PD at 20 and 30 % in CO-muffins were not significantly different from the CO-control

samples which gave the highest all sensory features because of one step of heating and moderate amounts of replaced fat. However, the appearance, color, and odor of CO-muffins with 30 % of PD were more similar to the CO-control sample than those ones with 20 %. Besides, the CO-muffins with 10 % of PD were similar to the CO-control samples except the color.

Table 3. Types of prebiotic and conditions of storage on the sensory characteristics of muffins

Type	Condition	Appearance	Color ns	Odor ns	Flavor	Taste	Texture	Overall liking
Control	CO	5.30±1.01^{ab}	6.18±0.67	5.48±0.87	5.52±1.04^{a}	5.43± 0.97^{a}	4.68±1.01^{a}	5.21±0.92^{a}
	BCM	5.35±0.97^{a}	6.09±0.70	5.43±0.78	5.10±0.95^{bcd}	5.28±0.94^{ab}	4.16±0.91^{bc}	4.89±0.94^{bc}
IN	CO	5.04±0.91^{bc}	6.07±0.67	5.42±0.84	5.23±0.99^{b}	5.27±0.95^{ab}	4.42±1.07^{ab}	5.09±0.96^{ab}
	BCM	5.15±0.93^{abc}	6.00±0.72	5.42±0.79	4.90±0.87^{cd}	5.09±0.89^{b}	3.92±1.01^{cd}	4.71±0.97^{c}
PD	CO	5.00±0.90^{c}	6.01±0.69	5.37±0.82	5.18±0.97^{bc}	5.21±0.87^{ab}	4.28±1.12^{b}	4.95±0.93^{abc}
	BCM	5.04±0.90^{bc}	5.97±0.73	5.42±0.79	4.84±0.92^{d}	5.01±0.76^{b}	3.86±1.02^{d}	4.67±0.95^{c}

$^{a, b, c, d}$Mean ± standard deviation within the same coloumn with different litters are significantly different ($p \leq 0.05$)

^{ns}Mean ± standard deviation within the same coloumn are not significantly different ($p > 0.05$)

Table 4. Levels of polydextrose and conditions of storage on the sensory characteristics of muffins

Level (%)	Process	Appearance	Color	Odor	Flavor	Taste	Texture	Overall liking
0	CO	5.76±0.79^{a}	5.96±0.82^{a}	5.67±1.04^{a}	5.69±0.96^{a}	5.70±0.97^{a}	5.52±1.09^{a}	5.70±0.86^{a}
	BCM	5.39±0.85^{bc}	5.89±0.83^{ab}	5.60±0.94^{ab}	5.68±0.83^{a}	5.07±1.57^{cd}	4.73±1.50^{b}	5.26±1.07^{bcd}
10	CO	5.52±0.98^{ab}	5.66±1.06^{bcd}	5.40±1.19^{abc}	5.43±1.13^{abc}	5.52±1.07^{ab}	5.27±1.08^{a}	5.39±1.11^{abc}
	BCM	4.85±1.20^{e}	5.35±0.94^{e}	4.87±1.23^{e}	4.84±1.27^{d}	4.53±1.49^{e}	4.22±1.58^{c}	4.59±1.19^{f}
20	CO	5.58±0.94^{ab}	5.82±1.03^{abc}	5.59±1.02^{ab}	5.51±1.14^{ab}	5.66±1.05^{a}	5.52±1.16^{a}	5.66±0.90^{a}
	BCM	4.99±1.18^{de}	5.51±0.96^{de}	5.00±1.25^{de}	5.11±1.17^{cd}	4.77±1.38^{de}	4.22±1.74^{c}	4.96±1.14^{de}
30	CO	5.73±0.81^{a}	5.97±0.69^{a}	5.73±1.04^{a}	5.62±1.01^{ab}	5.63±1.03^{a}	5.63±0.92^{a}	5.57±1.08^{ab}
	BCM	5.42±0.93^{bc}	5.75±0.74^{abcd}	5.29±1.17^{bcd}	5.45±0.99^{ab}	5.22±1.45^{bc}	4.61±1.58^{bc}	5.23±1.10^{cd}
40	CO	5.55±0.87^{ab}	5.80±0.96^{abc}	5.44±1.09^{abc}	5.32±1.11^{bc}	5.58±0.98^{ab}	5.49±0.96^{a}	5.29±1.18^{bc}
	BCM	5.18±1.00^{cd}	5.59±0.84^{cde}	5.13±1.19^{cde}	5.29±0.97^{bc}	4.95±1.39^{cd}	4.37±1.55^{bc}	4.79±1.21^{ef}

$^{a, b, \cdots}$Mean ± standard deviation within the same coloumn with different litters are significantly different ($p \leq 0.05$)

This related to fat substitution with 11.5 % of PD in cookies which gave the flavor and general acceptance similar to the control samples (14). Furthermore, the CO-muffins with 40 % of PD were similar to the control-CO samples except the flavor and overall liking. These indicated that a few and many amounts of PD for fat substitution in CO-muffins significantly reduced the sensory attributes but the medium amounts (20 and 30% of fat by weight) of PD gave the sensory attributes similar to the control-CO samples. Whereas the BCM-muffins with 30% of PD were similar to the BCM-control samples because the replacement of PD at <30 or >30% of fat dropped total sensory parameters.

In conclusion, at the 30% level of PD in CO-muffins gave the highest sensory attributes and were similar to the CO-control samples. This related to fat replacement with PD up to 30 % of the fat without any decrease in the sensory quality of pogaca (13).

4. CONCLUSIONS

The acceptance of the sensory features of CO-muffin was higher than BCM-muffin. The IN-CO muffins were not significantly different sensory acceptance from PD-CO muffins. While the PD-BCM muffin gave inferior appearance and texture than the control-BCM muffin. The amount of prebiotic for replacement of fat affected the organoleptic characteristics of muffin. It should not exceed 30 % in order to produce muffins with good consumer acceptability. Consequently, PD can be used as a prebiotic and a fat replacer in muffin together with CO process to produce the muffin with the consumer acceptability of sensory features and select as functional foods.

5. ACKNOWLEDGMENTS

This research was funded by Rajamangala University of Technology Krungthep, Bangkok. Inulin received from DPO (Thailand) Co., Ltd. Polydextrose received from Rama Production Co., Ltd.

6. REFERENCES

[1] Kolida S, Tuohy K, Gibson GR. Prebiotic effects of inulin and oligofructose. Br J Nutr 2002;87(suppl 2):S193-7.

[2] Roberfroid M. Inulin and oligofructose aslow- calorie. In: Roberfroid M, editor. Inulin- type fructans: functional foodingredients. Boca Raton, FL: CRC; 2005.p. 133-43.

[3] Young NWG, O' Sullivan GR. Theinfluence of ingredients on productstability and shelf life. In: Kilsast D,Subramaniam P, editors. Food and beverage stability and shelf life. Cambridge, UK: Woodhead; 2011. p. 132-78.

[4] Miremadi F, Shah NP. Applications of inulin and probiotics in health and nutrition. Int Food Res J 2012;19(4):1337-50.

[5] Tiefenbacher KF. The technology of waffers and waffles I: opereational aspects. Oxford, UK: Academic Press; 2017.

[6] BeMiller JN. Carbohydrate chemistry for food scientists. 5th ed. Duxfore, UK: Woodhead Publishing; 2019.

[7] Julianti E, Rusmarilin H, Ridwansyah R,Yusraini E. Effect of gluten free composite flour and egg replacer on physicochemical and sensory properties of cakes. Int Food Res J 2016;23(6):2413-18.

[8] Youtube. com [Internet]. Japan: YouTube;[updated 2016 Aug 16; cited 2020 May29] Available from https://youtu.be/v8AvLt8ETLc

[9] Arifin N, Siti Nur Izyan MA, Huda-Faujan N. Physical properties and consumer acceptability of basic muffin made from pumpkin puree as butter replacer. Food Res 2019;3(6):840-5.

[10] Pinto SS., Fritzen-Freire CB, Benedetti S, Murakami FS, Petrus JCC, Prudêncio E S, et al. Potential use of whey concentrate and prebiotics as carrier agents to protect *Bifidobacterium*- BB- 12 microencapsulated by spray drying. Food Res Int 2015;67:400-8.

[11] Srisuvor N, Julaya W, Sarawong C. The replacement of fat with prebiotic on the qualities of chilled gluten- free muffin.

Research report, Bangkok: Faculty of Home Economic Technology, Rajamangala University of Technology Krungthp, 2018.

[12] Moris C, Morris GA. The effect of inulin and fructo-oligosaccharide supplementation on the textural, rheological and sensory properties of bread and their role in weight management: A review. Food Chem 2012;133(2):237-48.

[13] Serin S, Sayar S. The effect of the replacement of fat with carbohydrate-based fat replacers on the dough properties and quality of the baked pogaca: A traditional high-fat bakery product. Food Sci Tech 2017;37(1):25-32.

[14] Zoulias EJ, Oreopoulou V, Tzia C. Effect of fat mimetics on physical, texture and sensory properties of cookies. Int J Food Prop 2000;3(3):385-97.

CreTech 2020
8th International Conference on Creative Technology
Multidisciplinary to Drive Economy and Social
http://utkcretech.rmutk.ac.th

The study of microgels by utilizing light scattering technique

Nettraporn Doungsong[1*], Terence Cosgrove[2], and Jeroen S. van Duijneveldt[2]

[1] Program in Materials Science, Faculty of Science, Maejo University, Chiang Mai, 50290, Thailand.
[2] School of Chemistry, University of Bristol, Cantock's Close, Bristol BS8 1TS, United Kingdom.
*Corresponding author. E-mail: nettraporn_ds@mju.ac.th

ABSTRACT

Microgels are cross-linked polymers so that they can swell enormously responding to specific environmental stimuli without destruction. Therefore, they are of great interest to be used in applications as carriers of drugs, diagnostic agents and agrochemicals, and microreactor. This study is to investigate the swelling behaviour of poly(acrylic acid) (PAA) microgels using light scattering technique. Dynamic light scattering (DLS) measures the hydrodynamic radius (R_H); whist static light scattering (SLS) evaluates the radius of gyration (R_G). Besides, the combined data of DLS and SLS inform the shape and internal structure of the microgels via shape factor (ρ). The results show that a higher pH leads to the increased particle size of microgels as a result of the electrostatic repulsion between carboxylate anions of ionized PAA. However, the presence of salt causes the de-swelling of microgels due to the charge screening effect. The shape factor values of microgels are in the range of 0.61 to 0.92 consistent with a core-shell structure or non-uniform cross-linked density distribution. Consequently, the LS technique is a powerful tool, providing information for better understanding the swelling behaviours of PAA microgels which might be further used as carriers with the controlled-release response triggered by pH and ionic strength.

Keywords: microgels, poly(acrylic acid), light scattering, the radius of gyration, hydrodynamic radius

1. INTRODUCTION

Microgel is a physically and/or chemically cross-linked polymer with the particle size range of 10-1,000 nm, and it may swell up to 1,000 times its original size at appropriate conditions [1]. For pH-responsive gels, changes in pH and salt concentration (or ionic strength) can control their swelling behaviours attributed to the presence of certain pendant groups along the polymer chains. They are divided into two types: anionic and cationic gels. The typical pendant groups of anionic gels are carboxyl groups (-COOH) and phosphoric acid (-PO_3H_2), while the cationic gels usually contain primary amine (-NH_2) [2,3].

Poly(acrylic acid) (PAA) microgels are anionic gels with carboxyl pendant group (pK_a of carboxyl group = 4.5 -5). This group can be ionized to the carboxylate anion (-COO^-) at pH above its pK_a. As a result, the electrostatic repulsion between the ionized groups leads to the swelling of the microgels. However, they become de-swollen at pH lower than its pK_a due to the protonation of the ionized groups or when the ionic strength increases due to the charge screening effect [4]. Since the controllable swelling behaviours triggered by pH and ionic strength, the applications of PAA-based microgels are mostly used in carrier systems with a targeted release of active ingredients (AIs) such as drug, agrochemicals and skincare

[5,6].

Light scattering (LS) can be generally divided into two categories: dynamic (DLS) and static light scattering (SLS) as shown in Figure 1. For DLS, the intensity of scattered light (I) is measured by a photon detector as a function of time (t) at a certain angle (normally 90˚) and subsequently transformed into a correlation function, giving the diffusion coefficient (D) of the particles. According to the Stokes-Einstein equation: $R_H = k_B T/6\pi\eta D$, where k_B is the Boltzmann constant, η is the viscosity of the solvent, and T is the absolute temperature, the hydrodynamic radius (R_H) of the observed particle can be calculated by assuming that its diffusion rate is similar to an equivalent hard-sphere [9]. For SLS, the intensity profile (I) is measured as a function of the degree of angle (θ), which is transformed to the scattering vector (Q) using the following equation:

$Q = (4\pi n_D/\lambda)\sin(\theta/2)$, where n_D is the refractive index of solvent and λ is the wavelength of the laser light. The plot of $I(Q)$ as a function of Q can be then analyzed using various methods such as Zimm plot and Guinier approximation to yield the weight average molecular weight ($\bar{M}_w$), the radius of gyration (R_G) and the second virial coefficient (A_2) [10]. The ratio R_G/R_H defined as shape factor (ρ) informs the shape and internal structure of particles. For example, the ρ of homogeneous hard spheres is 0.775; while that of random polymer coils in theta solvent varies between 1.5 and 1.8 [11].

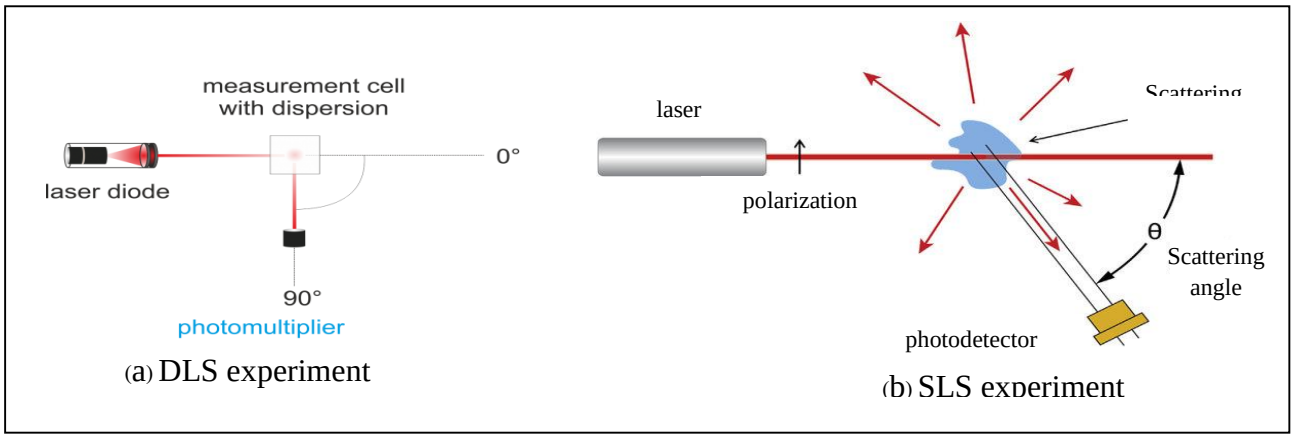

Figure 1. Light scattering with (a) DLS and (b) SLS measurements.
Revised and Reprinted from [7] and [8]. Copyright (2016) by Analytical Biochemistry.

For microgels, the shape factor (ρ) is a sensitive parameter to monitor the changes in the density distribution of microgels according to their swelling/de-swelling behaviours.

Generally, the shape factor of slightly cross-linked microgels is lower than 0.775 [11,12], indicating the non-uniform internal structure of the microgels as the R_H is larger than the R_G. It is due to the dangling chains in the outer surface of microgels detected by the DLS; while the SLS is mainly sensitive to the dense core of microgel.

In this study, the swelling behaviours of PAA microgels as a function of pH and ionic strength were determined by using both DLS and SLS experiments analyzed by two different approaches: the SasView software and Rayleigh–Gans–Debye (RGD) approximation.

2. MATERIALS AND METHODS

2.1 Materials

The preparation method of spherical PAA microgels with low cross-linking density was reported previously in the literature [13].

Sodium hydroxide (NaOH), hydrochloric acid (36%HCl), and sodium chloride (NaCl) were purchased from Fisher Scientific UK and used as received. Deionized (DI) water with a resistivity higher than 18.2 MΩ·cm was obtained from a Millipore Milli-Q Plus.

2.2 Sample preparation

As mentioned above, the pK_a of carboxyl group is about 4.5-5. The swelling behaviours of PAA microgels were hence investigated in pH 4 and pH 7 solutions to ensure that the microgels will be in their fully collapsed and swollen states, respectively.

The pH 4 and 7 solutions were prepared with 0.1 M HCl or NaOH. Then, a certain amount of NaCl was added into the pH solutions to obtain different NaCl concentrations (0, 5, 25 and 50 mM). Dry PAA microgels were then dispersed in the prepared solutions at a concentration of 0.1 mg/mL using an ultrasonic probe for 15 mins, filtered through a 2-micron pore filter paper and waiting for 30 mins to achieve the swelling/de-swelling equilibrium.

The R_H and R_G of PAA microgels were evaluated using a Malvern Auto-sizer 4800 equipped with a laser generating light of 532 nm wavelength, which is used for both DLS and SLS measurements. For DLS, the intensity of the scattered light (I) was measured at 90°, and the intensity correlation function is then fitted by monomodal distribution to yield the R_H. For SLS, the intensity (I) was measured as a function of scattering angles (θ) in a range of 30-140. Subsequently, the SLS data were analyzed using two different approaches: the SasView software and RGD approximation to obtain the R_S and R_G.

3. RESULTS AND DISCUSSION

The DSL measurement informs the size distribution of PAA microgels dispersed in pH 4 and pH 7 solutions with salt added, as shown in Figure 2. The results illustrate that the size distribution of PAA microgels is rather broad, mainly in a range of 100-1,000 nm.

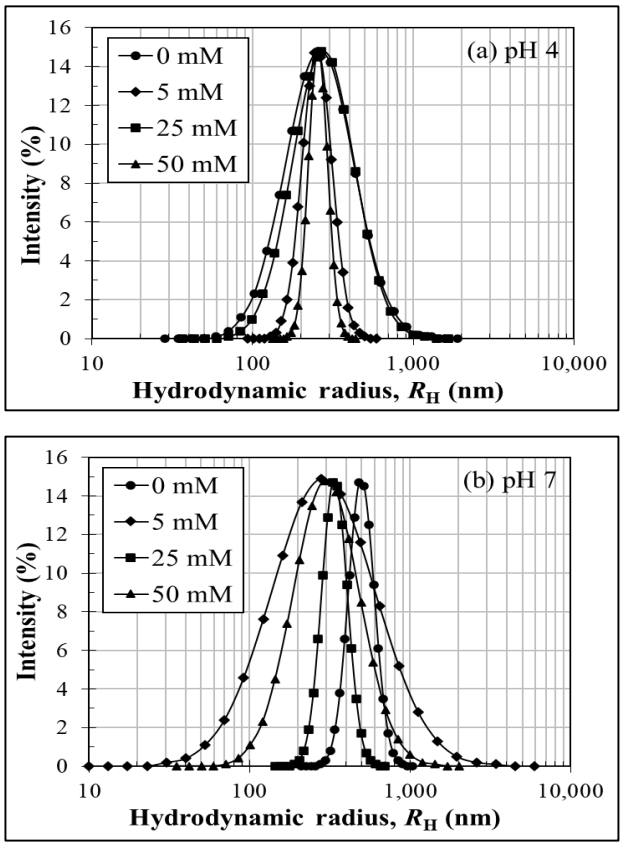

Figure 2. Hydrodynamic radius distribution curves in terms of intensity (%) obtained by DLS analysis of PAA microgels dispersed in (a) pH 4 and (b) pH 7 solutions with different salt concentrations (0, 5, 25 and 50 mM).

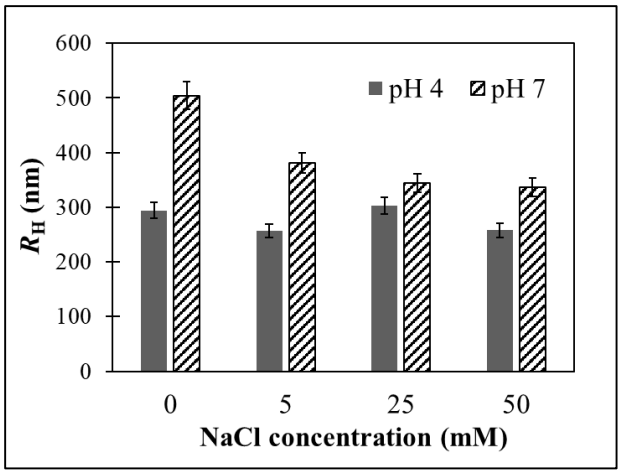

Figure 3. Hydrodynamic radius (R_H) obtained by DLS analysis of PAA microgels dispersed in (a) pH 4 and (b) pH 7 solutions with different salt concentrations (0, 5, 25 and 50 mM).

In Figure 3, PAA microgels become swollen when the pH of solutions is increased from 4 to 7 due to the electrostatic repulsion between the ionized carboxyl groups. Moreover, the maximum swelling ratio ($R_{H,\ pH7}/R_{H,\ pH4}$) is about 1.7 found in the solution without salt addition. In pH 4 solutions, the effect of salt concentration is not obvious; while the R_H of PAA microgels significantly decreases with an increase in salt concentration.

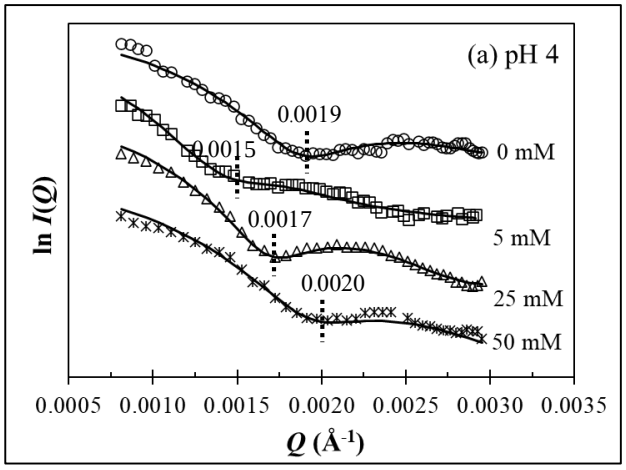

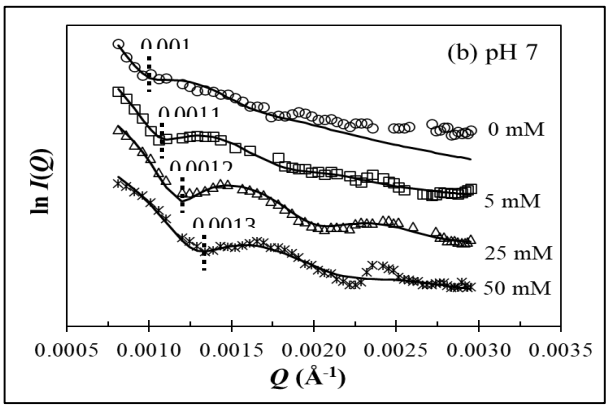

Figure 4. Scattering intensity profiles fitted by the SasView program with polydisperse sphere model of PAA microgels dispersed in (a) pH 4 and (b) pH 7 solutions with different salt concentrations (0, 5, 25 and 50 mM).

For SLS, the SasView software and RGD approximation were performed to evaluate the particle size of spherical PAA microgels. For a solid sphere, the static radius (R_S) and the radius of gyration (R_G) are related as $R_G = 0.775R_S$. With RGD approximation, the R_S is calculated from the value of Q at the location of the first minimum ln $I(Q)$ with a relationship of $Q_{min}R_S = 4.49$. With the SasView software, the SLS data (the plot of $I(Q)$ vs Q) was fitted using a polydisperse sphere model as shown in Figure 4. It is seen that the scattering intensity profiles of all samples can be fitted very well with the polydisperse sphere model, and the location of the Q_{min} can be observed and then calculated into the R_S.

The R_S of PAA microgels at pH 4 and 7 with different salt concentrations are shown in Figure 5. It is seen that the effect of pH and salt concentrations fitted by the SasView software are analogous to the RGD approximation. The maximum swelling ratios ($R_{H,\ pH7}/R_{H,\ pH4}$) are 1.8 and 1.9 corresponding to the RGD and SasView software, respectively. In addition, the swelling behaviours of PAA microgels triggered by changes in pH and salt concentrations analyzed

with the SLS are consistent with the results obtained by the DLS.

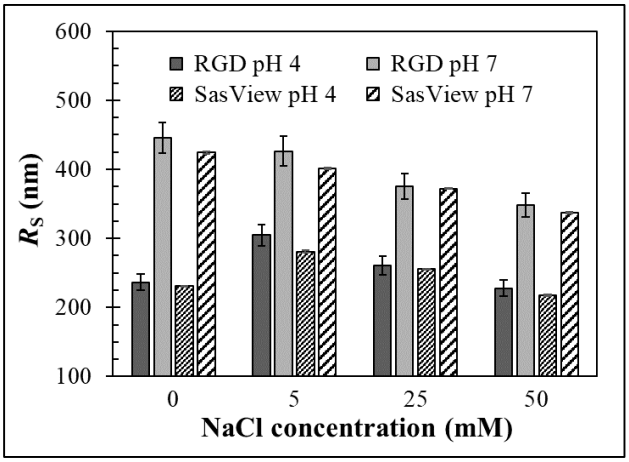

Figure 5. Static radius (R_S) of PAA microgels dispersed in pH 4 and pH 7 solutions with different salt concentrations (0, 5, 25 and 50 mM) obtained by fitting the SLS data with the SasView software and RGD approximation.

Combining the scattering data measured by DLS and SLS, the internal structure of PAA microgels can be investigated via the shape factor (R_G/R_H) as shown in Table 1. The shape factor values of PAA microgels at pH 4 are mostly lower than 0.775 (for homogeneous hard-sphere). These values are consistent with the dense core with a loose shell structure or non-uniform cross-linking density distribution as reported previously. However, the shape factor values at pH 7 with salt added are mostly above 0.775, indicating the heterogeneous swelling/de-swelling of PAA microgels.

Table 1. Comparison of the shape factor of PAA microgels analyzed with the SasView and RGD.

pH	NaCl concentration (mM)	Shape factor	
		$R_{G,SasView}/R_H$	$R_{G,RGD}/R_H$
4	0	0.62	0.61
	5	0.92	0.85
	25	0.67	0.65
	50	0.68	0.65
7	0	0.68	0.65
	5	0.87	0.81
	25	0.84	0.84
	50	0.80	0.78

4. CONCLUSIONS

In this study, DLS and SLS experiments were utilized to investigate both size (R_H, R_G and R_S) and internal structure of PAA microgels via shape factor defined as the ratio R_G/R_H.

Effects of pH and salt concentration on the swelling behaviours of PAA microgels obtained by the DLS are consistent with the results from the SLS.

The results of SLS data analyzed with the SasView software are comparable with those of RGD approximation.

The shape factor suggests that the PAA microgel structure is a dense core with a loose shell, and their swelling is heterogeneous due to non-uniform cross-linked density distribution in the microgel structure.

5. ACKNOWLEDGEMENTS

SLS data analysis benefited from SasView software, originally developed by the DANSE project under NSF award DMR-0520547 (see website: http://www.sasview.org/).

6. REFERENCES

[1] Bajpai AK, Shukla SK, Bhanu S, Kankane S. Responsive polymers in controlled drug delivery. Prog Polym Sci 2008; 33:1088-1118.

[2] Laftah WA, Hashim S, Ibrahim AN. Polymer hydrogels: A review. Polym Plast Technol Eng 2011; 50: 1475-1486.

[3] Ahn S, Kasi RM, Kim SC, Sharma N, Zhou Y. Stimuli-responsive polymer gels. Soft Matter 2008; 4: 1151-1157.

[4] Swift T, Swanson L, Geoghegan M, Rimmer S. The pH-responsive behaviour of poly(acrylic acid) in aqueous solution is dependent on molar mass. Soft Matter 2016; 12: 2542-2549.

[5] Bromberg L, Hatton TA, Barreiro-Iglesias R, Alvarez-Lorenzo C, Concheiro A. Controlled release camptothecin tablets based on pluronic and poly(acrylic acid) copolymer. Effect of fabrication technique on drug stability, tablet structure, and release mode. Drug Dev Ind Pharm 2007; 33: 607-615.

[6] Bromberg L, Temchenko M, Hatton TA. Dually responsive microgels from polyether-modified poly(acrylic acid): swelling and drug loading. Langmuir 2002; 18: 4944-4952.

[7] 3P instruments. Static light scattering [internet]. 2020 [cited 2020 June 30]. Available from: https://www.3p-instruments.com/measurement-methods/dynamic-light-scattering/

[8] Minton AP. Recent applications of light scattering measurement in the biological and biopharmaceutical sciences. Anal Biochem 2016; 501: 4-22.

[9] Stetefeld J, McKenna SA, Patel TR. Dynamic light scattering: a practical guide and applications in biomedical sciences. Biophys Rev 2016; 8: 409-427.

[10] Schärtl W. Light scattering from polymer solutions and nanoparticle dispersions; Berlin: Springer; 2007.

[11] Boon N, Schurtenberger P. Swelling of micro-hydrogels with a crosslinker gradient. Phys Chem Chem Phys 2017; 19: 23740-23746.

[12] Wu X, Pelton RH, Hamielec AE, Woods DR, McPhee W. Colloid Polym Sci 1994; 272: 467-477.

[13] Doungsong N. Synthesis and characterization of poly(acrylic acid) based microgels for formulation applications [Thesis]. Bristol: University of Bristol; 2018.

CreTech 2020
8th International Conference on Creative Technology
Multidisciplinary to Drive Economy and Social
http://utkcretech.rmutk.ac.th

Surviving the Disruptive Era: A Case Study through Voices of Leading Hoteliers in Bangkok, Thailand.

Komm Pechinthorn[1*], Ploy Umpornpet[2]

[1] International Business Management, International College, Rajamangala University of Technology Krungthep
[2] Innovative Tourism and Hospitality, Faculty of Business Administration, Thai-Nichi Institute of Technology
*Corresponding author. Email: Komm.p@mail.rmutk.ac.th

ABSTRACT

With many factors and situations that are now arises and affecting all of us unpredictably. This research aims to develop a study that is important to Thailand's tourism industry and its affiliated business, namely, hospitality business. While the world is now revolving and getting though the Disruptive Era, Thailand, like many other countries, is adjusting to the *adaptation phase and must act to survive* or else facing an economic ordeal. This research has provided both meanings and definitions of the Disruptive Era and Hoteliers but rather than convening simple findings of the study, research has targeted to reveal creative results, which in the near future, would stay in support to a broader study of an Economic Development based on the Thailand 4.0 model, that aims to unlock the country from several economic challenges resulting from past economic development models... (12) and to bring out creative guidelines in developing hospitality business which tailored to the needs of any travelers, through a theory related to *Customer Centric*. The Qualitative Method (Purposive Selection of an individual), has been chosen to analyze the *Two main Outcomes of this research;* 1. Reactions and concerns of the Hoteliers to the Disruptive Era through its major changes 2. Strategy and plans the Hoteliers have developed and implemented successfully. While the *result can be identified into the Two forms of theories, 1. The Six Sigma and 2. The Two – Factors Theory*, researcher has concluded that leadership skills no matter in hospitality and/or businesses with quick turn of outcome, such as "loyalty". To survive such dynamic and impacts of the Disruptive Era, People Skills, Inspiration Driven Leaders, together with their consciousness and experience have proved to successfully led their businesses and still surviving.

Keywords: disruptive era, disruptive innovation, hoteliers, Thailand's hospitality industry, hospitality business, disruption in hospitality, leading through change, strategic planning, lead and inspired, people management, customer satisfaction

1. INTRODUCTION

There is no denial to the fact that Disruptive Era has become one of the main discussion topics no matter in the academic level or the study of economics in Thailand. But to scope down our research areas, there are two main definitions the researcher would like to introduce; 1. Disruptive Era of the Hospitality Industry, according to JLL (13) Disruption is encouraging hotels to find opportunities to add value in their current models. Emerging technology is also playing a big role in helping hotels to operate more efficiently and enabling guests to have a smoother stay, in addition, brands (hotels) are looking to use new technology to improve their digital presence and improve guest loyalty. Guests on the other hand, could engage more deeply with a destination, as well as, with the hospitality brand itself. With facts

in mind, Disruptive Era also, brings certain conveniences especially, in sharing their opinions instantly via social media. More to the human factor and their perceptions, according to Hotelier Magazine (14) To counter competitive forces, there has been a major shift towards customer facing innovations The investment (in hospitality business) is now in visible things guests can see, from living walls to rooftop, charging stations and outside gardens – all of which add to the overall experience. Growing move towards digital replacements for almost all forward – facing facets: from check – in processes everyone is evolving, we are in an era of influx and everyone is adjusting to where the industry might be or is going (14). 2. The Hoteliers, as defined by Merriam Webster Dictionary (15): a proprietor or manager of a hotel. Leading Hoteliers, in this research are acquired to lead through Disruptive era, a major change, which does not happen easily therefore, leaders can facilitate change and thereby help organization adopt to external problems and opportunities. It is important for leaders to recognize that the change process goes through stages leaders are responsible for guiding employees and the organization (11). To successfully carry out valid and precise result, the researcher has chosen leading Hoteliers working in Bangkok, as stated a journal of factors influencing international visitors to revisit Bangkok, Thailand (4), both the World Tourism Organization and Time magazine (2013), Bangkok has been selected as the world's most visited city and Thailand itself has been considered as one of the top three most popular tourist destination in Asia. The businesses in hotel industry in Bangkok should compete with those other destinations based on outstanding service quality suggested also to enhance the convenience and reliability using online system and platforms for bookings (4). Researcher has chosen the Qualitative Method, though interviews with narrative transcript, which analyzed in conclusion and linked the key answers as Disruptive Era, presented in Bangkok, can be managed and handled effectively through leading Hoteliers with Strategic Management Plans and People Strategy.

2. MATERIALS AND METHODS

The Qualitative method chosen for this research has been observed and transcribed directly from the *Purposive Selection* of the Nine leading hoteliers selected from brands of hotel announced in the year of 2017 Table.1 (16) their planned to operate/expanded in Thailand by the year of 2020. Set of interview questions comprises of Five Open - Ended questions, and in the end, researcher has probed the interviewees into suggesting best plans they have yet explored and strategic tactics they have experienced to have used and successfully implemented in managing while in crisis/situation(s) during this so called Disruptive Era.

Table 1. Bangkok's Post Reported Year 2017 – Recent Hotel Announcement in Thailand (16).

RECENT HOTEL ANNOUNCEMENTS

Hotel chain	Projects/properties	Opening time
Miners Hospitality (Singapore)	Developing the Rizin Hotel & Residences Pattaya	2018
Frasers Hospitality (Singapore)	Looking for new project upcountry	-
Travelodge (US)	Opened hotels in Bangkok and Pattaya, planning for 50 properties or 10,000 keys by 2020	2017
Airbnb (US)	Planned for 68-million-baht investment in Asia-Pacific	By 2020
Erawan Group (Thailand)	Planned to operate 87 hotels and more than 10,000 rooms in Thailand and overseas	By 2020
Miracle Group	Opened new phase of Sleep Box in Don Mueang	2017
Proud Real Estate	Holiday Inn Vana Nava Hua Hin	2017
Minor Hotels and B&G Park Co	Avani Hua Hin Resort & Villas	2017
Enrich Group and Dusit International	DusitD2 and DusitD2 Residences Hua Hin Thailand is third highest levels for hotel	2020
JLL Hotels & Hospitality Group	Investment in the Asia-Pacific region	Jan-Sep 2017

Source: Bangkok Post BANGKOK POST GRAPHICS

As referred by Mohd and Mohd (3) some of the advantages of the Qualitative research in a hospitality research (Veal, 1992), the characteristics of the industry itself as a service industry which demands close interactions between people favors a Qualitative approach.

The method is more likely to be able to encompass changes over time (3). In support to best enhanced the context given by the interviewees, researcher has ensure that selected Nine individuals have a prior knowledge of the Disruption overview and/or at least, understand the technological revolution as defined by Buhalis et al., 2019 (2) the service management inevitably has been influenced by recent technological revolutions and smartness. The rapid evolving wave of technological advancements have major implications for service management and marketing and we can learn from tourism as a frontline service industry that integrates new knowledge on technological advancements in strategic planning processes, (Philips and Moutinho, 2014) Buhali et al., (2).

Enclosed space, and time limitation of *forty-five minutes* for each interviewee were also taken into the account and narrated fairly to best interpreted and concluded in form of summarized theories intended for future study and further research. Therefore, researcher has *omitted the method of a Focus Group Discussion* as appeared that selected individuals have limited time to spent and/or time as of the essence needed be considered.

Selected Nine interviewees are also *multi-nationals*, and *only communicate in English*. As this research has shown no valid data that correlates interviewees' nationalities to the perception and techniques on how they surpassed the Disruption Era while working in Bangkok, Thailand. Researcher trusts that Hoteliers as described by the Characteristics of Creative People and Organizations by Steiner, 1965 (10); they can be Conceptual fluency open-mindedness and, in the organization, they can also be resources allocated to creative personnel and projects without immediate payoff. Reward system encourages innovation. Inspiration and Motivation may be of help to the survival of service industries.

Unlike many areas of businesses, leading Hoteliers rely much on people, and with Disruptive Era, quick communication; reliable and timely information transfer and retrieval; sharing of information and achievement of common objectives as mentioned by Buhalis, 2020 (5), all have become quite a common sharing management tactics to hospitality leaders. The Qualitative approach would help support the researcher to compiled of interesting reasonings, strategic plans and results which can be further developed to a step forward the Thailand 4.0 Economic Model.

The same time, " *Think globally, act locally.* " Given the ease and speed at which information travels, every institution in the knowledge society has to be globally competitive, even though most organizations will continue to be local in their activities and market (7). To best suited the business during this era and time of global competitiveness, can this also be a strategy for the leading individuals to gear up their management strategy for the better? In order to survive. As displayed on Figure 1. (17) *a massive declined of -87%* only comparing the first two months of January and February of the year 2020. While crisis management and critical situation have not yet been proper defined as Disruptive factors. But a rapid change which resulted negative impact to the Hospitality industry can be defined as Disruptive act, and it is common for leading Hoteliers to provide and talk about a Strategic Management as defined by Daft, 2010 (6), the set of decisions and actions used to formulate and implement strategies that will provide a competitive superior fit between the organization and its environment so as to achieve organizational goals. As the set of strategic planning can always be adapted to implement for the business to survive the era.

Figure 1. International Tourists arriving in Thailand. ATTA's Members at Suvarnabhumi and Don Muang Airport. *As of 10 Feb. 2020* (17). (**1st quarter of Year 2020**) = (***minus***) – **87.51%**

YEAR	2559	2560	2561	2562	2563
MONTH	2016	2017	2018	2019	2020
January	490,545	433,996	542,326	492,967	**409,324**
February	518,335	472,562	539,199	489,938	**51,122**

3. RESULTS AND DISCUSSION

İnnovation cannot be separated from a firm's strategy or its competitive environment, which means that what we consider to be innovative is defined by the context... Firms innovate in a number of ways including business models, products, services, processes, and marketing channels with either the goal of maintaining or capturing markets or the desire to reduce cost or prices through greater efficiencies (8). Whilst Management always lives, works, and practices in and for an institution, which is human community held together by a bond: the work bond. And precisely because the object of management is a human community held together by the work bond for a common purpose, management always deals with the nature of man and with Good and Evil (7).

Therefore, to bridge and relate the surviving strategic tactics and plans to the Disruptive Era, this research has found a *significant inter- related connections between Disruptive causes*, no matter in Innovation and Rapid Change of situation to the Human Factor. To better deliver the results narrated into this Discussion part, the researcher chose to explain each discussion point in the following order:

Disruption Concerns and Points of Interest

According to the first couple of questions on how the interviewees understood of the Disruptive Era, how it has affected their establishments? All Nine leading Hoteliers agreed to the main fact that *Disruption itself, simply means, a change, in which, can be either planned or unplanned*. When proposed whether the interviewees see the Disruptive Era as their vulnerable period, almost all but one answered firmly that they see it as an *Era of Opportunities*, the latter requested for more details as *Disruption can be further explained into the change in an upper management, therefore, it can be vulnerable within one business*. One Interviewee has also, expressed his interests and compared the Disruptive Era to Maslow's Theory, the highest need category , self – actualization, represents the need for self- fulfilment: developing one's full potential, increasing one's competence, and becoming a better person (10). "*Innovative technology, much activated and discussed upon Disruptive Era, very little people realized that the world is disrupted due to the need, they longed for a better world...*" said one of the interviewee.

Possibility for leading Hoteliers to replace employees with the 'AI – Aritificial Intelligence', AI Is a narrowly applied decision – support tool, with potential application to a broard range of business operations. Expectations for its adoption and impact on types of services offered and business processes supported are considerable in service industries (2). As stated by Boonbumroongsuk and Panvisavas, 2019 "...because employees are the centric resources in providing its (hotels) services to customers, and they are the gateway to a hotel company's product "First–line" employees have to match the customers' needs with their company's service offerings... (1). It is undeniably tempting with such technology of an AI, but the interviewees entrusted, human development, and believed that the Disruption Era, brought much *Inventive Technologies to stay intertwined with*

human. Rather, interviewees, have expressed a much diverted concern into *"putting the right people to the industry"*. *Talent management is critical in the hotel industry*, where human capital, is one of the key success factors to having a competitive advantage in the business (1).

The most important part of each interview session was to find out, the thoughts behind selected leading Hoteliers in Bangkok, how they have succesfully implemented one or more Strategic Plan(s) and/or Technique(s) inorder to help support the organization during the Disruptive Era. Researcher has concluded important factors and related theories provided by the Nine leading Hoteliers:

3.1 Customer Centricity through the Six Sigma Culture, its goal is to delight customers. The quality of a product or services is measured from the customer's perspective by its contribution to their success... The Six Sigma is also a system of management to achieve lasting business leadership and top performance applied to benefit the business and its customers, associate and shareholders (9).

3.2 The Two – Factors Theory, a popular theory of motivation by Frederick Herzberg as described by Lim and Daft, 2017 (10) Herzberg interviewed hundreds of workers about times when they were highly motivated to work and other times when they were dissatisfied and unmotivated to work...(10) People in hospitality industry, similar to Herzberg's Motivator and Hygiene Factors, employee can be highly motivated by Achievement, Recognition, Responsibility, Work itself and Personal Growth. While the latter, influenced Dissatisfaction are those Working conditions, Pay and Security, Company Policies, Supervisors and Interpersonal Relationships (10). Interviewees entrusted in a fact of building a success though teamwork, therefore, employees shall first be motivated and trust in the organization enough to grow and further their capabilities for the success of business, resist and stand with an unexpected outcome or change.

Bridging to survive – Interviewees, have Discussed and in the end adhered that the Hospitality Industry in Bangkok is here to stay. And for certain would survive the Disruptive Era. Leaders should learn to *embrace and know to properly control any crisis, similar to any Disruptive impacts*, for selected leading Hoteliers, Disruptive Era is another period of change much like back in the days when no one would have thought that a landline/public telephone service would soon be deminished.

4. CONCLUSIONS

Surviving the Disruption Era, like any other changes that occurred over time. People would have to get through many phases, they learned to adapt themselves and thrive to move on. Leading Hoteliers, according to this research emphasized their opinions, thoughts and recommended the society to not feel overwhelmed, prepare to embrace with era and its innovation and never to neglect in managing people.

Regardless of which industry you have operating in, it is no longer linear and predictable; instead, it is all about uncertainty, ambiguity and unpredictability. Because the game has changed, we need to change our game in order to stay in the game (18). For the business to stay..., it should learn to disrupt themselves. This cannot be done unless leaders and executives start disrupting their thinking first in order to stay agile and relevant (18). Both the Six Sigma and the Two – Factors Theories were summarized and concluded in this research to solely presented the thoughts of selected leading Hoteliers working in Bangkok, Thailand. Therefore, they have expressed their readiness to the Disruptive Era itself, as the following 'rule of thumb' for the Hoteliers to know by heart that customers will always come first, there is very little room for any errors and/or unsatisfactory. Hotel business is fast paced, and highly competitive, especially in Bangkok. Therefore, the Six Sigma – Customer Centric theory does help strategically in creating loyalty and maintain high

standard of service, for a business to survive. While the Two - Factors theory supported highly in maintaining the ambience in an organization, a day-to-day inspiration, leaders should not forget to inspire their employee. It is important for hospitality business to act fast, maintain their high level of standards and build trust among their organizations, clients and other prospects.

With all the available materials and research on the Disruptive Era, how it affects a business. Researcher intended to deliver the result that can be in support to a future study of Disruptive term, in other aspects. Also, with limitation of time, one of the innovative technologies, such as, the AI Server/ Service Robot, believed to be replaced human, has not yet been released to any of the establishments of the selected leading Hoteliers. Therefore, researcher plans to develop an updated study in order to review and affirm whether such innovation occurred in the Disruptive Era, can be of help and support to the human employee ***or*** should be treated as a threat for a business

5. ACKNOWLEDGMENT

Researcher would like to express her gratitude to the CreTech 2020, Committee in providing the opportunity and for accepting research paper in Tourism & Hospitality. Researcher, with hopes in mind, would like for this research study to expand the knowledge of Disruptive Era, focusing on the Tourism & Hospitality Industries. And for those Academic readers, to understand more and truly of how (selected individuals) leading Hoteliers reflected back to the popular discussion topic of a Disruption, how they handled and embraced with the era.

6. REFERENCES

[1] Boonbumroongsuk B, Panvisavas V. Talent Management in the Thai Hotel Industry. Journal of Thai Hospitality and Tourism. 2019;14(1):78-91.

[2] Buhalis D, Harwood T, Bogicevic V, Viglia G, Beldona S, Hofacker C. Technological disruptions in services: lessons from tourism and hospitality. Journal of Service Management. 2019;30(4):484-506.

[3] Mohd, Yusof, and Fadil Mohd. "The Experience of Applying a Qualitative Methos in a Hospitality research" www.fp.utm.my/Epusatsumber/Listseminar/7.QRAM05/session2/87.MohdFadilMohd Yusuf.pdf, Fp.utm.my, 21 Aug. 2005, pdfs.semanticscholar.org/a82c/109cb8da5cef1a57ca69cc0e9ad2fc24ee78.pdf.

[4] Thiumsak T, Ruangkanjanases A. Factors Influencing International Visitors to Revisit Bangkok, Thailand. Journal of Economics, Business and Management. 2016Mar;4(3):220-30.

[5] Buhalis D. ETourism: information technology for strategic tourism management. Harlow, England: Financial Times Prentice Hall; 2010.

[6] Daft RL. New Era of Management. London: Cengage Learning; 2010.

[7] Drucker PF, Maciariello JA. The Daily Drucker: 366 days of insight and motivation for getting the right things done. London: Routledge; 2011.

[8] Enz CA, Harrison JS. Hospitality Strategic Management Concepts and Cases. Hoboken, NJ: Wiley; 2010.

[9] George ML. Lean Six Sigma: combining Six Sigma quality with lean speed. New York: McGraw-Hill; 2005.

[10] Lim, Ghee Soon, and Richard L. Daft. The Leadership Experience in Asia. Cengage Learning Asia Pte Ltd, 2017.

[11] Ireland RD, Hitt MA, Hoskisson RE. The management of strategy: Concepts and Cases. Australia: South-Western Cengage Learning; 2013.

[12] Beat Z. What is Thailand 4.0? [Internet]. CEBIT ASEAN Thailand. 2018 [cited 2020Feb15]. Available from: https://cebitasean.com/what-is-thailand-4-0/

[13] Jll. How disruption is driving change for hotels [Internet]. JLL Thailand. JLL; 2017 [cited 2020Feb15]Available from: https://www.jll.co.th/th/trends-and-insights/workplace/how-disruption-is-driving-change-for-hotels.

[14] Kostuch Media Ltd., Kostuch Media Ltd. Hotels in the Age of Disruption [Internet]. Hotelier Magazine. 2017 [cited 2020Feb15]. Available from: https://www.hoteliermagazine.com/hotels-age-disruption/

[15] Hotelier | Definition of Hotelier by Merriam-Webster. www.merriam-webster.com/dictionary/hotelier.

[16] Sritama S. Hotel chains are following the swarm of tourists [Internet]. https://www.bangkokpost.com. Bangkok Post Group; 2017 [cited 2020Feb15]. Available from: https://www.bangkokpost.com/business/1364271/hotel-chains-are-following-the-swarm-of-tourists.

[17] Statistics International Tourists Arriving in Thailand as of 10 February 2020: ATTA: Association of Thai Travel Agency [Internet]. Go to ATTA |. Association of Thai Travel Agency; 2020 [cited 2020Feb15]. Available from: http://www.atta.or.th/statistics-international-tourists-arriving-in-thailand-as-of-10-feb-2020/.

[18] Talerngsri, Arinya. "Inconvenient Truths in the Disruptive Era." Bangkok Post Group, September 26, 2017. https://www.bangkokpost.com/business/1331199/inconvenient-truths-in-the-disruptive-era.

CreTech 2020
8th International Conference on Creative Technology
Multidisciplinary to Drive Economy and Social
http://utkcretech.rmutk.ac.th

The impact of service quality and service recovery on customer satisfaction and brand loyalty : a case study of an e-commerce company in China

Jingwei Yang[1*], Sasithorn Suwandee[1], Pavadee Surakomol[1], Felicito Jabutay[1]

[1]Kasem Bundit University, Thailand
*Corresponding author. E-mail: 275945465@qq.com

ABSTRACT

Customer satisfaction affects the loyalty of customers to enterprises, which is an important competitive advantage, especially in e-commerce enterprises. This research enhances the understanding the role of e-service quality and e-service recovery on customer satisfaction and customer loyalty in e-commerce business. This study provides managerial implication for an e-commerce company to improve its strategies. Respondents are 308 customers who used the most popular e-commerce company to online shopping. The research result confirmed the positive effect of e-service quality and e-service recovery on customer satisfaction and customer loyalty. The study also found that e-service recovery has stronger impact on customer satisfaction than e-service quality. This reflected that e-commerce company should focus on remedial service failure to improve customer satisfaction and loyalty.

Keywords: E-service quality, E-service recovery, Customer satisfaction, Customer loyalty

1. INTRODUCTION

With the rapid development of B2C e-commerce, more and more people buy goods through e-shopping platform instead of a physical store [1]. China is the fastest growing internet market in Asia, and accounts for a large share of the global internet market. Ghalandari [2] identified that the quality of service provided determine customer satisfaction and attitude loyalty. Especially for the e-stores, the service staff did not contact with customers in person. E-service quality directly affects e-trust and e-satisfaction, and indirectly affects e-satisfaction through e-trust, which means that the higher the quality of e-service, the higher the e-trust and e-satisfaction of e-shop service. By promoting user-oriented network communication, marketing personnel help customers purchase goods and services provided on the internet. Through this kind of communication and assuming appropriate customer participation skills, the process quality of internet products has been enhanced, and customers can perceive the result of high service quality provided [3]. Prior research does not extensively investigate the role of e-service recovery. Hence, the objectives of this research are: 1.) explore the effect of e-service quality and e-service recovery on customer satisfaction; 2.) examine the effect of customer satisfaction on customer loyalty; 3.) provide managerial implication to improve services.

Parasuraman et al. [4] introduced electronic service quality (E-S-QUAL) for measuring the service quality delivered by Web sites on which customers shop online. It includes: 1.) Efficiency, the ease and speed of accessing and using the site; 2.) Fulfillment, the extent to which the site's promises about order delivery and item availability are fulfilled; 3.) System availability, the correct technical functioning of the site; 4.) Privacy, the

degree to which the site is safe and protects customer information. They also propose recovery service quality scale (E-RecS-QUAL) consisting of three dimensions: 1.) responsiveness, effectiveness of handling problems and returns through the site; 2.) compensation, the degree to which the site compensates customers for problems; 3.) availability, assistance through telephone or online representatives.

Ghane et al. [5] studied the relationship between E-service quality and E-satisfaction. The study focused on 965 students from four universities and found that service quality dimensions are positively related to customer satisfaction. The quality of e-service has a direct and indirect impact on e-satisfaction [5]. Consistently, Shanka [6] found that the relationship between service quality dimension and customer satisfaction is confirmed through study on 245 customers of e-banking. The service quality provided has a positive impact on the overall customer satisfaction [6]. Service quality is the foundation of service integrity through customer satisfaction [7]. The improvement of service quality can satisfy and develop customer satisfaction, and ultimately retain valuable customers [4]. Therefore, this study proposes

Hypothesis 1: E-service quality has positive effect on customer satisfaction.

Jung & Seock [8] examined the effect of service recovery on customer's satisfaction on online shopping websites. Using Qualtrics.com, 368 participants were recruited for the main survey. This study confirms that within the context of service recovery, customers perceive distributive and interactional justice differently depending on the type of service recovery they receive. Customers' perceptions of justice significantly affect their post recovery satisfaction, and, eventually, customer satisfaction is improved by service recovery.

Therefore, this study proposes

Hypothesis 2: E-service recovery has positive impact on customer satisfaction.

As good service leads to a positive correlation between customer satisfaction and customer loyalty [9]. This means that the more satisfied customers are with the service, the more loyal customers are to the industry. Therefore, satisfying customers is important in developing loyal customers [6]. Additionally, the strong positive correlation between customer satisfaction and customer loyalty means that customers will recommend the company to others. Therefore, it can ensure that the company has a loyal and stable customer base, thereby reducing costs in acquiring new customers [10].

Since the severity of service failure is related to satisfaction, remedy for service failure in e-retailing company based on interactive fairness to dissatisfied customers can improve customer loyalty and alleviate the negative relationship between the severity of service failure and customer loyalty [1]. These customers are more likely to visit service providers in the future and share their positive experiences with others [11]. Therefore, this study proposes:

Hypothesis 3: Customer satisfaction has positive impact on customer loyalty.

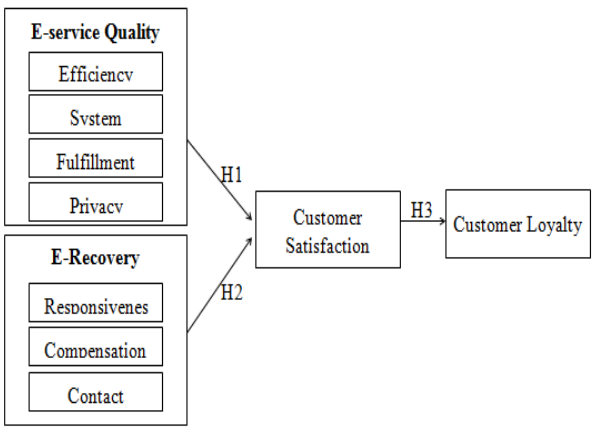

Figure 1: Conceptual framework

2. MATERIALS AND METHODS

This study randomly distributed 1,000 questionnaires to customers of the selected e-commerce company who experience service failure while shopping online. This study uses simple regression to verify hypotheses. The study found 308 valid questionnaires. 52 % (n=160) of respondents are female and 48% (n=148) of respondents are male. 31% of respondents are in the age between 26 to 35 years old. 76% of respondents obtained a bachelor degree. 39% of respondents have monthly income between 7,001 to 10,000 CNY. 29% of respondents use online shopping a few times per month. 35% of respondents spent between 200 to 500 CNY per month for online shopping.

The measurement items of all four variables are in a 5-point Likert scale (ranging from 1 for Strongly Disagree to 5 for strongly agree). For *E-service quality*, 22 items are adopted from Parasuraman et al [4]. It is divided to four dimensions, include efficiency, fulfillment, system availability, and privacy. For *E-service recovery*, 10 measurement items are adopted from [4]. It is divided to three dimensions, include responsiveness, compensation, and contact. For *E-loyalty*, 11 measurement items are adopted from Harris & Goode [12]. It is divided to four dimensions include cognitive loyalty, affective loyalty, conative loyalty, and action loyalty. For *Customer Satisfaction*, three measurement items are adopted from Anderson & Srinivasan [14]. The items are: 1.) "I am satisfied with my decision to purchase from XXX."; 2.) "I think I did the right thing by buying from XXX."; 3.) "My choice to purchase from XXX was a wise one."

Factor loadings of e-service quality (>0.70), e-service recovery (>0.762), customer satisfaction (>0.935), and customer e-Loyalty (>0.912) are above 0.6 confirming validity [14].

The study found that e-service quality, E-service recovery, customer satisfaction, and customer E-loyalty have sufficient convergent validity and reliability. The average variances extracted (AVEs) for E-service quality (0.761), E-service recovery (0.655), E-loyalty (0.858) and customer satisfaction (0.888) were above 0.5, confirming convergent validity [15]. In addition, the composite reliability and Cronbach's alpha of variables exceeded 0.7, showing internal consistency for reliability. This study employed Cronbach's Alpha to test the internal consistency of measurement items of each variable. All variables have Cronbach's Alpha value above 0.8 which reflected that all variables have high internal consistency (E-service quality=.961, E-service recovery=.904, E-loyalty=.0.949 and Customer Satisfaction=0.904).

3. RESULTS AND DISCUSSION

The current study conducted simple regression to test the direct effect of three hypotheses. The findings of hypothesis 1 suggested that E-service quality has positive impact on customer satisfaction (p = 0.000, β = 0.969). This study also confirm hypothesis 2 that E-service recovery has positive impacts on customer satisfaction (p = 0.000, β = 0.849). In addition, this study found that e-service recovery (β = 0.569) has stronger impact on customer satisfaction that e-service quality (β = 0.298). The current study found that customer satisfaction has positive impact on customer loyalty (p = 0.000, β = .809). Thus, hypothesis 3 is supported.

This paper explores the impact of E-service quality and E-service recovery on customer satisfaction and verify the relationship between customer satisfaction and customer loyalty. Employing quantitative approach induce the findings that all three hypotheses are supported.

The research confirms that the good e-service quality and great e-recovery have positive impact on customer satisfaction. Meanwhile, high customer satisfaction is prone to improve their loyalty.

The present study found that E-service quality has positive influence on customer satisfaction. Among four dimensions of E-service quality, the efficiency, system availability, fulfillment, and privacy dimension, fulfillment is the most critical. The correlation between the fulfillment and customer satisfaction is the highest at 0.770 while system availability has the lowest correlation with customer satisfaction at 0.658. Thus, e-commerce company should seek to improve fulfillment dimension of E-service quality. This finding is consistent with finding of Shanka [6] that found the quality service provided has a positive impact on the overall customer satisfaction.

This study adopted the three dimensions of E-service recovery measurement (E-RecS-QUAL) of Ravichandran et al. [4]. The three dimensions are responsiveness, compensation, and contact. The finding from the present study is consistent with Singh & Crisafulli [16] that found the online service recovery is the key driver of customer satisfaction. Similarly, Jung & Seock [8] also confirmed the positive relationship between service-recovery and customer satisfaction. The finding from the present study compensation (0.757) is highly correlated with customer satisfaction compared to other dimensions. Hence, compensation can be the most effective means of E-service recovery. Therefore, e-commerce company should let compensation as most important methods to resolve service failures and improve customer satisfaction. In addition, e-commerce company needs to make timely communication and show their responsiveness, and pay attention to the way of communication with customer so that customer's satisfaction will be improved from effective E-service recovery.

Additionally, the standardized coefficient of e-service recovery on customer satisfaction is 0.569 which is more than that of e-service quality (β=0.298) so the impact of E-service recovery on customer satisfaction is stronger than E-service quality. This is consistent with Anderson & Srinivasan [13] that found that effective service recovery is especially important in services provided on the Internet. This is because online customers are difficult to attract and retain. However, customer still can feel the quality of product and service, thus, e-commerce company should pay attention more on E-service recovery.

The result of this study has suggested implications for e-commerce business operation and web-customer satisfaction. Online customers commonly have repeated experiences with various websites. This study focuses on the China famous website. The finding from the present study confirm that e-service quality and e-recovery are the two important factors to influence on customer satisfaction.

Also, this study confirmed the relationship between customer satisfaction and customer loyalty. This finding is consistent with finding of Ghane et al. [5] and Shanka [6] that found the customer's satisfaction has effective impact on customer loyalty. Therefore, e-commerce company should try to improve customer satisfaction to enhance customer loyalty.

4. CONCLUSIONS

E-commerce companies should focus on how to improve their e-service quality, including efficiency, fulfillment, system availability and privacy. This study found that system availability has the lowest correlation with customer satisfaction so e-commerce companies should pay more attention on efficiency, fulfillment and privacy as well as adopt ways to improve their e-service quality according to their actual situation.

The selected e-commerce company in this study needs to improve the search engine to make customers more convenient to find the products they need. The company should recognize that customers are very concerned about personal privacy. Respondents are worried that the selected e-commerce company will disclose their personal information so the company needs to improve the protection measures for customers to retain users, which will help to improve the service quality of the selected e-commerce company.

In addition, the selected e-commerce company should understand how to recover from online service failures as it is very crucial for service managers to design effective service recovery strategies. According to the present study, the contact dimension has lowest influence on customer satisfaction. Therefore, the e-commerce company should pay more attention on compensation and responsiveness to improve service recovery. The company should make effective compensation to customer, and provide online procedures in the form of FAQs, online help pages and discussion forums enable timely resolution of the service failure. Additionally, since the influence of e-service recovery is stronger than service quality, thus, E-service recovery is more important work for improving customer satisfaction.

This study also found that the selected e-commerce company needs to improve the compensation for users who have not successfully traded, so that the company can obtain higher rating in e-service recovery. In addition, the company needs to provide customers with better services and lower prices than competitors, and improve users' comprehensive evaluation of the company. The company needs to make customers feel that this purchase is very wise decision. Also, the company needs to strengthen the positive impact on its customers repeatedly because this can effectively improve customer loyalty.

In an e-commerce context, improve customer satisfaction and building e-loyalty are a difficult challenge. The difficult point is to differentiate themselves from competitors. The result confirms that loyalty of customer is directly affected by customer satisfaction, then, e-service quality and e-recovery are two key factors. Hence, the company should try to provide the sound e-service quality and e-recovery to increase customer satisfaction. It would enhance customer uses frequency of these services, intention to recommend, and likelihood of repurchase from these services in the future Ghane et al. [5].

There are several possible limitations to the research study. First, online questionnaire may cause discrepancies between reported behaviors and their actual behaviors. So, in future research, researcher should try to communicate with the respondents face to face. Second, this study did not provide details for service quality improvements, especially for E-service quality improvements as each website is not in the same situation. In future research, author should focus on how to improve e- service quality. Third, this study focuses on research how company deliver online recovery but did not address on the impact of online service recovery on customer perceptions and post-recovery behavior. So, further research shall focus on detail of service-quality, impact of customer perceptions, and post-recovery behavio

5. ACKNOWLEDGMENTS

I am grateful to many people who gave me guidance and help in the process of writing this paper. First of all, I sincerely thank to my advisor Dr.Sasithorn Suwandee[2], who is a respected and responsible scholar. I thank her for reading my paper, commenting on my ideas, helping me understand and enrich my ideas. I got a lot of encouragement and practical advice from her. Thanks for her suggestions and corrections to the

questionnaire. I would also like to thank my friends for their very cooperative participation in this study.

Most of all, without the love and patience of my family, it's impossible. I have to show my parents' support in particular. I want to express my heartfelt thanks to my family. My lovely family has been helping and encouraging me.

In addition, I would like to thank those who didn't mention their names. They gave me a lot of inspiration and encouragement until the completion of this independent study.

6. REFERENCES

[1] Wang YS, Wu SC, Lin HH, Wang YY. The relationship of service failure severity, service recovery justice and perceived switching costs with customer loyalty in the context of e-tailing. International journal of information management. 2011 Aug 1;31(4):350-9.

[2] Ghalandari K. The effect of e-service quality on e-trust and e-satisfaction as key factors influencing creation of e- loyalty in e-business context: The moderating role of situational factors. Journal of Basic and Applied Scientific Research. 2012;2(12):12847-55.

[3] Ojasalo J. E-service quality: a conceptual model. International Journal of Arts and Sciences. 2010;3(7):127-43.

[4] Ravichandran, K. Influence of Service Quality on Customer Satisfaction Application of Servqual Model, International Journal of Business and Management. 2010;5(4): 117-124.

[5] Ghane SO, Fathian M, Gholamian MR. Full relationship among e-satisfaction, e-trust, e-service quality, and e-loyalty: The case of Iran e-banking. Journal of Theoretical and Applied Information Technology. 2011 Nov 15;33(1):1-6.

[6] Shanka MS. Bank service quality, customer satisfaction and loyalty in Ethiopian banking sector. Journal of Business Administration and Management Sciences Research. 2012 Dec;1(1):001-9.

[7] Caruana, A. Service loyalty: The effects of service quality and the mediating role of customer satisfaction. European Journal of Marketing. 2002; 36(7/8): 811-28.

[8] Jung NY, Seock YK. Effect of service recovery on customers' perceived justice, satisfaction, and word-of-mouth intentions on online shopping websites. Journal of Retailing and Consumer Services. 2017 Jul 1;37:23-30.

[9] Jahanshahi AA, Gashti MA, Mirdamadi SA, Nawaser K, Khaksar SM. Study the effects of customer service and product quality on customer satisfaction and loyalty. International Journal of Humanities and Social Science. 2011 Jun;1(7):253-60.

[10] Siddiqi KO. Interrelations between service quality attributes, customer satisfaction and customer loyalty in the retail banking sector in Bangladesh. International journal of business and management. 2011 Mar 1;6(3):12.

[11] Gustafsson A. Customer satisfaction with service recovery. Journal of Business Research. 2009 Nov 1;62(11):1220-2.

[12] Harris LC, Goode MM. The four levels of loyalty and the pivotal role of trust: a study of online service dynamics. Journal of retailing. 2004 Jan 1;80(2):139-58.

[13] Anderson RE, Srinivasan SS. E□satisfaction and e□loyalty: A contingency framework. Psychology & marketing. 2003 Feb;20(2):123-138.

[14] Nunnally JC, Bernstein IH. Psychometric theory 3rd edn. New York: McGraw- Hill. 1994.

[15] Fornell C, Larcker DF. Evaluating structural equation models with unobservable variables and measurement error. Journal of marketing research. 1981 Feb;18(1):39-50.

[16] Singh J, Crisafulli B. Managing online service recovery: procedures, justice and customer satisfaction. Journal of Service Theory and Practice. 2016 Nov; 26(6): 764-87.

CreTech 2020
8th International Conference on Creative Technology
Multidisciplinary to Drive Economy and Social
http://utkcretech.rmutk.ac.th

The factors that influence students' decision towards work destination choices: A case study of public university

Komm Pechinthorn[1*], Ada Marie Mascarinas[1], Kyawt Shinn Thant Zin[1], Ploy Umpornpet[1]

[1]International College of Rajamangala University of Technology Krungthep, Thailand,
*Corresponding author. E-mail: Komm.p@mail.rmutk.ac.th

ABSTRACT

This research developed and tested the factors that influence students' decision towards work destination choices of the international college students in public university of Rajamangala University of Technology Krungthep (ICUTK). The variables in the hypothesis included Age, Gender, Grade Point Average (GPA), Expected Income and Maximum Traveling Time to work destination. By using the multiple regression analysis of the Minitab software, findings of this research presented all the included variables are the influenced factors for this group of respondents.

Keywords: Work destination**,** Public company, Private Company, Employment, Influence factor, Decision process

1. INTRODUCTION

The economy and the employmentcontext of Thailand have been rapidly changing recently. As a consequence of globalization, rapid technological changes, downsizing and outsourcing of activities, an increase in short-term contracts and self- employment have occurred [13]. However, the hiring process from private or public companies are not diminishing. In fact, people choose their careers that could provide improvement for their lives [5]. The meaning of occupation or job is explained by Jones & Larke [10] as a means of living, which has the power to change personalities, determine social status, predict expected earnings, determine social groups etc. Therefore, its importance of job selection cannot be undermined. Students do not usually think about their careers at the point of choosing departments in universities where they will be educated but often plan their careers after graduation [12]. It is not a bad idea to be able to identify any important factors that could impact the decision makin process for the young workforce being produced by the public universities in Thailand.

1.1 Scope and Objective

This research is attempted to study various factors that have relationship with the decision process of young university students' selection of work destination, public or private company, after graduation by testing on various selected factors.

1.2 Literature Review

In the past two decades, gender roles in the work force in many countries have been quite uneven and unfair. Females usually had lower paying jobs than men [4]. Despite how developed the country is, there is no guarantee on the equality in society with Japan as a good example. Currently, the playing field between the two are more even. However, when looking closely at the workforce, people can still witness men and women in stereotypical job fields [8]. According to many researches, gender is an important factor that influences career choice. It affects not only the chosen careers are affected by the reason that contribute to his or her choices. Hence, males and females usually prefer careers that are consistent with their genders [9].

King (2003) conducted a research by using UK graduates as respondents and found out that the important factors of them selecting a job is based on the security of traditional career [11]. They feel less tempting on other factors in boundary less-career today. Chapman et al (2005) conducted a research and found out that perceived

information to job seekers about the company, specifically promotion within short time no longer than 3 years are the vital motivation [7]. This links to values and policies of that organization. According to Chan and Ho (2000) organizations are looking for talented and qualified job applicants but the well-known reputation is a very important factor [6]. If organizations have highly satisfactory reputation, applicants will apply for the jobs to support their self-esteem.

Many young people believe that they would like to be economically stable and have a comfortable lifestyle. Therefore, when they look into a major or a career path, they seek out the higher paying jobs or anything with most job security. In fact, some may even look at job stability ahead to retirement plan [18].

Bani-Khaled (2014) points out the people in the research weigh their options according to the environment in their interests and their educational performance and where they live [2]. Because the amount of travel time from home to work is a factor. This is linked to both genders who lay the emphasis on social type and investigate the type of occupations.

According to Beggs et al (2008) the students usually settle on a different path due to many uncontrollable factors [3]. They would not choose the job with salary and benefits of that job do not play a role in this decision. When considering about money, they include high earning potential, benefits, and opportunities for advancement. Mcglynn (2007) agrees with such findings most of the students in this generations are more highly concerned with the amount of money they can get [14]. However, there are some students who pursue their dreams. Similar finding by Wildman and Torres (2002) students want to be economically stable and look for a career path with higher salary and most job security [18]. Moreover, Rojatzl et al (2017) present a finding that environment in workplace as the combined efforts of employers, employees and society to enhance the health and well-being of people at work [16]. It can be any kind of interaction between interventions and stakeholders that provides significant benefits for employees.

2. MATERIALS AND METHODS

The respondents in this study are the 3rd year and 4th year students of the ICUTK. Both male and female students who are older than 20 years of age were selected through convenience probability sampling method. Questionnaires were distributed to 120 student respondents with the complete of 100 qualified after screening process.

Data collection was keyed and run through questionnaires and Regression Model Analysis. The questionnaire consisted of different parts. First, the demographic data, second, the personal opinion through their Rating Scale of the factors that influences their selection of a workplace in private or public companies.

The five variables of this research are Gender, Age, GPA, Expected Income and Expected Travel Time to workplace. The GPA range considered is from 2.00 to 4.00 as the minimum required for graduation is 2.00. The Expected Income is based on the current market's rate for fresh graduate employees which ranges from 15,000 to 20,000 baht. In fact, most companies would not pay the public university fresh graduate more than 20,000 baht. While the Expected Travel Time considered is from less than 30 to maximum of 90 minutes which is the usual travel duration during working hours in the Bangkok city using public transportation.

The data collected were processed through the study instrument using the multi- regression program by Minitab program.

The Conceptual Framework for this research is as follows:

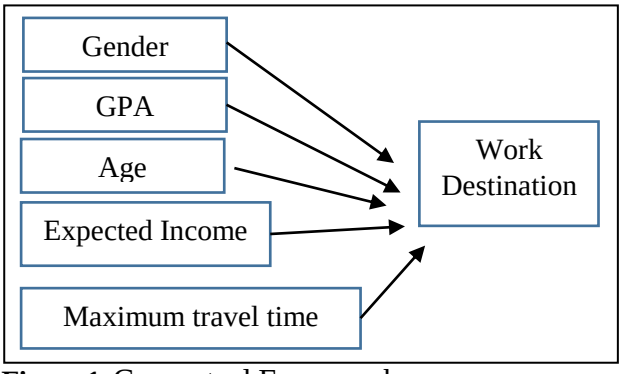

Figure 1. Conceptual Framework

Research Hypothesis

H_0 Gender, GPA, Age, Expected Income and Maximum travel time duration for traveling to work *do not have* any influences in selecting process to work destination.

H_1 Gender has influence in selecting process to work destination.

H_2 GPA has influence in selecting process to work destination.

H_3 Age has influence in selecting process to work destination.

H_4 Expected income of the graduate has influence in selecting process to work destination.

H_5 Maximum travel time for traveling to work has influence in selecting process to work destination.

3. RESULTS AND DISCUSSION

Table 1. Demographic Profile of Survey Participants

No.	Characteristics	Frequency	Percentage
1		Age	
	20	11	11%
	21	11	11%
	22	59	59%
	23	15	15%
	24	4	4%
	25	0	0%
2		Gender	
	Male	55	55%
	Female	45	45%
3		Expected Income	
	15000 Baht	11	11%
	16000 Baht	22	22%
	17000 Baht	42	42%
	18000 Baht	15	15%
	19000 Baht	10	10%
	20000 Baht	0	0%
4		Maximum Travel Time	
	<30 min	25	25%
	30 to 60 min	51	51%
	60 to 90 min	24	24%
5		GPA	
	<2.00	0	0%
	2.00-2.49	10	10%
	2.50-2.99	77	77%
	3.00-3.49	12	12%
	3.50-3.99	1	1%
	4.00	0	0%

The study population consisted of 100 undergraduate students of ICUTK. In terms of gender, Table 1 indicates that there are more male 55% and the rest of the 45% are females. All of the respondents are predominantly young people between 20 to 24 years old. Majority are 22 years old that shares 59% of the total number, while the 20 and 21 age groups share the same number which is 11%. The second biggest number of respondents comprised of individuals with 23 years of age that's 15%, while the least number is from the 24 years old of 4%.

With respect to GPA level, most of the respondents (77%) are within the 2.50-2.99 bracket, followed by 12% with 3.00-3.49, while those within the minimum GPA range of 2.00-2.49 are 10% of the respondents. The least number of students are in 3.50-3.99 GPA range that is 1%. No one among the respondents have GPA below 2.00 and more than 4.00.

Most of the respondents (42%) expect to earn a monthly salary of 17,000 baht on their first job. Twenty two percent (22%) of them expects 16,000 baht followed by 15% hoping for an 18,000 baht income while the least numbers of 11% and 10% expects the minimum starting salary of 15,000 baht and maximum of 19,000 baht respectively. It is worth noting that in Bangkok, Thailand, a starting salary of 15,000 baht per month is an appealing prospect for a young university graduate. However, since our respondents will be graduated from an International College, slightly higher salary is expected.

Lastly, with regard to Maximum Travelling Time to Work, most of the respondents would like to allot only within 30 to 60 minutes to commute to work. Twenty Five (25%) percent wants travel time to work be only less than 30 minutes, while the least percentage of 24 can accept a travel duration of 60 to 90 minutes to work.

Table 2. Multiple Regression Analysis

Variables	Coefficients	Std. error	T stat	P-value
Intercept	-2.490	0.721	-3.451	0.000
Gender	0.270	0.028	9.761	0.000
GPA	-0.416	0.057	-7.207	0.000
Age	0.242	0.019	12.475	0.000
Expected Income	0.000	0.000	-2.329	0.022
Maximum Time	0.017	0.001	11.516	0.000

The five independent variables in this study are Gender, GPA, Age, Expected Income, and Maximum Travel Time (See table 2). Out of 100 respondents in this research, P-value score for Gender, which is the only categorical data, is 0.000. This rejects the null hypothesis due to the fact that P-value is less than 0.05. The second and third variables, GPA and Age, have the same P-value score of 0.000. Both variables reject the null hypothesis. The fourth variable, Expected Income, has P-value score of 0.022. And the last variable, Maximum Traveling Time, has P- value score of 0.000. Therefore, 5 variables all reject the null hypothesis. There was no requirement to exclude any of the 5 selected variables in this research.

Table 3. R and R^2

Multiple R	R Square	Adjusted R Square
0.945	0.892	0.890

The value of Multiple R is 0.945 indicating a strong positive relationship between independent and dependent variables. In this research, the value of R^2 is 0.892 implying that Gender, GPA, Age, Expected Income, and Expected Maximum Travel Time influence the students in the selecting to work in private and public company. Moreover, the adjusted R^2 value is as high as 89.0% while the rest 11% is other factors which is not included in this research.

Table 4. The Regression Model for Calculation

Female	-2.489- 0.4161 GPA+ 0.2421 AGE + 0.01703 Max travel time
Male	-2.219 - 0.4161 GPA+ 0.2421 AGE + 0.01703 Max travel time

4. CONCLUSIONS

This research was conducted to measure the factors that influences the students' decision of selecting work destination either to private or public company. Due to the fact that majority of the students have personal goal and some idea on work destination, they tend to keep high GPA to have competitive edge after graduation. GPA along with age and gender all have enough evidence to reject the null hypothesis and prove to be factors on whether these respondents are willing to work for private or public companies. One notable factor in this research is the expected income which is similar to researches done by Beggs et al (2008) as the students consider high earning potential, benefits and opportunities for advancement [3], Saeed (2013) where financial income and employee performance have strong relationship [17] and Parvin and Kabir (2011) which money is a great motivator [15]. However, this research put one more specific factor, the Expected Travel Time from home to work, to allow private and public organization to be familiar with the need of this young generation. The raw data shows that it is acceptable for them to travel up to 90 minutes each from home to workplace. By profoundly understanding these factors, both private and public companies can use the model provided in this research to estimate the most suitable offers to these young students from public university.

Research limitation and suggestion

Arthur et al (2005) argue the fact that the career development is a really complicated topic and with only questionnaires or survey is considered as one-dimensional [1]. To enhance it, qualitative research is recommended. Based on the findings, 5 variables were proven to be influenced. Furthermore, more variables such as health benefits offered from stakeholders should be included as it has been conducted in the research [15].

6. REFERENCES

[1] Arthur MB, Khapove SN & Wilderom, CPM. Career success in a boundaryless career world, Journal of Organizational Behavior 2005; 26(2), 177-202.

[2] Bani-Khaled, TA. Career Intentions of Jordanian Undergraduate Students of English, Middle-East Journal of Scientific Research 2014; 21(1), 249-262.

[3] Beggs, JM. Bantham, J.H. & Taylor,S. Distinguishing the factors influencing college students' choice of major, College Student Journal, 2008; 42(2), 381-394.

[4] Bronstein, P & Farnsworth, L. Gender differences in faculty experiences of interpersonal climate and processes for advancement. Research in Higher Education 1998; 39(5), 557-585.

[5] Cavus, S Geri, S & Turgunbayeva, K. Factors Affecting the Career Plans of University Students after Graduation, International Journal of Humanities and Social Science 2015; 5(5), 94-99.

[6] Chan, SY & Ho, SSM. Desired attributes of public accounting firms in the job selection process: An empirical examination of accounting graduates' perceptions, Accounting Education: An International Journal 2000; 9(4), 315-327.

[7] Chapman, DS Uggerslev, KL Carroll, SA Piasentin, KA & Jones, DA. Applicant attraction to organizations and job choice: A meta-analytic review of the correlates of recruiting outcomes, Journal of Applied Psychology 2005; 90(5), 928-944.

[8] Greenwood, AM. Gender and jobs: Sex segregation of occupations in the world. Jour. of International Labour Review 1999; 138(3), 341-343.

[9] Huda, N. & Yousuf, S. Career preference of final year medical students of Ziauddin Medical University. Education for health (Abingdon, England), 2006; 19(3), 345-53.

[10] Jones, WA & Larke, A. Enhancing the quality of life for Hispanic individuals through career preparation. Journal of Hispanic Higher Education 2005; 4(1), 5-18.

[11] King, Z. New or traditional careers? A study of UK graduates' preferences, Human Resource Management Journal 2003; 13(1), 5-26.

[12] Kozak, MA & Dalkıranoğlu, T Mezun Öğrencilerin Kariyer Algılamaları: Anadolu Üniversitesi Örneği, Anadolu Üniversitesi Sosyal Bilimler Dergisi 2013; 13(1), 41-52.

[13] Mayrhofer, W Steyrer, J Meyrer, M Strunk, G Schiffinger, M & Iellatchitch, A. Graduates' career aspirations and individual characteristics, Human Resource Management Journal 2005; 15(1), 38-56.

[14] Mcglynn, AP. Achieving the Dream – What is it, and What's new? The Hispanic Outlook in Higher Education 2007; 18(4), 44-45.

[15] Parvin MM & Kabir MMN. (2011), Factors Affecting Employee Job Satisfaction of Pharmaceutical Sector, Australian Journal of Business and Management Research 2011; 1(9),113-123.

[16] Rojatzl, D Merchant, A & Nits, M. Factors influencing workplace health promotion intervention, Health Promotion International 2017; 32(5),831–839.

[17] Saeed, R. Factors Affecting the Performance of Employees at Work Place in the Banking Sector of Pakistan, Middle-East Journal of Scientific Research 2013; 17(9), 1200-1208.

[18] Wildman, M & Torres, RM. Factors Identified When Selecting a Major in Agriculture, Journal of Agricultural Education 2002; 46(2), 46-55.

CreTech 2020
8th International Conference on Creative Technology
Multidisciplinary to Drive Economy and Social
http://utkcretech.rmutk.ac.th

Transition to online learning during COVID-19 pandemic: Impact on students' learning motivation

Jiraporn Yiamkhamnuan[1], Jurairat Phuttharak[2*]

[1]Department of Business English, Prince of Songkla University (Trang campus), Thailand
[2]Department of Management Information Technology, Prince of Songkla University (Trang campus), Thailand
[*]Corresponding author. E-mail: jiraporn.yi@psu.ac.th

ABSTRACT

The study aims to investigate the impact of a disruptive shift from the in-class face-to-face learning to an online mode as a result of the sudden emergence of the COVID-19. A particular focus was given on students' development of motivation to learn. This study was carried out with a group of 54 Thai students registering for a course at a university. Both quantitative and qualitative methods were used to collect the data. Questionnaires were administered to the students, followed by semi-structured interviews. The findings from quantitative analysis revealed that the students became less motivated when learning via online platforms. Based on an analysis of qualitative data, four factors that possibly explain these quantitative findings are related to the students' ability to manage their own study environments, perceived lack of support and interactive collaboration, regulating attention and effort, and technical problems. Findings are helpful with regard to the formulation of pedagogical strategies that practitioners may consider when designing online courses to enhance students' learning motivation and engagement.

Keywords: COVID-19, learning motivation, online education

1. INTRODUCTION

Since early 2020, with the widespread of Coronavirus disease (COVID-19), universities across the world, including in those in Thailand, have been experiencing an unprecedented transition from in-class face-to-face learning to online spaces for distance learning. Following the Thai government's declaration of a state of emergency and precautionary measures against COVID-19, educational institutions nationwide have enforced sudden closures with face-to-face classes suspended. Online learning modes thus started.

Education has changed abruptly. Online teaching is no more an option but a necessity. Lecturers have indulged them in remote teaching while their students, either staying at home or dorms, have learned via the Internet. E-learning applications or video conferencing, though have not been widely used before, has been embraced after shutdown. It seems to be a tool appropriate for teaching in this time of crisis [1]. Adopting this e-technology can however affect the success of learning acquisition [2]. This study thus aims to see the impact of this sudden shift to online teaching, as compared to traditional methods of teaching in a form of face-to-face lectures. The particular focus was given to examine students' development of their motivation to learn, one of the factors considered significant for online learning and its achievement [3]. Factors that may be involved were also examined. Findings of this study put some light on the formulation of pedagogical strategies for designing online courses that enhance students' motivation and engagement. They include suggestions of how to deal with challenges associated with the online learning.

2. RELATED WORKS

2.1 On-line learning as innovation

Online learning has been viewed as one of the most prominent innovations. According to Rogers [4], an innovation is defined as "an idea, practice, or object that is perceived as new by an individual" (p. 12). Newness is subjectively-determined [4]. One innovation, although being known for some time, might be viewed as new since it has not been adopted yet in particular situations or for particular purposes to solve problems that institutes and teachers are facing.

In the contexts of this study, it can be said that the sudden transition from habitual in-class teaching to online platforms during the COVID-19 crisis is part of educational innovation in an attempt to control the pandemic of COVID-19 and ensure continuation of teaching operation. When, however, the instructional innovation has been mandated, the stakeholders (i.e., teachers and students) might adopt e-teaching with levels of uncertainty due to a lack of online teaching experience.

As Rogers [4] suggested, the information about the effectiveness of the outcomes of innovation needs to be actively measured, especially when its implementation is mandated by external factors, rather than by an individual's interest. This study thus seeks to see lecturers' teaching practice via online platforms and its impact on the development of motivational attributes in students.

2.2 Motivation to learn

Motivation is defined as an internal drive moving individuals to learn meaningfully [5]. Motivation leads learners to initiate a particular activity and determines how long they are willing to persist in that activity through effort put in it [5]. The motivated learners will actively adopt a deep approach to their learning. In a Self-Determination Theory, learning motivation is categorized into intrinsic and extrinsic types [6].

Intrinsic motivation is considered to be the most autonomous form of learners' self-regulation. It refers to their interest in, enjoyment of, and satisfaction with, doing tasks in and of themselves. This type of motivation emanates from their "full sense of volition and choice" [6] and will be endorsed when their behavior is perceived as autonomous [6]. Extrinsically motivated behavior is, however, instrumental or controlling. It occurs when individuals perform tasks out of an expectation for external outcomes such as receiving a reward, avoiding punishment, or even gaining acceptance [7].

In self-regulated learning, motivation to learn is closely related to goal-orientation that underlies the purposes of performing tasks [8]. Goal orientation can be both intrinsic and extrinsic. Intrinsic goal-oriented learners will participate in a task for internal driving such as challenge, interest and mastery. By contrast, the behavior of extrinsic goal-oriented learners is driven by external forces, such as expectations for good grades, rewards or positive evaluation of others.

2.3 Motivation and online learning

Understanding students' motivation to learn in online environments has been gaining much interest among researchers. For example, Martens, Gulikers, and Bastiaens [9] argue that online learners are required to be intrinsically motivated since the success of this learning requires them to use self-regulated strategies and be engaged in learning with curiosity. Similar findings are found in the study by [10] indicating that online students are more intrinsically motivated than their on-campus counterparts. Poor motivation has been asserted by [11, 12] as a key factor that result in a high rate of students' dropout.

Online environment itself is perceived as motivating. Online learning has been perceived to be favorable due to their potential for learning

flexibility—physical barriers that normally exist in face-to-face instruction are removed [13]. As a result of better access to learning, students with other responsibilities (e.g., family or work) can study at a distance.

Nevertheless, a cautious remark is made about limitations of online learning. The isolated atmosphere of e-learning is found to eliminate or reduce face-to-face, interactional aspects [14, 15] which are the key elements for effective teaching [16]. Students' feelings of frustrations with technical difficulties also influence their decisions to withdraw from e-courses. Issues about students' high attrition rates as a result of lacking self-regulated learning skills [17] are also raised.

Based the literature discussed above, we see that motivation is a crucial key to success in online learning and thus become a primary reason for conducting this study. Additionally, research exploring motivation in online learning has been found limited [18], especially during the time of pandemic. Little evidence has been reported about tangible outcomes of such online learning. A report on students' attrition rates in online educational contexts [19, 20] highlights the complexity of the factors that influence their motivation to learn and consequently the need for greater understanding of it. The current study aims to address this gap. It seeks to investigate students' motivation to learn online during the Covid-19 outbreak where lecturers have shifted their pedagogical approach to adapt to changing situations.

3. METHODS

The current study set out to investigate the extent to which the online learning impacts upon learning motivation of a specific group of Thai students. Specifically, it sought to discover how the students perceived online learning with a focus given to their motivation to learn. In this study, motivation was particularly examined as it has been viewed as one of the most important prerequisites contributing to accomplishment of online learning [5]. Based on this main purpose, two research questions (RQ) are posed as follows:

Research questions:

1. To what extent do the students develop their motivation to learn via video conferencing platforms?
2. What are the factors influencing students' development of motivation to learn in their online environments?

Participants

The setting of the study was a university in Thailand. The 54 Thai students were recruited into this study, among of whom were 27 females and 27 males. Their participation was voluntary. The 15-week course consisted of 45 hours of instruction focusing on IT skills development. In response to the COVID-19, the 3-week course instruction had been suspended and then shift to online modes conducted via video conferencing applications or e-platforms: Zoom, Webex and Google Meet, where the permission to access cameras was given with videos kept on.

Instruments and data collection

In addressing RQ1, the levels of students' motivation were measured after participation in the online learning, compared to that perceived in face-to-face instruction. A shorter version of Deci and Ryan's Intrinsic Motivation Inventory (IMI) with 22 items was adopted in the study as it has been proved a reliable measurement with predictive validity [6].

The modified IMI measured four areas of intrinsic motivation: interest/enjoyment, perceived competence, effort, and perceived choice. The interest/enjoyment subscale is the only subscale that directly measured learners' intrinsic motivation while the effort, perceived competence and perceived choice are predictors positive to motivation [21]. The Cronbach's

alphas for the scales of interest/enjoyment, perceived competence, and effort were considered as robust ($\alpha > .70$). The low alpha value in the perceived choice ($\alpha > .62$) was in part due to the small number of items made up the sub-scale.

To provide further insight into students' development of motivation in online learning, as addressed in RQ 2, a semi-structured interview was conducted with five of the students who were purposively selected by their academic achievement. These students were assured of their anonymity and encouraged to give honest responses. The interviews were analyzed by the authors who checked for keywords and recurring themes.

Data analysis

The collected data underwent quantitative and qualitative analyses. Quantitative data were derived from the 5-point Likert-type scales questionnaire. The data were analyzed using the Statistical Package for the Social Sciences (SPSS) program (version 21). To address the research questions, both descriptive and inferential statistical tests (dependent T-Test) were carried out. Two hypotheses have been put forward as follows:

H_0 = There is no change in students' motivation in online learning environments.

H_1 = There is a positive change in learners' motivation in online learning environments.

Each item on the IMI was given a score from 1 to 5 (a Likert-type scale). The scores were collated according to the participants and question number, bearing in mind that questions 4, 6, 12 - 16, 21 and 23 were reverse-scored. The final scores were averaged for each of the four subscales.

The qualitative data derived from student interviews were conducted in Thai and digitally recorded. The recordings were then transcribed verbatim and translated into English for the thematic analysis. The themes emerging from the data were identified, coded, reviewed, and finally defined before writing a report.

4. RESULTS AND DISCUSSION

RQ1. To what extent do the students develop their motivation to learn via video conferencing platforms?

This section first reports the findings for RQ1 examining the extent to which the students perceive a change in their motivation to learn in video conferencing-based environments. This question was posed to track levels of students' motivation in the areas of interest/enjoyment, perceived competence, effort/importance, perceived choice and value/usefulness.

Means (M) for motivation obtained in the questionnaire, together with standard deviations (SD), were calculated. The criteria used as a basis for the interpretation of the mean ratings are as follows: 4.51–5.00 = very high; 3.51–4.50 = high; 2.51–3.50 = moderate; 1.51–2.50 = low; and 1.00–1.50 = very low. Subsequently, a paired-samples t-test was conducted to measure whether rates of change in means of each construct differed in students' motivation in online environments as compared to in-class learning (α=0.05). Results of the analyses are presented in Table 1.

Table 1. Means and significance tests for students' motivation

Motivation	N	Means (SD)		Means difference	t	p (two-tailed)
		In-class	Online			
Interest/enjoyment	54	4.21 (.69)	2.7407 (1.04)	1.47 (1.39)	7.767	.000
Competence	54	3.90 (.65)	2.4704 (.93)	1.43 (1.10)	7.883	.000
Effort/importance	54	4.04 (.68)	3.1620 (.86)	0.88 (1.34)	5.641	.000
Perceived choice	54	3.65 (.69)	2.6111 (.95)	1.04 (1.15)	6.971	.000
Value/usefulness	54	4.54 (.60)	3.3630 (1.05)	1.18 (1.24)	6.989	.000

The results from the dependent-samples t-test analyses as depicted in Table 1 indicate the statistically significant changes in a negative direction for all of the five sub-constructs of motivation, suggesting that the online learning, as compared to traditional, in-class instruction, had a negative impact upon the development of students' motivation to learn. In other words, the students became less motivated when learning via e-platforms: they lacked interest in engaging with online activities, felt incompetent in their ability to learn, felt having no choice to learn, and devalued experiences they derived from this learning with less effort put into it.

RQ2. What are the factors influencing students' development of motivation to learn in their online environments?

This section presents qualitative findings from an analysis of the student interviews. The four themes emerged as factors influencing their motivation for online learning were identified as follows:

Management of learning environments

The most identified aspect of online learning viewed by all students as disadvantaged was related to their experience in unfavorable learning atmosphere. For example, Student1, though perceiving freedom to learn anywhere, still had difficulties in managing her learning environments, as said, "At home, while I was learning, my mother was doing the housework and my little sister was playing around. I found it disturbing." Similarly, as getting "distracted very easily" when studying online at home, Student2 expressed her preference for in-class learning since she felt more focused on the ongoing lectures.

Learning interactions and support

In the online learning, it seems that the learning process cannot reach its full potential due to a lack of direct interactions and support. In other words, students' limited contact with a lecturer might be at the root of students' frustration. For example, although being structured to learn online via Zoom under the supervision of her lecturer in the perceived "non-threatening" learning atmosphere, Student2 felt lost due to a perceived lack of sufficient support: "...It's not convenient for me to seek immediate help either from my peers or teacher." There are reasons underlying the students' reluctance to seek help in this online learning.

The particular characteristics of the online learning seems to influence students' decisions about whether to seek help. The students in this study preferred not to seek help as viewing behavior of interrupting the ongoing lectures as impolite. Besides, students' dissatisfaction with peer collaboration was noted in the responses of Student2; that is, her project team members were found less engaged in online discussion. Feeling a lack of learning community, the student found online learning boring and unengaging.

Regulating attention and effort

From the interviews, the students reported on poor ability to regulate their effort, as shown in their use of poor learning strategies: "a computer was left on and I was doing other things else. I hardly pay attention to the [online] learning." (Student3) and "I often shift to Facebook after a few minutes of [online] learning." (Student4). Furthermore, completing examinations online from home, some students admitted cheating on quizzes just to obtain good scores.

It seems that all students vary in degrees of their capabilities and confidence while learning online. Based on the students' self-reflection responses, the failure to regulate their learning effort is caused by a lack of autonomous learning attributes. For example, the student4 who rated herself as having a low academic competence said: "I have no motivation to preview lessons my lecturer posted before [online] class meetings. I didn't even watch the clips which was recorded for self-study revisions." She thus expressed her preference for teacher-dependent class in which the lecturers physically present in her brick-and-mortar class helped stimulate her to learn.

Additionally, students reported on a need for more effort invested into online learning. The intense focus on words and sustained eye contact made them feel exhausting. For them, more than an hour of e-learning was considered too long to be attentive, resulting in a subsequent report on lapses in their attention to lectures.

Technical problems

Unsurprisingly, technical difficulties were found to hinder students' learning process. More than half of the students reported on a lack of a computer, which hampered them from actively engaging in online activities and developing into more active learners. Frustration with turning microphones on and off, lagging connections and background noise was found to impact upon the quality learning acquisition, as remarked by Student1: "There were delays between images and sounds, and I had difficulties to understand or catch up with lectures." Due to this problem, the students seemed to be less motivated and less persistent in the learning.

5. CONCLUSIONS

COVID pandemic made us realize the importance of technology as providing solutions during COVID pandemic crisis. However, there have been concerns over how the shift to online learning is adopted in a way that provides quality e-learning.

The findings in this study reveals students' lack of sufficient motivation in online learning. This lack is manifested in students' report on difficulties in managing study environments, regulating effort, and disciplining themselves to learn. It appears that this disinclination to take on active roles in learning was demonstrated in the forms of being easily distracted and using poor learning strategies. These may be explained by taking into account an interplay of contextual factors that imposed constraints on the learning.

Online learning modes may not be viewed as a panacea in the time of Covid-19 crisis. Due to the abrupt shift from a face-to-face class, the problems emerging in this study may be partly rooted from poor preparedness for e-learning pedagogy with a lack of key elements associated with quality learning—Internet accessibility, learning flexibility and IT infrastructure support [15]. Apart from that, students' attributes are the factors involved. The students' inability to take control of their learning may negatively affect their engagement in the learning, as noted in this study.

There is thus a need to re-design the online learning either for future use or in times of crisis. Lecturers should start by guiding their students on how to learn online effectively. The finding that suggested the preference for lecturer control might indicate students' insufficient confidence

and lack of strategies needed for learning online. As such, training in self-directed learning should be arranged to psychologically prepare them for challenges that might happen.

The provision of autonomy support should not be overlooked. Lecturers need to make clear the kind of support they should provide if their students need it. Consultations via e-mails or other platforms after online meeting is needed especially for the academically underprepared students. technical difficulties can also be solved by prerecording video lectures [15]. Learning atmosphere needs to be managed in a way that promotes interactions and collaboration; that is, students could seek help, share ideas and search for learning solutions with their friends. In short, provided with sufficient help, students are likely to feel cared for and supported [22], possibly boosting motivation and preventing them from resistance to this kind of 'perceived' insolated learning.

As the progress of online learning depends on students' levels of active learning outside of class, emphasis should be placed on pedagogical issues. Rather than restricting assessment to formal tests, lecturers may employ various types of formative assessment possibly administered either in synchronous and asynchronous forms. Learning experience should also be personalized by making use of self-reflection learning tools (e.g., logs) since the tools are useful in helping the students reflect on their learning by looking into problems they faced, trying out solutions to those problems and evaluating strategies they use. In so doing, the students will be given an opportunity to exercise skills in attention control and develop into more motivated, responsible learners.

Based on the findings as discussed above, there is a compelling argument that lecturers also need to update their IT skills and be trained for professional development that is focused more on e-learning pedagogies. By the training they will be equipped with strategies that help make their online teaching effective even at the time of crisis.

6. REFERENCES

[1]. Mueller M, Schrie C, Holzer M, Roeggla M, Laggner AN, Ettl F. Education in academic emergency medicine during the COVID-19 pandemic – our experience from an ongoing crisis 2020 [cited 2020 15 June]. Available from: file:///D:/Downloads/Education_in_academic_emergency_medicine_during_th.pdf.

[2]. Alkhaldi A, Abualkishik A. The mobile blackboard system in higher education: Discovering benefits and challenges facing students. International Journal of Advanced and Applied Sciences. 2019;6(6):6-14.

[3]. Gedera D, Williams J, Wright N. Identifying Factors Influencing Students' Motivation and Engagement in Online Courses. In: C. K, editor. Motivation, Leadership and Curriculum design. Singapore: Springer; 2015.

[4] Rogers EM. Diffusion of innovations. 5th ed. New York, NY: Free Press; 2003.

[5]. Dörnyei Z. Teaching and researching motivation. Harlow, England: Longman; 2000.

[6]. Deci EL, Ryan RM. Intrinsic and extrinsic motivations: Classic definitions and new directions. Contemporary Educational Psychology. 2000;25:54-67.

[7]. Deci EL, Vallerand RJ, Pelletier LG, Ryan RM. Motivation and education: The self-determination perspective. Educational Psychologist. 1991;26(3 & 4):325–46.

[8]. Zimmerman BJ. Motivational sources and outcomes of self- regulated learning and performance. In: Zimmerman BJ, Schunk DH, editors. Handbook of self-regulation of learning and performance. New York, NY: Routledge; 2011. p. 49-64.

[9]. Martens R, Gulikers J, Bastiaens T. The impact of intrinsic motivation on e-learning in authentic computer tasks. J Comp Assisted Learning. 2004;20:368-76.

[10] Wighting MJ, Liu J, Rovai AP. Distinguishing Sense of Community and Motivation Characteristics between Online and Traditional College Students. Quarterly Review of Distance Education. 2008;9(3):285-95.
[11] Artino AR. Motivational beliefs and perceptions of instructional quality: Predicting satisfaction with online training. Journal of computer assisted learning. 2008;24(3):260-70.
[12] Keller JM. An integrative theory of motivation, volition, and performance. Technology, Instruction, Cognition, and Learning. 2008;6(2):79-104.
[13] Blake R, Wilson NL, Cetto M, Pardo-Ballester C. Measuring oral proficiency in distance, face- to- face, and blended classrooms. Language Learning & Technology. 2008;12(3):114-27.
[14] Sitter V, Carter C, Mahan, R., Massello C, Carter T. Hybrid course design: Faculty and student perceptions. In: Smith P, editor. Proceedings of the 2009 ASCUE Summer Conference 42st Annual Conference Association of Small Computer Users in Education. Myrtle Beach, SC: ASCUE; 2009. p. 40-51.
[15] Dhawan S. Online Learning: A Panacea in the Time of COVID-19 Crisis. Journal of Educational Technology Systems. 2020.
[16] Littlewood W. Autonomy: An anatomy and framework. System. 1996;24(4):427-35.
[17] Van den Branden K. Diffusion and implementation of innovations. 2009 06 July 2014. In: The handbook of language teaching [Internet] .Malden,MA : Blackwell; [659-72]. Available from: http://www.blackwellreference.com.
[18] Teklu Abate B. Motivation and Satisfaction in Internet-Supported Learning Environments: A Review. Journal of Educational Technology & Society. 2010;13(2):116-27.
[19] Lee Y, Choi J, Kim T. Discriminating factors between completers of and dropouts from online learning courses. British Journal of Educational Technology. 2013;44(2):328-37.
[20] Liyanagunawardena TR, Adams AA, Williams SA. MOOCs: A systematic study of the published literature 2008- 2012. International Review of Research in Open & Distance Learning [Internet]. 2013 15 June 2020; 14(3):[202-27 pp.]. Available from: http://www.irrodl.org/index.php/irrodl/article/view/1455/2531.
[21] Mitchell- Barrett R. An analysis of the Storyline method in primary school; its theoretical underpinnings and its impact on pupils' intrinsic motivation: Durham University; 2010.
[22] Deci EL, Ryan RM. Intrinsic motivation and self-determination in human behavior. Ryan RM, editor. New York, NY: Plenum; 1985.

CreTech 2020

8th International Conference on Creative Technlogy

RAJAMANGALA KRUNGTHEP

For More Information CreTech

Research and Development Institute
Rajamangala University of Technology Krungthep

Tel. +(66) 2 287 9600 ext 1177
Fax +(66) 2 287 9684